

Winter 2016

Size specific transfection to mammalian cells by micropillar array electroporation

Yingbo Zu

Follow this and additional works at: <https://digitalcommons.latech.edu/dissertations>



Part of the [Genetics Commons](#), and the [Nanoscience and Nanotechnology Commons](#)

**SIZE SPECIFIC TRANSFECTION TO MAMMALIAN
CELLS BY MICROPILLAR ARRAY
ELECTROPORATION**

by

Yingbo Zu, B.S., M.S.

A Dissertation Presented in Partial Fulfillment
of the Requirements of the Degree
Doctor of Philosophy

COLLEGE OF ENGINEERING AND SCIENCE
LOUISIANA TECH UNIVERSITY

November 2015

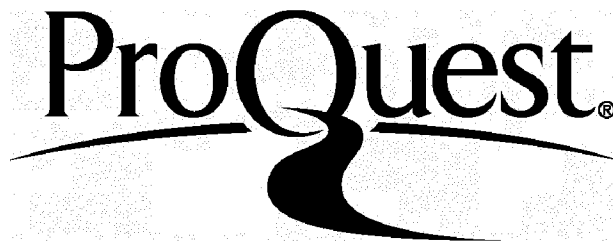
ProQuest Number: 10301616

All rights reserved

INFORMATION TO ALL USERS

The quality of this reproduction is dependent upon the quality of the copy submitted.

In the unlikely event that the author did not send a complete manuscript and there are missing pages, these will be noted. Also, if material had to be removed, a note will indicate the deletion.



ProQuest 10301616

Published by ProQuest LLC(2017). Copyright of the Dissertation is held by the Author.

All rights reserved.

This work is protected against unauthorized copying under Title 17, United States Code.
Microform Edition © ProQuest LLC.

ProQuest LLC
789 East Eisenhower Parkway
P.O. Box 1346
Ann Arbor, MI 48106-1346

LOUISIANA TECH UNIVERSITY

THE GRADUATE SCHOOL

OCTOBER 9, 2015

Date

We hereby recommend that the dissertation prepared under our supervision by

Yingbo Zu, B.S., M.S.

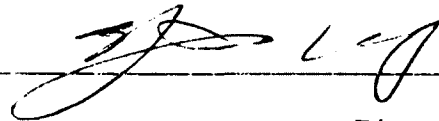
entitled Size Specific Transfection to Mammalian

Cells by Micropillar Array

Electroporation

be accepted in partial fulfillment of the requirements for the Degree of

Doctor of Philosophy in Engineering



Supervisor of Dissertation Research



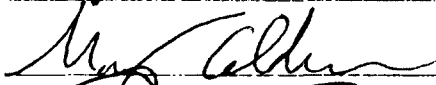
Head of Department

Engineering
Department

Recommendation concurred in:

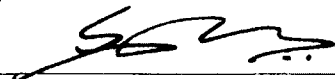


Yuei Luou



Advisory Committee

Approved:



Director of Graduate Studies



Dean of the College

Approved:



Dean of the Graduate School

ABSTRACT

Electroporation serves as a promising non-viral gene delivery approach, while its current configurations carry drawbacks associated with high-voltage electrical pulses and heterogeneous treatment on individual cells. Here, we developed a new micropillar array electroporation (MAE) platform to advance the delivery of plasmid DNA and RNA to mammalian cells. By introducing well-patterned micropillar array on the electrode surface, the number of pillars each cell faces varies with its cell membrane surface area, despite their large population and random locations. In this way, cell size specific electroporation is conveniently done and contributed to a 2.5~3 fold increase on plasmid DNA transfection and an additional 10-55% knockdown with targeting siRNA, respectively. The delivery efficiency varies with the number and size of the micropillars as well as their pattern density. As MAE works like many single cell electroporation is carried out in a parallel fashion, the electrophysiology response of individual cells is representative, which has the potential to gear up the tedious, cell-specific protocol screening process in the current *in vitro* bulk electroporation (i.e., electroporation to a large population of cells). Its success might facilitate the wide adoption of electroporation as a safe and effective non-viral gene delivery approach needed in many biological research and clinical treatments.

APPROVAL FOR SCHOLARLY DISSEMINATION

The author grants to the Prescott Memorial Library of Louisiana Tech University the right to reproduce, by appropriate methods, upon request, any or all portions of this Dissertation. It is understood that "proper request" consists of the agreement, on the part of the requesting party, that said reproduction is for his personal use and that subsequent reproduction will not occur without written approval of the author of this Dissertation. Further, any portions of the Dissertation used in books, papers, and other works must be appropriately referenced to this Dissertation.

Finally, the author of this Dissertation reserves the right to publish freely, in the literature, at any time, any or all portions of this Dissertation.

Author *W. E.*

Date 12/1/15

DEDICATION

This dissertation is dedicated to my parents, Dehuai Zu and Yanxia Wang, my wife, Zhongjing Huang and my children, Ashley Zu and Aaron Zu, whose unwavering encouragement provided me with the strength to complete this quest.

TABLE OF CONTENTS

ABSTRACT	iii
DEDICATION	v
LIST OF FIGURES	x
LIST OF TABLES	xiii
ACKNOWLEDGMENTS	xiv
CHAPTER 1 INTRODUCTION	1
CHAPTER 2 LITERATURE REVIEW	7
2.1 Gene Delivery	7
2.1.1 Viral Vectors Gene Delivery	8
2.1.2 Non-Viral Delivery Methods	10
2.1.3 Chemical Transfection Methods	12
2.1.3.1 Lipoplex	13
2.1.3.2 Polyplex	14
2.1.4 Physical Transfection Methods	14
2.1.4.1 Biolistics (gene gun)	14
2.1.4.2 Microinjection	15
2.1.4.3 Electroporation	15
2.2 Electroporation	17
2.2.1 Theory	17
2.2.2 Physical Mechanism	19
2.2.3 Effect Factors in Electroporation	20

2.2.4	<i>In Vivo</i> Electroporation	22
2.2.4.1	Electric field distribution	23
2.2.4.2	Vascular effects.....	23
2.2.5	<i>In Vitro</i> Electroporation	23
2.2.6	Laboratory Practice.....	24
2.2.1	Electroporation Cuvettes Electrodes Material	25
2.3	Carbonization.....	26
2.3.1	Glass-Like Carbon	26
2.3.2	Temperature and Pressure Factors for Carbonization.....	28
2.3.3	Composition of Precursors.....	31
CHAPTER 3 MICRO-PILLAR ARRAY ELECTROPORATION TO ENHANCE GENE DELIVERY TO MAMMALIAN CELLS		32
3.1	Introduction.....	32
3.2	Materials and Methods.....	34
3.2.1	Materials and Reagents	34
3.2.2	Cell Culture.....	34
3.2.3	Micropillar Array Electrode Fabrication	34
3.2.4	Measurement of the Gap Size of Electrodes in MAE.....	36
3.2.5	Device Assembling	37
3.2.6	Electroporation Setup and Process	38
3.2.7	Transfection Efficiency and Cell Viability	38
3.3	Simulation on the Electric Field of MAE	40
3.4	Results and Discussion	41
3.4.1	Enhancement of micro-pillar array electroporation on reporter gene transfection.....	41
3.4.2	Focusing of the Electric Pulses	46

3.4.3	Cell Size-Dependence Transfection.....	47
3.4.4	Effect of Size and Density of Micro-pillars on Electroporation Enhancement.....	50
3.5	Conclusions.....	51
CHAPTER 4 CARBON ELECTRODE MICRO-PILLAR ARRAY ELECTROPORATION		53
4.1	Introduction.....	53
4.2	Materials and Methods.....	54
4.2.1	Materials and Reagents	54
4.2.2	Cell Culture.....	55
4.2.3	Small Interfering RNA.....	55
4.2.4	Micro-Pillar Array Fabrication	56
4.2.5	Carbonization.....	58
4.2.5.1	Micro-Pillar Array Electrode Carbonization Protocol.....	60
4.2.6	Transfection Efficiency and Cell Viability.....	64
4.3	Results and Discussions.....	65
4.3.1	Structure Characterization by Scanning Electron Microscopy (SEM)	65
4.3.2	Carbon Micro-Pillar Array Electroporation.....	67
4.3.3	Enhancement of Micro-pillar Array Electroporation on Sima Delivery	71
4.4	Conclusions.....	74
CHAPTER 5 FLOW GUIDED MICRO-PILLAR ARRAY ELECTROPORATION		76
5.1	Introduction.....	76
5.2	Materials and Methods.....	77
5.2.1	Cell Culture.....	77
5.2.2	Fabrication and Assembly of Microfluidic Device.....	77
5.2.3	Electroporation Procedure	79

5.2.4	Polymer Based Nano-Fiber Fabrication	80
5.2.5	Nano-Fiber Electrode Carbonization Protocol.....	81
5.3	Results and Discussions.....	82
5.3.1	Comparison of FME with Bulk Electroporation.....	82
5.3.2	Comparison of MFE with Different Pulse Frequency	87
5.3.1	Comparison of MFE with Different Pulse Frequency	90
5.4	Conclusions.....	92
CHAPTER 6 CONCLUSIONS		94
REFERENCES		96

LIST OF FIGURES

Figure 1-1: Estimated cancer deaths in the US in 2014 (American Cancer Society).....	1
Figure 2-1: Gene delivery methods	7
Figure 2-2: The schematic of the working principles of chemical transfection method.	13
Figure 2-3: Schematic of the working principles of electroporation.	16
Figure 2-4: Cell membrane lipids arrangement in hydrophobic (top) and hydrophilic (bottom) pore.	20
Figure 2-5: <i>In vitro</i> electroporation processes.	24
Figure 2-6: Electroporator BTX 830 (https://www.btxonline.com/ecm-830-square-wave-electroporation-system/).....	25
Figure 2-7: Carbonization process.....	28
Figure 2-8: Pressure-temperature Conditions for the Formation of Carbon Spheres from Different Precursors.	30
Figure 3-1: Schematic of the micropillar array electrodes integrated with the SU-8 spacer and connecting the microchannel in MAE.	35
Figure 3-2: The working principle of the micropillar array electroporation (MAE). (a) Schematic of the cell size-specific treatment mechanism (large cells face more micropillars with each providing focused electric pulse during electroporation); (b) a SEM image of 2- μ m micropillars; (c) schematic illustration of MAE operation.	37
Figure 3-3: The model geometry and mesh setup for the electric field simulation of a single micropillar protruding towards a single cell. Location “A” is the chosen point in later transmembrane potential calculation.	41
Figure 3-4: Fluorescence and phase contrast microscopic images of pGFP plasmid transfection by a commercial system (“BTX”) and MAE on K562 cells.....	43

Figure 3-5: Transfection enhancement of pGFP plasmids in 2- μ m micropillar MAE. (a) Phase contrast and fluorescence microscopic images of NIH 3T3 cells after transfection by a commercial system (“BTX”), “Au plain plate”, and MAE; quantitative results of transfection efficiency (b) and cell viability (c) for 3T3 cells and K562 cells, respectively. (**) represents $p < 0.01$, (***) represents $p < 0.005$, (****) represents $p < 0.0001$.	45
Figure 3-6: COMSOL simulation of the calculated electric potential and field lines around a cell facing an “Au plain plate” electrode (a) and a 2- μ m micropillar (b). (c) The calculated transmembrane potential at location “A” (marked in Figure 3-3) of the cell.	47
Figure 3-7: The plot of fluorescence intensity of GFP in transfected K562 cells to the cell size in a commercial bulk electroporation system (“BTX”, panel a and b) and a 2- μ m micropillar MAE system (a, c).	49
Figure 3-8: The effect of micropillar size and density on MAE electroporation enhancement. (a-b) Phase contrast images of cell coverage on 6- μ m micropillar array (a) and 2- μ m micropillar array (b); the comparison on the enhancement performance for MAE based on micropillars of various sizes: transfection efficiency (c) and cell viability (d). (**) represents $p < 0.01$, (***) represents $p < 0.005$.	51
Figure 4-1: Carbonization set up used for produce conductive carbon material (http://www.scielo.br/img/revistas/mr/2012nahead/aop_1346fig01.jpg).	60
Figure 4-2: Images for pyrolysis protocols I (a); II (b) and III (c).	63
Figure 4-3: Three stages of SU-8 carbonization protocol.	64
Figure 4-4: SEM images (a) and (b) SU-8 micro-pillar array, (c) and (d) carbon micro-pillar array, (e) single SU-8 micro-pillar (f) single carbon micro-pillar.	66
Figure 4-5: Transfection enhancement of pGFP plasmids in fluorescence microscopic and phase contrast images (a) gold coated plain plate; (b) carbon coated plain plate; (c) gold coated MAE; (d) carbon coated MAE.	70
Figure 4-6: The effect of micropillar materials on electroporation performance. The transfection efficiency (a) and the cell viability (b) comparison of gold-coated electrodes and carbon-based electrodes: for micropillar array electrode (“MAE”), plain plate electrode without micropillar pattern (“Plain Plate”), and a commercial system (“BTX”). (**) represents $p < 0.01$, (***) represents $p < 0.005$, (****) represents $p < 0.0001$.	71

Figure 4-7: Enhancement on siRNA delivery in 2- μ m micropillar MAE. (a) Fluorescence images of K562 cells and (b) fluorescence intensity measurement on GFP expression level in K562 and A549 cells when co-transfecting pMaxGFP and its corresponding siRNA; (c) the luminescence measurement on Luciferase expression level in K562 cells and cell viability when co-transfecting pLuc and knockdown siRNA probe (“GL3”); (d) cell viability of K562 and A549 cells in panel (b). (*) represents $p < 0.05$, (**) represents $p < 0.01$, (***) represents $p < 0.005$	74
Figure 5-1: Micro-fluidic device assembling.....	78
Figure 5-2: Schematic diagram of fiber formation by electrospinning process where a droplet of a polymer solution is elongated by a high electrical field.....	81
Figure 5-3: Three stages of PAN nano-fiber carbonization protocol	82
Figure 5-4: Transfection enhancements of pGFP plasmids in FME. Fluorescence microscopic and phase contrast images of K562 cells after transfection by 2 μ m (a) and 6 μ m (b) pillar structure enhanced microfluidic electroporation and conventional bulk electroporation (“BTX”) (c)	83
Figure 5-5: Transfection enhancements of pGFP plasmids in MFE. Fluorescence microscopic and phase contrast images of A549 cells after transfection by 2 μ m (a) and 6 μ m (b) pillar structure enhanced microfluidic electroporation and conventional bulk electroporation (“BTX”) (c)	84
Figure 5-6: Quantitative results of pGFP plasmids transfection efficiency for K562 (a) and A549 (b) cells by 2 μ m and 6 μ m pillar structure enhanced micro-fluidic electroporation and conventional bulk electroporation (“BTX”)	86
Figure 5-7: Quantitative results of electroporation cell viability for K562 (a) and A549 (b) cells by 2 μ m and 6 μ m pillar structure enhanced micro-fluidic electroporation and conventional bulk electroporation (“BTX”)	87
Figure 5-8: Transfection enhancements of pGFP plasmids in FME. Fluorescence microscopic and phase contrast images of K562 cells 24 hours after electroporation by 2 μ m pillar structure enhanced micro-fluidic electroporation for pulse frequency 1 Hz, 10 Hz, and infinite (a, b and c).	88
Figure 5-9: K562 cell transfection efficiency and cell viability on various pulse frequencies	90
Figure 5-10: Transfection enhancement of pGFP plasmids in fluorescence microscopic and phase contrast images of carbon nano-fiber based electroporation.....	91
Figure 5-11: Presents the pGFP transfection efficiency (a) and cell viability (b) difference between plain plate, fiber-based and pillar-based electroporation	92

LIST OF TABLES

Table 1: Different steps of pyrolysis.....	59
Table 2: Protocols tested for carbonization	61
Table 3: Technical specifications of the multi-functional pulse generator.....	79

ACKNOWLEDGMENTS

I would like to express my sincere gratitude to my advisor Dr. Shengnian Wang for his patient guidance, constructive advice, and continuous support during my Ph.D. study at Louisiana Tech University. I would also like to thank my committee members, Dr. James Palmer, Dr. Yuri Lvov, Dr. Weizhong Dai, and Dr. Mary Caldorera-Moore for providing valuable feedback on this dissertation.

I would like to extend my gratitude to all of the members in Dr. Wang's lab that worked alongside me and provided help in their expertise: Mrs. Fangfang Ren, Dr. Shuyan Huang, Mr. Xuan Liu, Miss Juan Chen, Mr. Baiyang Lv, Mr. Yang Lv, Dr. Yuxin Wang, Mr. Hong Tian, and Mr. Kartik Rajgopalan.

Finally, I would like to thank my parents Dehuai Zu and Yanxia Wang for their love and dedication in raising, supporting, and educating me. Great appreciation to my wife, Zhongjing Huang, for her love, support, company and understanding through all these years. Gratitude and best wishes to my children, Ashley Zu and Aaron Zu, for the happiness they bring me.

CHAPTER 1

INTRODUCTION

Cancer has a serious impact in the United States. According to the Centers for Disease Control and Prevention (CDC), cancer is the second cause of death in the United States in adults (NVSR 2014). The American Cancer Society (ACS) gives out specific data that shows there were 1,665,540 cancer cases diagnosed and 585,720 cancer deaths in 2014 (ACS 2014). The ACS also indicates if this situation lasts during an American's lifetime, one in two men and one in three women will develop cancer. As shown in Figure 1-1, the top cancers that killed the most people in the United States in males are: lung and bronchus (87,260 deaths), prostate (29,720 deaths), colon and rectum (26,300 deaths), pancreas (19,480 deaths), and liver and intrahepatic bile duct (14,890 deaths), and in females they are: lung and bronchus (72,220 deaths), breast (39,620 deaths), colon and rectum (24,530 deaths), pancreas (18,980 deaths), and ovary (14,030 deaths) (ACS 2014).

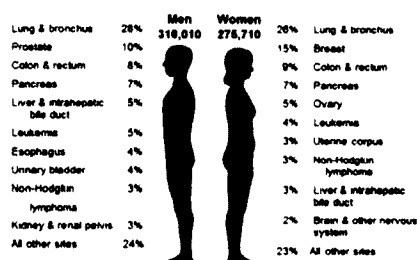


Figure 1-1: Estimated cancer deaths in the US in 2014 (American Cancer Society)

To prevent deterioration, many types of cancer treatment were developed. To date, the primary cancer treatment methods include surgery following chemotherapy and/or radiation therapy. However, this traditional treatment will cost greatly both economically and psychosomatically. Thus, some other options were researched and developed. Some mature and already applied methods immunotherapy, targeted therapy and hormone therapy. Individual treatment will be suggested according to the diagnosis. However in most cases, a multiple combined treatments will be applied (NCI 2014).

As a cancer treatment method, immunotherapy shows great potential. Immunotherapy is defined as the treatment that fights diseases with certain parts of a patient's own immune system. The immune system is a functional system with the composition of organs, special cells, and substances. It protects people from infections and some other diseases. The popular immunotherapy on cancer treatment include: monoclonal antibodies, immune checkpoint inhibitors, genetic vaccines, and other non-specific immunotherapies (ACS 2014).

A vaccine is a biological agent to fight against a particular disease, making it possible to obtain active acquired immunity. The typical vaccines are usually pathogenic microorganisms. They are the results of weakened or dead form (Fiore *et al*, 2009). When the biological agent is injected into human bodies, the immune system begins to work and identify such formulations as a threat. To protect from infection, antigens would be produced to destroy the microorganisms. Such behavior will be recorded. So the immune system can more easily identify and destroy it in the later encounters (CDC 2011).

In the history of the development of vaccines, genetic vaccines are considered one of the most important discoveries. From the early 1990's, an immune response in the plasmidencoded antigen by the introduction of plasmid DNA led to the rapid development of genetic vaccines (Alarcon, 1999). Generally, the DNA vaccine is produced through delivering the plasmid with genetic information into the target cells. While information encoded on plasmids was expressed, the transfected cells obtained the antigen, resulting in an immune response. Compared to traditional vaccine (recombinant bacteria or viruses), the genetic vaccine contains only the genetic information, produced under the water environment of living cells and unwanted activities that do not occur besides antibody responses (Robinson, 2000).

The distinct advantages of a genetic vaccine are relatively low in cost and the simplicity of manufacturing and use. In the past 20 years, through the efforts of scientists, the study of genetic vaccine has developed from laboratory to human clinical trials. To date, genetic vaccine has been conducted for cancer (Robinson, 2000), HIV-infection (Douek, 2009), or malaria (Nadjm & Behrens, 2012).

Plasmid DNA and mRNA are the main research areas in genetic vaccine. A typical case of DNA vaccine manufacture is gene gun delivery. Inert particles are usually used for precipitate plasmid. Through external factors, like a helium blast, genetic DNA is transferred into the cell (Fisher *et al.*, 2007). An mRNA is an immunogenic and programmable molecule, which is preferred as an antigen encoding gene for cell-based immunotherapy. In contrast to the DNA vaccine, the expression of mRNA vaccine is more efficient because it does not need to cross the nuclear envelope. This advantage aroused the interest of scientists and developed a series of methods to stimulate immune

responses through the use of mRNA. However, the shortages are always accompanied by inconveniences. A major disadvantage of using the mRNA vaccine is the time expense on the processes of harvesting, culturing, and loading. The efficacy of genetic vaccines in some immunotherapy systems is still considered not satisfactory enough. To improve gene delivery, efficiency becomes an urgent problem.

To achieve gene delivery from the external environment to the interior biological tissues or cells is an important procedure in immunotherapy. Along with the genetic technology growth, vested and foreseeable benefits had driven scientists to develop multiple approaches to implement gene delivery. Viral methods were used to transfer genes into the target cells. The viruses have very high gene transfer efficiency. Non-viral gene methods were also researched and used to overcome the negative effects caused by viral vectors. Chemical methods and physical methods are the two main research directions (Kamimura *et al.*, 2011).

Due to the unique advantages, electroporation was researched and applied frequently as a physical Non-viral gene delivery method. When working in a sterile environment, the risk of infection is considered is redundant in electroporation. The undemanding requirement on device and operation gained a wide application in all gene research area. Although electroporation experienced low performance at the very beginning of its development, the transfection efficiency and cell viability improved a lot during decade's of research and showed great potential (Neumann *et al.*, 1982; Sugar & Neumann, 1984).

Scientists are paying more attention to electroporation. However, challenges are also significant and arduous. In the current bulk electroporation protocols, the actual

pulse strength adopted in most bulk electroporation protocols fall in 0.5~1.0 KV/cm for mammalian cells and varies with cell type, source, and population. Such high-voltage pulses, though effective in improving the cell membrane's permeability and probe uptake, inevitably lead to severe problems such as slow membrane recovery, harmful electrochemical reactions (e.g., water hydrolysis, leading to pH changes and bubble burst damage), and Joule heating (temperature variations), all detrimental to the cell's survival fate.

To tackle the high-voltage issues, new systems with micro-/nanoscale features have recently been introduced by several research groups through closely patterning electrode pairs and/or sophisticated focusing the applied electric pulses. The rationale behind these micro-electroporation systems comes from when the two electrodes are brought close together and a low voltage is sufficient to generate pulses with a high enough field strength required for cell electroporation. However, most of these micro/nanoscale systems still ignore the local electrical variations on individual cells among a large population, leaving many uncontrollable factors similar to what is in the bulk electroporation systems.

In order to solve this problem and accomplish size specific electroporation, we propose a new electroporation system named the Micro-pillar Array Electroporation (MAE) approach. In MAE, cells will be sandwiched between a plain plate electrode and a plate electrode composed of thousands of micro-pillars in a well-patterned array format. This way, the number of micro-pillars each cell faces varies with its membrane surface area, or the size of the cells. This MAE setup is expected to leverage the current electroporation-based delivery approach in terms of efficiency and cell viability. To test

our hypothesis with mammalian cell transfection, NIH 3T3 cells (use as model anchor cells) and K562 cells (use as model suspension cells) were used here. Cell viability and transfection efficiency were the focused areas of the electroporation evaluation of reporter genes (pMaxGFP and pWizLuciferase) and their corresponding SiRNAs to demonstrate its broad effectiveness in electroporation enhancement.

CHAPTER 2

LITERATURE REVIEW

2.1 Gene Delivery

Gene delivery methods can be divided into two types: viral and non-viral methods, or vectors which are summarized in Figure 2-1. From the scheme we can figure out the viral methods which include the use of viruses such as adenovirus, retrovirus, and vacciniavirus. The non-viral methods are also researched in two areas: chemical methods, including lipoplex and polyplex, and physical methods, including microinjection, gene gun, and electroporation.

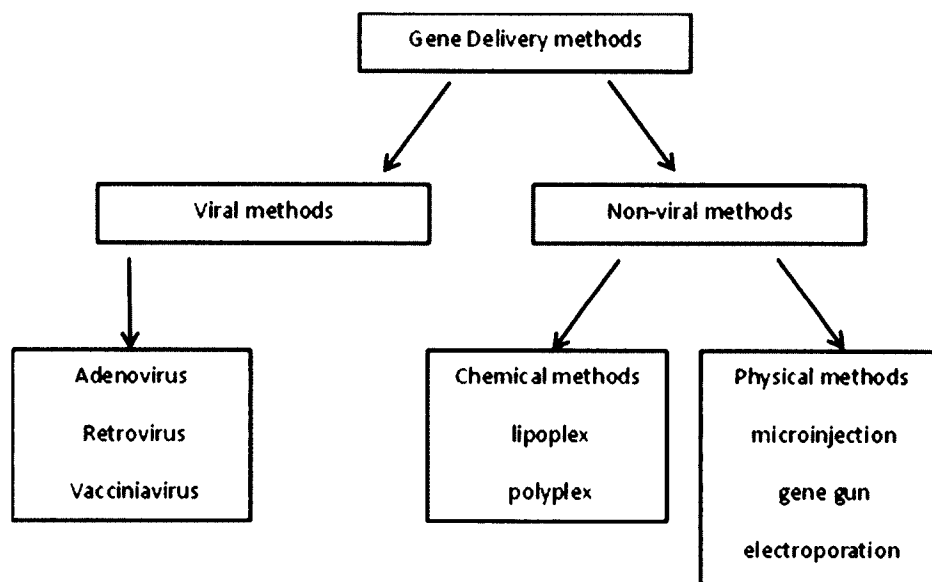


Figure 2-1: Gene delivery methods

Gene therapy generally requires a specific delivery of genes into the chromosome of a target cell. Treatment success rate is up to whether the agent or vector might be used for delivering therapeutic genes. Vector is a carrier of useful therapeutic gene. Vector has multiple functions, including avoidance degradation, promoting the gene into the target cells, and to ensure that the gene transcription is in the nucleus (Walther & Stein, 2000). In an ideal case, the gene delivery vectors should be efficient and safe. Safe transfer is described as a no-risk of introducing an infection or vector immune response is minimal (Walther & Stein, 2000; Peng, 1999).

A recent study suggests that some carriers have been well researched and developed. A common carrier has not been found to be used universally. So, how to choose a carrier that people need to consider many factors, such as the entire course of treatment, if a short-term or chronic treatment is better. As of spring 2014, there have been about 40 variants of the vectors have been evaluated or applied to gene therapy clinical trials (Wiley, 2013). These carriers are usually divided into two main categories: viral or non-viral methods.

2.1.1 Viral Vectors Gene Delivery

Viruses can be used to transfer genes into the target cells. Typically, working as the infection agent, the viruses have very high gene transfer efficiency. On the other hand, for the host organisms, viruses have very good adaptability. These advantages often make the viruses considered in gene therapy to transfer therapeutic genes into the targeted cells.

Although viruses differ in structures, almost all viruses have some universal feature. Such as, all viruses have a structure called capsid. Its role is used to save proteins

and glycoproteins of genetic material. There is a very interesting phenomenon: genetic material viruses carried is also varied, including the DNA, RNA, or even certain enzymes are also different. Therefore, it is necessary to identify the virus based on the characteristics of the composition of the virus genes. Furthermore, there are some particular viruses in their capsid surrounding a membrane structure. It can penetrate the host's cell membranes through membrane fusion (Campbell & Robinson, 1998; Coffin, 2014).

The working principle of the viral vector is to utilize the ability of the viruses that can enter the cells and the genetic material can be delivered into the nucleus. In general, after the operation by the researchers, the majority of the original viruses' genes are replaced by the therapeutic genes. Thus, the viruses injected into the vector do not cause the disease. Common viral vectors include: retrovirus, lentivirus, and adenovirus. Different viruses vectors vary in gene delivery efficiency. As a result, depending on the required characteristics of each case and the associated clinical studies, researchers can select a specific viral vector (Ginn *et al.*, 2013; Campbell & Robinson, 1998; Coffin, 2014; Nisole & Saib, 2014; Coffin, 1997; Cooray *et al.*, 2012; Sakuma *et al.*, 2012).

In earlier studies, the viral vector has been widely developed. However, in the actual treatment, there are usually more than one type of cells infected with the virus. Therefore, not only the targeted cells, but the healthy cells also present the risk of being infected. During therapy, once the vaccine or treatment fails, the validity of the use of viral vectors again proved to be difficult. On the other hand, the same viral vector is typically not used in various vaccines or gene therapies. Introducing a variety of viral vectors would increase the risk of infection. In addition, sometimes the patient's immune

system might cause gene therapy to fail eventually (Nayak & Herzog, 2009; Zhou *et al.*, 2004).

If the introduction of the virus is not accepted, there is another consideration. The smooth insertion of genetic material and transduction, effectively splitting the target cells to become one of the essential conditions of viral vectors. However, there are some cells that are highly resistant to retroviral infection and transduction in humans. On the other hand, in the copy process, transcriptional gene may be an over-expression, to produce beyond the desired amount of protein. Also, this situation will lead to harmful effects, such as inflammation or allergies. In addition, integrase enzyme is able to insert genetic material in the target cell genome at any point. This posed some problems. If the genetic material is inserted into the wrong position of the genome, gene mutation may occur, which has been demonstrated in clinical trials (Thrasher *et al.*, 2006; Urnov *et al.*, 2005).

2.1.2 Non-Viral Delivery Methods

In order to overcome the negative effects caused by viral vectors, non-viral gene vectors have been frequently used. Common forms of non-viral vectors for gene therapy are: plasmid DNA encoding of a transgene, transgenic, local or systemic such as injection into the blood vessel. In these processes, the expression yield of the desired therapeutic protein would treat the disease. Peripheral arterial occlusive disease (Comerota *et al.*, 2002), arthritis (Bloquel *et al.*, 2004) and cancer (Daugimont *et al.*, 2001) are the most popular non-viral gene therapy clinical application.

Non-viral delivery techniques offer cost-effective and less toxic alternatives to viral methods. Non-viral methods for transfection can be categorized into two groups, chemical and physical methods. Chemical methods of transfection include lipoplex and

polyplex. Unlike the viral transfection, chemical transfection is not limited by the size of the genetic payload. Physical methods involve creation of transient pores in the cell membrane using physical forces. The major current physical methods are microinjection, gene gun, and electroporation.

Using a plasmid vector is one of the many methods to insert therapeutic genes. Most commonly it occurs in bacteria and unicellular microorganism's plasmid, a small circular double stranded DNA molecule. In the biological world, organism keeps functioning by a plasmid gene delivery, such as antibiotics. In the world of bacteria, the plasmid can often be delivered by a non-breeding gene transfer. It happens frequently while genetic materials exchange between bacteria. For example, a plasmid containing genes to obtain the antibiotic resistance, by gene transfer, the gene can be used on the bacteria.

Natural and artificial plasmids now had been regarded as a basic tool of genetics and biotechnology. Plasmids normally used in the laboratory for small DNA and gene replication. Sometimes it also works as a method in the production of large-scale proteins. This technology is very mature; many plasmids have been fully commercialized.

Plasmid DNA may be used alone and expressed therapeutic gene. This feature was first discovered in an intramuscular injection. The plasmid DNA was used as a marker for validation and gene expression measurement (Wolff *et al.*, 1990). Reporter gene (marker gene) is a very effective method of marking. In recent clinical applications, this labeling method has been widely used in vascular disease. The principle is the expression of a therapeutic gene, which encodes for antigenic growth, basic fibroblast growth, or hepatocyte growth (Nikol *et al.*, 2008; Powell *et al.*, 2008).

Another active area of the plasmid DNA therapy lies in the development of genetic vaccines. There have been several already achieved approaches of plasmid DNA genetic vaccines in influenza, HIV and hepatitis C (Seaman *et al.*, 2005; Gudmundsdotter *et al.*, 2006; Sandstrom *et al.*, 2008). Using these genetic vaccines may reduce or limit gene transcription (Li & Huang, 2000). When the plasmid vector DNA goes into the nucleus of a target cell, the efficiency of DNA must be transcribed because of transgene expression and cell division is achieved. Introduction of therapeutic DNA into target cells will hold this function.

When an unrecognized substance enters the patient's body, his immune system would be activated. Affected immune system can be reduced by therapeutic efficacy. This effect is significant during recurring treatment. Therefore, before introducing of the vector, the protein purification process is necessary. In the commercial system, this step is usually achieved by separating the DNA vector. Therefore, the yield and purity of the antigen will cause problems. In treatment, it is often taking risks caused by antibody response. Furthermore, the size of the inserted DNA also has a requirement. It is usually 30-40 kb of base pairs (Del *et al.*, 1998; Vivian *et al.*, 2001; Pinto *et al.*, 2012).

2.1.3 Chemical Transfection Methods

Figure 2-2 shows the general chemical methods for gene delivery. Typically, genetic plasmids are mixed with polycation complex and delivered in to the target cells.

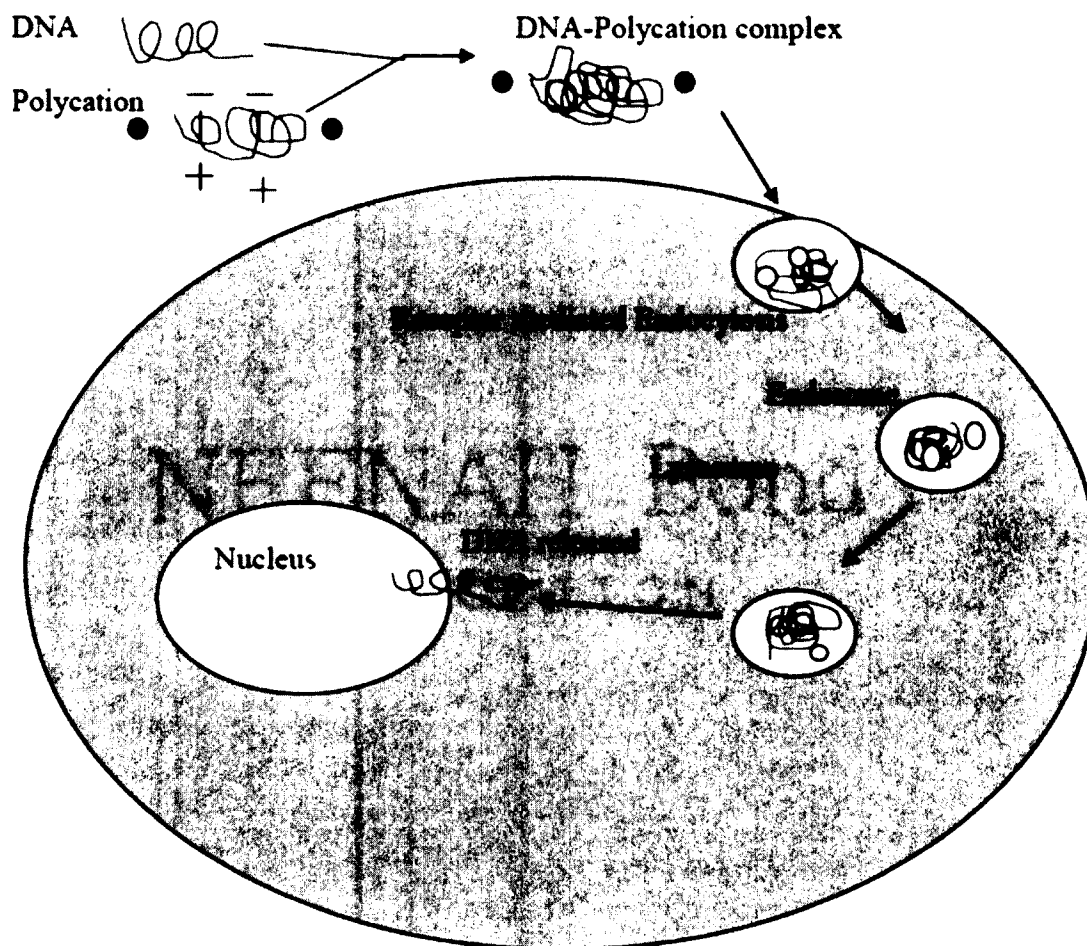


Figure 2-2: The schematic of the working principles of chemical transfection method.

2.1.3.1 Lipoplex. Lipoplex is a complex of cationic lipids with DNA. Lipoplex mediated DNA delivery was first introduced by Felgner in 1980 (Felgner *et al.*, 1987) and extensively explored thereafter for both *in vivo* and *in vitro* therapeutic probe delivery. Lipoplexes were synthesized through the electrostatic interactions between positively charged lipids and negatively charged DNA (Ma *et al.*, 2007). Early studies believed that DNA molecules enter cells when lipoplex is directly fused with cell plasma membrane. However, the recent studies showed that the DNA delivery by lipoplex mainly proceeded through endocytosis (Felgner *et al.*, 1987).

The transfection efficiency of lipoplex is low when compared to the viral vectors. Because of its advantages over viral vectors in terms of health risks, they still attract much attention for both *in vivo* and *in vitro* delivery investigations. Great efforts have been made to improve its delivery effectiveness (Zuhorn *et al.*, 2002; Jordan & Wurm, 2004; Davis, 2002).

2.1.3.2 Polyplex. The polyplex is a complex of cationic polymers with DNA (Yang & May, 2008). Like lipoplex, polyplex is regulated by ionic interactions between cationic polymers and DNA (How *et al.*, 2004). One big difference between polyplex and lipoplex lies on their different DNA release processes inside the cell cytoplasm. Polyplex made of DNA and polyethylenimine, chitosan, or trimethylchitosan have their own ways for endosome disruption (How *et al.*, 2004) compared to other vectors.

The use of polyplex has several advantages, such as low immune response, convenience for cell or tissue targeting, and no restriction on the size of the DNA to be transported. Moreover, it is very easy to produce polyplex with a large quantity (Ulasov *et al.*, 2011). In the past decades, the polyplex research has achieved very promising progress in both *in vivo* and *in vitro* gene delivery. Among the polyplexes, the polyethylenimine based polyplex was found to be one of the most efficient ones (Ulasov *et al.*, 2011). Their high density of amino groups results in efficient condensation of DNA and reasonable transfection in eukaryotic cells at physiological pH value (Vancha *et al.*, 2004).

2.1.4 Physical Transfection Methods

2.1.4.1 Biolistics (gene gun). Biolistics, also known as a gene gun, has been widely used for gene delivery. A Helios gun with a modified barrel is used to deliver

carrier particles over a wide area during biolistic transfection (O'Brien & Lummis, 2011). Obviously, the barrel could cause severe damage to cells or tissues (Uchida *et al.*, 2009). The most commonly used carrier particle size is $\sim 1 \mu\text{m}$. The biolistic damage can be reduced by choosing smaller particles to carry DNA (Cui & Mumper, 2003). It has been reported that particles of 100-180 nm in size had shown successful transfection (O'Brien & Lummis, 2011). Even though the gene gun can successfully deliver naked DNA inside cells, its efficiency is quite low when compared to other delivery methods. In addition, DNA molecules inside the cells are often hindered by nuclease enzyme and further degraded before successful transfection (Mintzer & Simanek, 2009).

2.1.4.2 Microinjection. Microinjection is the process which uses micropipettes for DNA delivery to cells (Ansorge & Pepperkok, 1988). Microinjection can deliver DNA directly to the cell cytoplasm or the nuclei. However, the process was very time consuming and labor intensive. With the assistance of computer controlled systems, microinjection could be done faster (Ansorge & Pepperkok, 1988), although still slow as compared to other approaches.

2.1.4.3 Electroporation. In 1982, Neumann and Zimmermann proposed an electrically mediated gene delivery system, i.e. electroporation. Nowadays, it has become one of the most powerful and effective techniques for the introduction of DNA into the cells (Kim *et al.*, 2008). Figure 2-3 shows an overview of electroporation. In electroporation, an electric pulse is applied, resulting in the formation of pores on the cell membrane which facilitates the delivery of genes into the cells (Kim *et al.*, 2008). Both electroporation conditions and the cell properties have a significant effect on the delivery

efficiency (Olofsson *et al.*, 2007). Depending on the electroporation conditions, the pores can be transient, short-lived or long lived (Agarwal *et al.*, 2009).

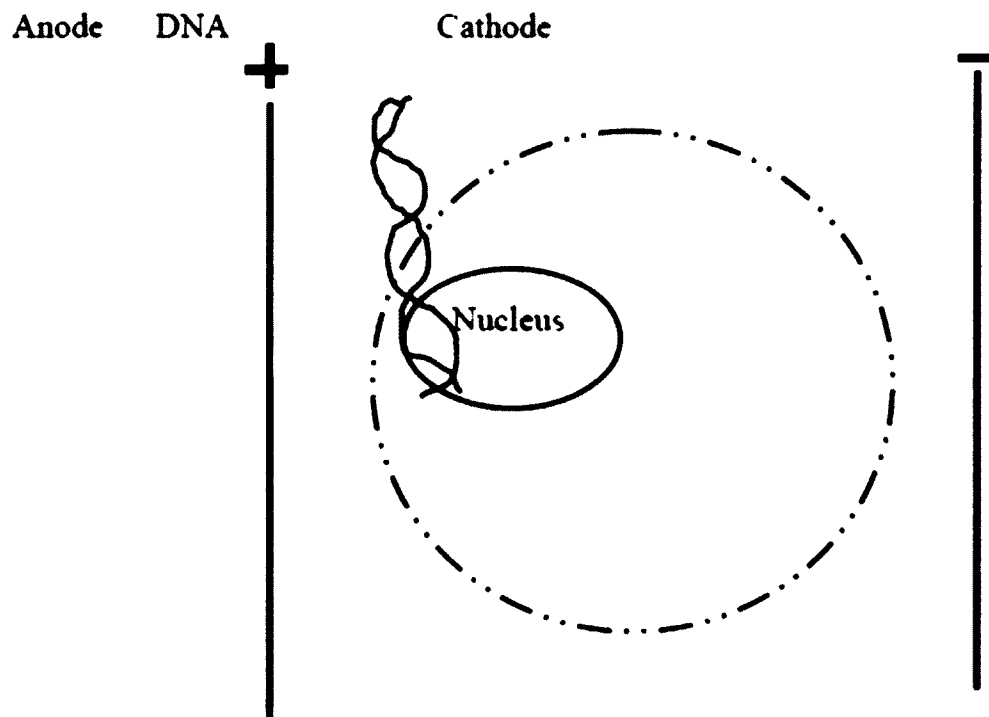


Figure 2-3: Schematic of the working principles of electroporation.

Two areas of electroporation studies are focused on gene delivery: bulk electroporation and single cell electroporation (Agarwal *et al.*, 2009). A uniform electric field is involved in bulk electroporation (BE). A large number of cells will be permeabilized at the same time (Teissie *et al.*, 2005). On the other hand, only one single cell is involved in single cell electroporation (SCE) at a time. Usually, it happens in a micro-scaled device (Teissie *et al.*, 2005).

2.2 Electroporation

Electroporation is a biophysical phenomenon by applying an electrical field to the cells or tissues in order to increase cell membrane permeability so that it will achieve the chemicals, drugs, DNA, and other macromolecules introduced into the interior of the cells (Neumann *et al.*, 1982). Typically, the cells and plasmids would be mixed together, after the electroporation, and the plasmids can be within the cells. After this process, the cells will be cultured in the medium. Breed until they split again, creating new cells containing the plasmids information replication (Neumann *et al.*, 1982; Sugar & Neumann, 1984). Electroporation is a very efficient method for introducing foreign genes into the tissue cells, especially mammalian cells.

2.2.1 Theory

Dr. Weaver had given a standard operation protocol of electroporation in 2000.

1. Cells or tissues would be exposed in a high intensity electrical field. The duration was from nanosecond to millisecond.
2. The cell membrane would be charged.
3. The molecular structures within the cell membrane would localize reorganized.
4. Transient pores would format.
5. Gene delivery and mass exchange would achieve through the transient pores.
6. Cell membrane recovery (Weaver, 2000).

Cell membrane has a semi-permeable Bilayer structure. Molecules of water and small soluble molecular can be freely transmitted, while macromolecules such as nucleic

acids will not be allowed to pass through. Membranes can be viewed as separate and outside the boundaries of the cell conductive electrolyte. When an external electric field was applied, the cell membrane would perform as a capacitor being charged. Equation 1 describes the transmembrane potential $\Delta V_m(t)$ induced across the cell membrane when an externally electric field E_{ext} is applied:

$$\Delta V_m(t) = -f E_{ext} r \cos \varphi [1 - e^{-\frac{t}{\tau}}], \quad \text{Equation 1}$$

where f represents the form factor of the cell.

r represents the radius of the cell.

φ is the angle between the membrane site and the direction of the applied field.

t is the time after the electric pulse onset.

τ is the membrane charging time constant (Bernhardt & Pauly, 1973; J. M. Escoffre *et al.*, 2009; Neumann, 1992).

Equation 2 describes the impact of the cell on the electric field distribution on the form factor f . The external solution σ_0 , cell interior σ_i , the cell membrane σ_m and thickness of the membrane d defined the form factor. For a spherical cell, when $\sigma_m \ll \sigma_0$ and σ_i (Neumann, 1992):

$$f = [1 + \frac{\sigma_m(2 + \frac{\sigma_i}{\sigma_0})}{\frac{2\sigma_i d}{r}}]^{-1}. \quad \text{Equation 2}$$

Sometimes due to the applied electric field at that site and resting membrane potential ΔV_{res} , the transmembrane potential can be the sum of the induced potential and presented as Equation 3 (Mehrlé *et al.*, 1992):

$$\Delta V_c = f E_c r \cos \varphi [1 - e^{-\frac{t}{\tau}}] + \Delta V_{res}, \quad \text{Equation 3}$$

where ΔV_c is the transmembrane potential of the cell exceeding a certain threshold.

According to the research data, usually the value of ΔV_c is in the range of 0.2 – 0.3 V (Gabriel & Teissie, 1997; Teissie & Rols, 1993). ΔV_c is important, for it works as a dielectric breakdown of the membrane. It means it is the power for forming aqueous pores (Hibino *et al.*, 1991; Weaver, 2003; Zimmermann *et al.*, 1974). Therefore, from Equation 3, another critical electric field is necessary for electroporation which is Equation 4:

$$E_c = \frac{\Delta V_c - \Delta V_{res}}{fr \cos \varphi [1 - e^{-\frac{t}{\tau}}]} . \quad \text{Equation 4}$$

Equation 4 tells us if an electric field E_c is applied, electroporation would process for φ , which is close to 0 and π . This means the aqueous pores will show up on the membrane facing the electrodes.

2.2.2 Physical Mechanism

Under normal circumstances, macromolecules such as DNA would not go through the hydrophobic bilayer membrane by diffusion. Electroporation techniques can highly charge macromolecules and take them from one side to the other side of the membrane. For the mechanism concerning an aqueous environment, it is an operation of opening the nanoscale holes on the bilayer structure. For phenomenon, electroporation and dielectric breakdown are very similar. By studying the mechanism's action, they are completely different. The dielectric breakdown would ionize the target material, thereby forming an electrically conductive path. In this process, the nature of the material produced a chemical change. However, electroporation is just the opposite. The chemical changes do not occur, and it is purely a physical displacement by pore formation on the lipid molecules as shown in Figure 2-4.

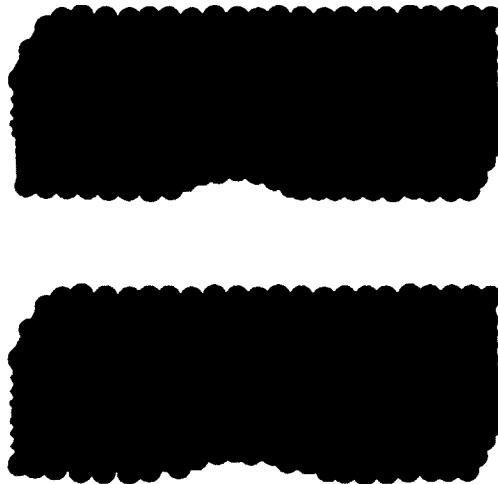


Figure 2-4: Cell membrane lipids arrangement in hydrophobic (top) and hydrophilic (bottom) pore.

(https://en.wikipedia.org/wiki/Electroporation#/media/File:Pore_schema.svg)

As described previously, while an electrical pulse is applied, typical parameters would be 300-400 mV across the membrane (Weaver *et al.*, 1996). Upon the existence of potential differences, the performance of the cell membrane is more like a capacitor. With the accumulation of a charge, when the electric field strength reaches a critical value, the cell membrane will rearrange. Then a hydrophilic interface will be created by the bending of lipid heads. Lastly, these conductive pores are going to face polar fates: reseal and heal or expand and rupture. The key factor to determine their fate is the critical defect size (Joshi & Schoenbach, 2000). To tell if the pores exceed the limitation of critical defect size, the applied electric field, local mechanical stress, and bilayer edge energy are considered effective.

2.2.3 Effect Factors in Electroporation

Physical mechanism explains the working principle. However, under real lab or clinical conditions, besides the electric properties, there are still several factors which

might bring affections when performing an electroporation. These factors are listed as follows:

1. Cell size. According to Equation 1, when plasmids permeabilization is achieved, a larger size cell requires a relatively larger transmembrane potential. Thus, it is necessary to provide a different treatment for various sizes of the cells. In the actual case, when the cell size distribution is very wide (eg, Ehrlich ascites cells) if specific treatment is not provided, it is difficult to get good results. Furthermore, it is conceivable that when electroporation is applied on non-spherical shaped cells, the cells orientation is also very important.

2. Temperature. It has been proven that it is good for the cell closure process to operate at a relative lower temperature. Also, after plasmids transfection, cell membrane resealing is in direct proportion to the temperature (Kinosita & Tsong, 1977b). More specifically, in gene delivery, lower temperature while transient pores format and higher temperature in an incubator for cell recovery had a good effect on transfection efficiency and cell viability (Rols *et al.* 1994).

3. Post pulse operation. Since the cells would be exposed in the electric field and the membrane would be recognized, cells suffer and are vulnerable at the moment when the transient pores form. Scientists have suggested that 15 min is a good period of time for cell resealing after the electroporation (Gehl *et al.*, 1998). Also, after the cells pipet into the culturing petri dishes to avoid any manipulation is good for cell viability (Zerbib *et al.*, 1985).

4. Electrodes material. Electroporation process requires a short duration pulse. Good conductive metal are considered as electrodes material. Aluminum is the

most popular choice. Usually, there would not be a problem for the short pulse. However, along with the requirement of growth, the release of the metal is a concern in a long duration pulse or a multiple pulses electroporation (Rols *et al.*, 1994). Both the vibration of the PH value and the release of metal ion would decrease the cells' viability and transfection efficiency. Inert materials are highly recommended if working as an electrode.

5. Medium. Since the plasmids, genes or any particles are in the environment of complicated chemicals during the electroporation, it is wise to be careful with the medium composition. Some researchers preferred the low conductivity media. Also, the careful usage of calcium is necessary to avoid a sudden high intracellular level of the electrolyte (Rols *et al.*, 1994). However, the research on the affection of medium composition is still under development. The opinions are not identical. Some authors advocate a right amount of calcium or magnesium in the buffer would increase cell viability and transfection efficiency (Neumann *et al.*, 1996).

Additionally, heating during the electroporation has been proven to be not a problem, which is always a concern. In standard electroporation conditions (BTX cuvette), the temperature change caused by generated heating is less than 1°C (Bhatt *et al.*, 1990).

2.2.4 *In Vivo* Electroporation

In vivo electroporation has been introduced and has many applications in gene therapy. A pair of plates or needles usually works as electrodes. Organs have been carried out for *in vivo* drug and gene delivery through electroporation. Two important features are discussed most frequently on *in vivo* electroporation.

2.2.4.1 Electric field distribution. When performing an *in vitro* electroporation, it is obvious that needles electrodes would be more convenient during operation. Compared with the electric field of the plate electrodes, the distribution of the electric field of the needles electrodes play a critical role. Since there is not a uniform distribution of the electric field and usually the field strength is in the scale of kilovolts per cm, it is much dangerous to operate *in vivo* electroporation on the body.

2.2.4.2 Vascular effects. *In vivo* electroporation, area covered by the scope of the electric pulse will produce a phenomenon called hypoperfusion. This is mainly due to two reasons. One is because of the reflex contraction of vascular resistance in the range of an electric field. The other is the inter impact of interstitial edema and intravascular lactone structure due to the pressure drop caused by the projection effect (Gehl *et al.*, 2002). Reflex contraction of the artery will continue about 1-2 minutes. During this period, interstitial edema will disappear because of the reorganization of the cell membrane. It is worth mentioning that the vascular effect of cancer treatment seems particularly prominent, and is considered advantageous in cancer treatment (Sersa *et al.*, 1999; Gehl & Geertsen, 2000; Cemazar *et al.*, 2001).

2.2.5 In Vitro Electroporation

In vitro gene delivery involves performing the experiments in a controlled environment outside a living organism. This type of research aims at describing the effects of an experimental variable on a subset of an organism's constituent parts. Currently, electroporation is one of the most popular research tools used for gene transfer into mammalian cells *in vitro*. Figure 2-5 briefly describes the *in vitro* electroporation process.

In vitro Electroporation

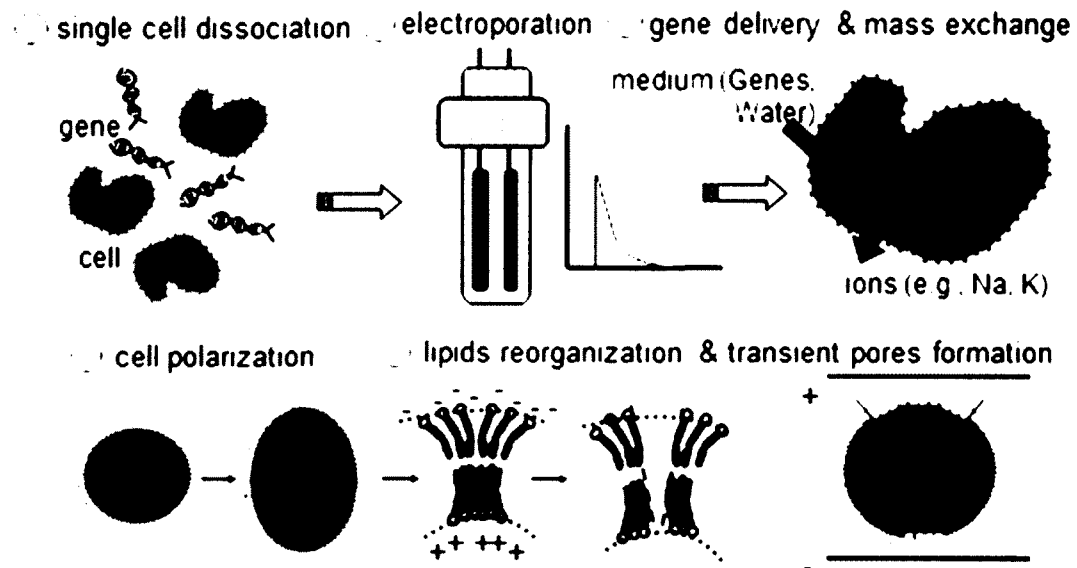


Figure 2-5: *In vitro* electroporation processes.

Generally, cells are mixed with genetic plasmids and suspended in the appropriate medium. After being loaded between two electrodes, a typical electroporation process will be experienced. After the cell polarization and genetic plasmids and mass exchange as described previously, cells will be collected and cultured for further observation or treatment.

2.2.6 Laboratory Practice

The electroporation device is named electroporator. Components include a pulse generator, electroporation cuvettes and cuvette holder. Figure 2-6 showed the pulse generator, electroporation cuvettes and cuvette holder used in the experiment. A glass or plastic cuvette has two aluminum electrodes in a parallel manner on its sides. For electroporation operation, the voltage and capacitance will be set. The cell suspended in

medium will be pipetted into the cuvette. Electric pulse will be given after the cuvette is inserted into the holder.

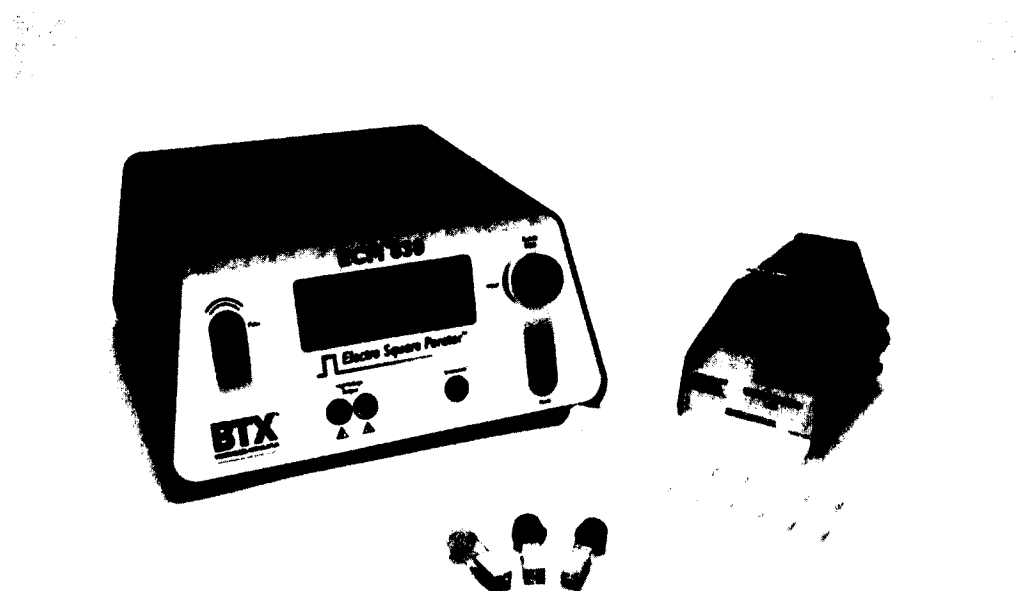


Figure 2-6: Electroporator BTX 830 (<https://www.btxonline.com/ecm-830-square-wave-electroporation-system/>).

2.2.1 Electroporation Cuvettes Electrodes Material

As they directly contact with biological samples, the choice of electrodes is extremely important in electroporation. Materials change along with the development of electroporation. Initially, aluminum or stainless-steel was chosen. Since the solution worked in the environment, metal ion might be released. It is seen as harmful for cell viability. The conventional electroporator uses platinum, gold or inert metal coated material as the electrodes. The cost of manufacturing or the shedding of the coated material turns into another focused issue. Recently, due to the good bio-compatibility and low manufacture expense, conductive carbon material becomes a new hot research topic.

High molecular weight organic material carbonization process is the pathway to fabricate conductive carbon material. Carbonization is the process by which solid residues with a high content of carbon are obtained from organic materials. Through the pyrolysis process, polymer materials will decompose and gain new desired properties. Different precursors to glass-like carbon exist. The degree of shrinkage and carbon yield, the ratio of the weight of carbon to the weight of the original polymer sample, varies depending on the choice.

2.3 Carbonization

2.3.1 Glass-Like Carbon

Glass-like carbon is obtained from pyrolysis, or derived from the thermal degradation process. Since it is an organic polymer material, inert atmosphere during pyrolysis is a necessary condition. After carbonization, the product is carbon and it is generally smooth, glossy and exhibits a conchoidal fracture. It is referred to as glass-like carbon. As an allotrope of carbon, glass-like carbon has a very high isotropic in its structure and physical properties while liquid and gas permeability is very low. As for its crystal structure, until now, scientists have different opinions, but the most widely accepted model is the tangles and ribbon wrinkle aromatic molecules randomly cross-linked carbon - carbon covalent bond (Jenkins & Kawamura, 1971; Pesin, 2002). Like some non-continuous graphene fragments, this structure reflects the thermosetting resins, usually used as structural features of the carbon precursor.

In addition, this model can also explain the most characteristic glass-like carbon by existing detection means such as its impermeability, brittle and conductivity (Jenkins & Kawamura, 1971; Pesin, 2002; Jenkins *et al.*, 1972; Kakinoki, 1965). Here, we want to

emphasize one thing even though we still cannot describe the exact structure of glass-like carbon, and its structure is called glassy and amorphous, but it is not an amorphous carbon. The International Union of Pure and Applied Physics (IUPAC) has defined the amorphous carbon as carbon materials with localized π -electrons (Fitzer *et al.*, 1995).

Glass-like carbon has become popular because it has a very reliable performance. With strong acids (sulfuric acid, hydrofluoric acid) and a corrosive chemical attack, such as bromine, it showed significant inertia. This point indicates that it is very stable. It may be oxidized in the presence of oxygen under high temperature environment; however, tests showed that the oxidation rate compared to other carbon allotropes are much lower. From electrochemical point of view, it even has a wider stability window than platinum and gold, which makes it a very suitable alternative to platinum and gold and other precious metals in electrochemical experiments (Zittel & Miller, 1965; Linde *et al.*, 1980).

In the mechanical properties, glass-like carbon has the same outstanding performance. The Young's modulus range between 10 and 40 GPa and features 6-7 Mohs, a value comparable to the hardness of quartz, and its density stays between 1.4 and 1.5 g/cm³, compared to graphite of 2.3 g/cm³ (Yamada & Sato, 1962). This slight decrease drives scientists to speculate that perhaps there are some closed pores in the internal structure of glass-like carbon. X-ray diffraction studies proved this speculation; there is a very small (about 50 Å) pore structure inside the glass-like carbon (Rothwell, 1968; McFeely *et al.*, 1974). In thermodynamics, the thermal expansion coefficient of the glass-like carbon is $2.2\text{-}3.2 \times 10^{-6}/\text{K}$, similar to some of the borosilicate glass. It is also considered to be thermally inert. Its thermal conductivity is about one tenth of the value

of the typical graphite (Pesin, 2002; Pesin & Baitinger, 2002; Yoshida *et al.*, 1991; Spain, 1981; Ranganathan *et al.*, 2000).

2.3.2 Temperature and Pressure Factors for Carbonization

The process of carbonization can be seen as the elimination process of different hydrocarbons and gases, as shown in Figure 2-7. Most of these reactions are closely related to the temperature and pressure. Modifying temperature and pressure is the key point to have a good control of the carbonization process. The application of pressure in certain temperatures can prevent the carbon atom from being released during the gas phase (particularly hydrocarbon gases). Detaining carbon atom in the final products can improve the carbonization yield rate. Mechanical and chemical properties such as solubility, viscosity, and density can also be modified. In addition, carbonization under pressure is also expected on the possibility of controlling the phase change on carbon allotrope to obtain specific particle morphology of the resultant carbons.

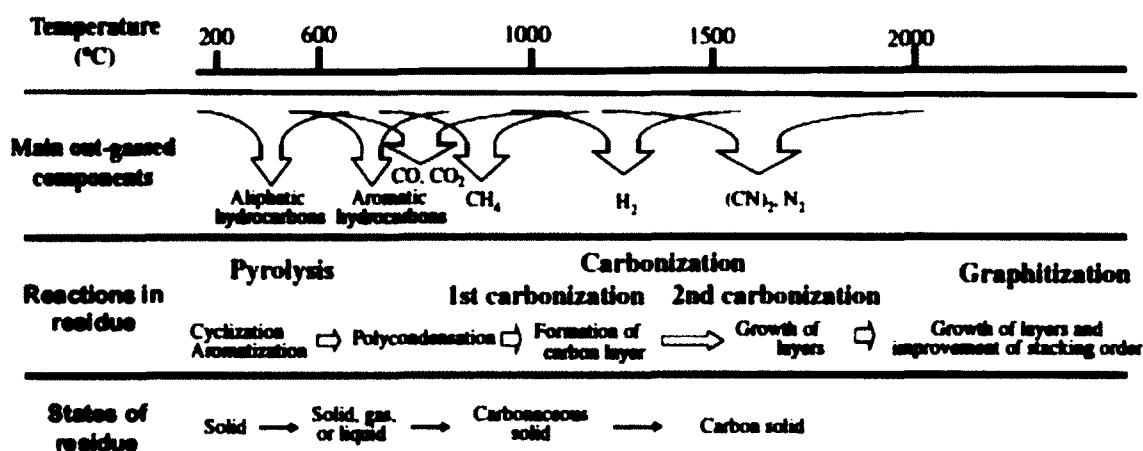


Figure 2-2: Carbonization process [book: Advanced Materials Science and Engineering of Carbon]

Carbonization under pressure has been classified into three routes: carbonization under built-up pressure by decomposition gases from carbon precursors, hydrothermal conditions, and the reduction of CO₂ under pressure. Under pressure built up by the decomposition gases from carbon precursors, such as pitches, the acceleration of the formation of mesosphere spheres was confirmed and their coalescence was suppressed at a temperature a little higher than under atmospheric pressure, even though their coalescence could not be inhibited. A marked increase in carbonization yield was observed on all precursors, suggesting that the evolution of hydrocarbon gases from the organic precursors was strongly suppressed during pyrolysis and carbonization. However, it has to be pointed out that an efficient increase in carbonization yield was possible only in the sealed capsule (closed system) where all decomposition gases were included in the capsule. When the capsule was open, even in the autoclave, a marked improvement in carbonization yield was not observed in most cases because the decomposition gases were deposited on low-temperature parts of the autoclave. In order to get carbon materials from polyethylene, which does not give any carbon residues under atmospheric pressure, the whole of the autoclave itself had to be heated to a high temperature. Different carbon materials, carbon nanotubes, fullerenes, diamond, and carbons with various morphologies, were often formed as a mixture. However, carbon materials with spherical morphology (carbon spheres) were synthesized without appreciable amounts of other forms of carbon by selecting the conditions of pressure carbonization. On the basis of the results published, the formation conditions of single carbon spheres with different nanotextures are discussed here with relation to the temperature-pressure conditions and also the chemical composition of the precursors.

The pressure and temperature ranges for carbonization process are shown in Figure 2-8. The spherical morphology of carbon materials has been reviewed, focusing on their nano texture and preparation processes (Davis *et al.*, 2004). Carbonization of different organic precursors in the atmosphere of their decomposition gases has been carried out in relatively limited ranges of temperature (500-700°C) and pressure (50-250 MPa). In supercritical water, carbon spheres were obtained from benzene at a slightly lower temperature of 400°C by adding a small amount of H_2O_2 as an initiator of radical reactions. Under hydrothermal conditions, pressure carbonization of saccharides occurred at an even lower temperature of 200°C to give carbon spheres that still contained hydrogen and oxygen, as shown by the H/C of around 0.7-0.8 and the O/C of about 0.3-0.4.

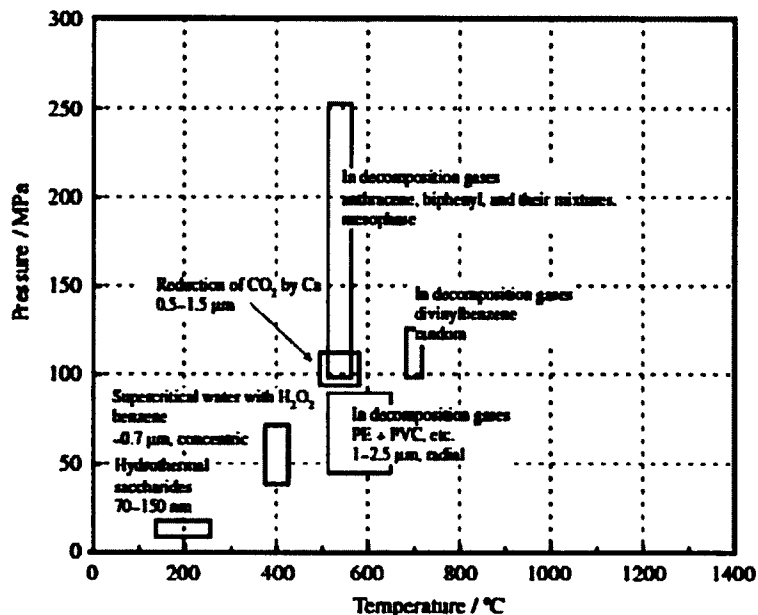


Figure 2-8: Pressure-temperature Conditions for the Formation of Carbon Spheres from Different Precursors. [Book: Advanced Materials Science and Engineering of Carbon]

2.3.3 Composition of Precursors

The carbonization behavior of the carbon precursor changes under pressure and the resultant carbon is different in structure, properties, and even particle morphology from that obtained without pressure. The departure of various hydrocarbons and carbon oxides results in the loss of carbon atoms from the precursor; in other words, it lowers the carbonization yield.

CHAPTER 3

MICRO-PILLAR ARRAY ELECTROPORATION TO ENHANCE GENE DELIVERY TO MAMMALIAN CELLS

3.1 Introduction

A number of new systems with micro-/nanoscale features have recently been introduced to tackle the high-voltage issues through closely patterning electrode pairs and/or sophisticatedly focusing the electric pulses (Kim *et al.*, 2007; Huang *et al.*, 2014). The rationale behind these microelectroporation concepts comes from the fact that when the two electrodes are brought very close, e.g. $\sim 20\text{ }\mu\text{m}$, a low voltage (1-2 V) is sufficient to generate pulses with a high enough field strength (e.g., 500-1000 V/cm) required for successful cell electroporation. The micro/nanoscale pathways that stand between electrodes could further concentrate the applied electric pulses (Wang *et al.*, 2008). These micro-devices opened new routes towards the elimination of many induced apoptosis of electroporation and indeed offer several advantages over commercial systems (Wang & Lee, 2013).

However, most of these micro-electroporation systems still ignore the local electrical variations on individual cells of a large population, leaving many uncontrollable factors similar to that in the bulk electroporation systems. For example, according to Equation 1, the needed transmembrane potential is not only related to the field strength,

but also the size and electrical properties of the treated cells. Unfortunately, this issue did not attract enough attentions in the past due to the lack of simple but effective tools.

In this chapter, we propose a much more efficient gene delivery method, called the Micro-pillar Array Electroporation (MAE) approach to accomplish size specific electroporation. We loaded cells on a pre-treated micro-pillar array structure. By placing a piece of conductive plain plate surface on the top, we applied a low voltage pulse to achieve temporarily dielectric breakdown of the cell membrane and gene delivery. We observed a significant improvement of gene transfection with minimal cell damage.

Unlike some pioneer work in which a few micro- or nanoscale pillar electrodes were used as the replacement of capillary electrodes to monitor the intracellular electrical signals of single or a few cells for electrophysiology study (i.e., SCE) (Spira & Hai, 2013; Xie *et al.*, 2012), this new MAE setup utilizes well-patterned, large-scale (center-meter size) micropillar array to achieve size specific treatment to cells of a large population (i.e., BE) for the efficient uptake of an exogenous payload. In fact, it works like many SCE units that are carried out in parallel with no need for cell positioning. As every cell electroporation becomes representative, the cellular uptake dynamics study on individual cells in MAE might provide useful information in electroporation protocol identification for unknown cell sources (e.g., primary cells). Therefore, it has the potential to facilitate the communication between SCE (for cell electrophysiology study) and BE (for large scale gene transfection tests) to leverage the current electroporation-based delivery technology. In this contribution, we evaluated its transfection enhancement of reporter genes (pMaxGFP and gWizLuc). Both anchor cells (e.g., NIH

3T3 and A549 cells) and suspension cells (e.g., K562 cells) were tested to demonstrate its broad effectiveness.

3.2 Materials and Methods

3.2.1 Materials and Reagents

DNA plasmids with gWiz Luciferase and pMax GFP reporter genes were purchased from Aldevron, Inc. and Lonza, Inc., respectively. All other chemicals were purchased from Sigma-Aldrich and the cell culture reagents were purchased from Life Technologies (Carlsbad, CA) unless specified.

3.2.2 Cell Culture

NIH/3T3 cells (ATCC, CRL-1658) were routinely grown and maintained in high glucose DMEM supplemented with 10% newborn calf serum (NCS), 1% penicillin and streptomycin, 1% L-glutamine, and 1% sodium pyruvate. K562 cells (ATCC, CCL-243) and A549 (ATCC, CCL-185) were cultured in RPMI 1640 supplemented with 10% NCS, 100 µg/mL penicillin, 100 µg/mL streptomycin, and 100 µg/mL L-glutamine. All cultures were maintained at 37°C with 5% CO₂ and 100% relative humidity.

3.2.3 Micropillar Array Electrode Fabrication

Micropillar arrays were fabricated by BioMEMS technologies. Briefly, SU-8 photoresist was patterned on a Si (100) wafer via photolithography. Micropillars of 2 or 6 µm in diameter and a pitch size of 2 µm (Figure 3-2b) were defined in several 12-mm disc regions (Figure 3-1).

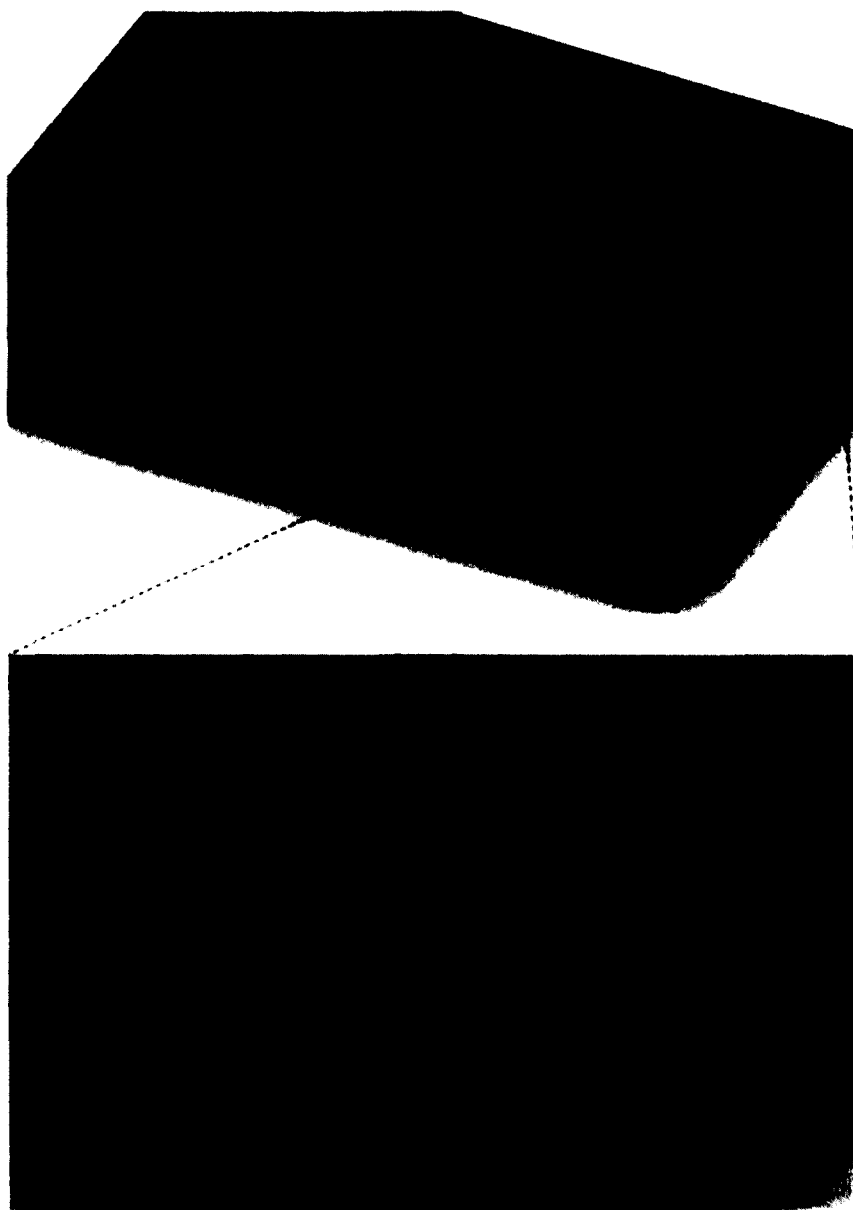


Figure 3-1: Schematic of the micropillar array electrodes integrated with the SU-8 spacer and connecting the microchannel in MAE.

The actual height of the finished micropillars was found to be $\sim 4\ \mu\text{m}$. Conductive micropillars were made by sputter coating with gold (for gold coated micropillar electrode). A second SU-8 layer was then applied to cover the non-electrode area and define two 100- μm long, 20- μm wide connecting channels to the micropillar array chamber, one on each side (Figure 3-1). When the cell solution drop is squeezed to fill

the entire micropillar chamber, the extra solution is guided into these channels and push air out to avoid potential bubble trapping issues during the chamber closure. Ball wire bonding was applied to connect the microelectrodes to wires that were plugged to a pulse generator (BTX 830).

3.2.4 Measurement of the Gap Size of Electrodes in MAE

As the sealing of the liquid chamber between the two electrodes in the MAE system and “Au plain plate” systems was done by a PDMS gasket, some deformation occurred when the top micropillar electrode was firmly pressed down for closure. Therefore, the actual gap size between the two electrodes was smaller than the sum of the measured thickness of the epoxy spacer (10 μm) and the PDMS gasket (200 μm). To find out the actual distance between the two electrodes, we measured the amount of excess liquid in the connecting channels that was squeezed out of the liquid chamber when the two plates were closed (see Figure 3-2). The actual gap size was then calculated based on the total volume of the loaded cell solution and the dimensions of the liquid chamber and the connecting channels:

$$\begin{aligned} V_{\text{total cell solution}} &= V_{\text{cell solution in liquid chamber}} + V_{\text{cell solution in connecting channel}} \\ &= \pi D^2 H / 4 + 2WLH = (\pi D^2 / 4 + 2WL)H \end{aligned} \quad , \text{Equation 5}$$

where D is the diameter of the liquid chamber, W is the width of the connecting channel, L is the length of the liquid connecting the channel, and H is the height of the gap between the two electrodes (Figure 3-2). The gap size, H, is then calculated by:

$$H = \frac{V_{\text{total cell solution}}}{\pi D^2 / 4 + 2WL} \quad \text{Equation 6}$$

3.2.5 Device Assembling

In MAE, cells will be sandwiched between a plain plate electrode and a plate electrode composed of thousands of micropillars in a well-patterned array format. In this way, the number of micropillars in each cell varies with its membrane surface area, or the size of the cells, as schematically shown in Figure 3-2.

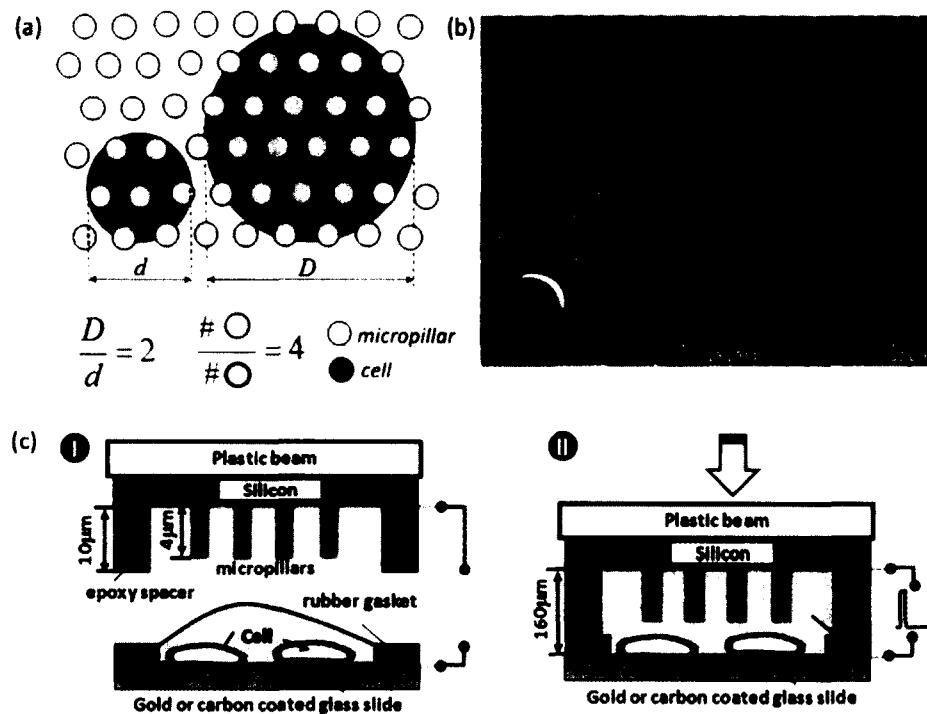


Figure 3-2: The working principle of the micropillar array electroporation (MAE). (a) Schematic of the cell size-specific treatment mechanism (large cells face more micropillars with each providing focused electric pulse during electroporation); (b) a SEM image of 2-μm micropillars; (c) schematic illustration of MAE operation.

In other words, larger cells likely receive more electroporation locations and area, which means more transient pores are created on their cell membrane with each smaller pore. Such size dependent pore formation mechanism is hardly affected by the random dispersion fact of cells as micro-pillars are configured in a well-patterned large array.

3.2.6 Electroporation Setup and Process

Cells were first centrifuged and re-suspended in fresh OPTI-MEM I (a serum free medium) at a density of 0.5×10^6 cells/ml. Plasmid DNA (pGFP or pLuc) of 10 μ g was then added to make the electroporation sample solution. In MAE electroporation (Figure 3-2c), a piece of gold or carbon coated plate electrode with a PDMS gasket of 200 μ m in height was first mounted on a mini mechanic press. One drop of cell solution (20 μ L) was then loaded into the formed liquid holding chamber. The micropillar array electrode, mounted on the other plate of the press, was loaded down to squeeze the liquid drop until the edge of the pre-defined SU-8 spacer (\sim 10 μ m) surrounding the micropillars firmly touched the PDMS gasket to seal the liquid chamber. The SU-8 spacer protects micropillars from destruction and controls the gap between the two electrodes of MAE. A single, 10-ms electric pulse of 10V was then applied across the two electrodes for electroporation. For comparison, standard electroporation was also done using a commercial BTX system (ECM 830, Harvard Apparatus). Samples of 100 μ L each were loaded into 2-mm electroporation cuvettes and a standard electroporation protocol (125 V, single 10-ms pulse) was applied. As the measured gap size between the two electrodes of MAE system is \sim 160 μ m, this is designated to ensure that the overall electric field strengths are the same (625 V/cm) in all three systems. After treatment, cells were transferred to 6-well plates and cultured for another 24 hours and then harvested for analysis.

3.2.7 Transfection Efficiency and Cell Viability

The expression of pGFP plasmids was evaluated both qualitatively by visualizing cells with green fluorescence within some representative areas under an inverted

fluorescence microscope (Olympus, Japan) and quantitatively by counting cells using an Agilent 2100 Bioanalyzer (Agilent Technologies, Santa Clara, CA). The fluorescence intensity of GFP was measured using the Cell Assay Module with live cells stained with carboxy-naphthofluorescein (CBNF). The results were analyzed with Agilent 2100 Expert Software and 500-1,500 events were counted for each sample. The transfection efficiency of pGFP is defined as the number of cells emitting fluorescence signal to the total number of cells in a sample (gated fluorescence signal of GFP). The Luciferase expression was quantified by One-Glo™ Luciferase assay system (Promega, Madison, WI). One-Glo™ reagent of 100 μ L was added to the cell growth medium of 100 μ L in 96-well plate. Luminescence was measured with a plate reader (FLUOstar OPTIMA, BMG LABTECH, Germany) after 10 min incubation at room temperature for complete cell lysis. The transfection efficiency of pLuc is presented as the luminescence of the total live cells in a sample.

The cell viability was evaluated by an MTS cell proliferation assay (Promega, Madison, WI). Briefly, the cells in 100 μ L/well of the medium were transferred to a 96-well plate and incubated. CellTiter 96 AQueous One solution (Promega, Madison, WI) of 20 μ L was added to each well and all samples were incubated at 37°C for another 4 hours. Absorbance was measured at 492 nm on an automated plate reader (Elx 800, Biotek, VT). Data points were represented as the mean \pm standard deviation (SD) of triplicates, unless otherwise indicated. The cell viability is calculated as the ratio of light absorbance of an electroporated cell sample to that of the negative control cell sample in MTS assay 24 hours post electroporation.

3.3 Simulation on the Electric Field of MAE

COMSOL (Mathworks, MA) was used to calculate the electric field in MAE based on a finite-element method (FEM). We considered an axial symmetric model with one micropillar (2 or 6 μm in diameter) and a single cell ($d = 16 \mu\text{m}$) in the computation domain ($35 \mu\text{m} \times 21 \mu\text{m}$). An electric field ($E = 625 \text{ V/cm}$) was assigned across the top and bottom of the computation domain whose right side boundary was set as the insulated wall. The cell was placed at the center of the left side boundary (the symmetrical axis) and a three-layer cell model, divided as the external medium, the cell membrane (5 nm in thickness), and the cell cytoplasm, was setup (Stewart *et al.*, 2005; Fei *et al.*, 2010). A gold micropillar was placed at the top of the cell, 0.5 μm and 1.0 μm away from the cell and the symmetrical axis, respectively. With a pitch size of 2 μm , cell membrane deformation in the gap of the micropillars seems essential (Kulangara *et al.*, 2012). Therefore, a quarter-circle raised arch (with a radius of 0.5 μm) was created on the cell membrane close to the micropillar to mimic its deformation. Detailed model dimensions and mesh setup are illustrated in Figure 3-3. The electric potential distribution around the micropillar and the cell was calculated. In this three-layer cell model, the electrical conductivity of the buffer, the cytoplasm, the membrane, and the gold-coated micropillar was set as 0.8, 0.2, 5×10^{-7} , and $4 \times 10^7 \text{ S/m}$, respectively.

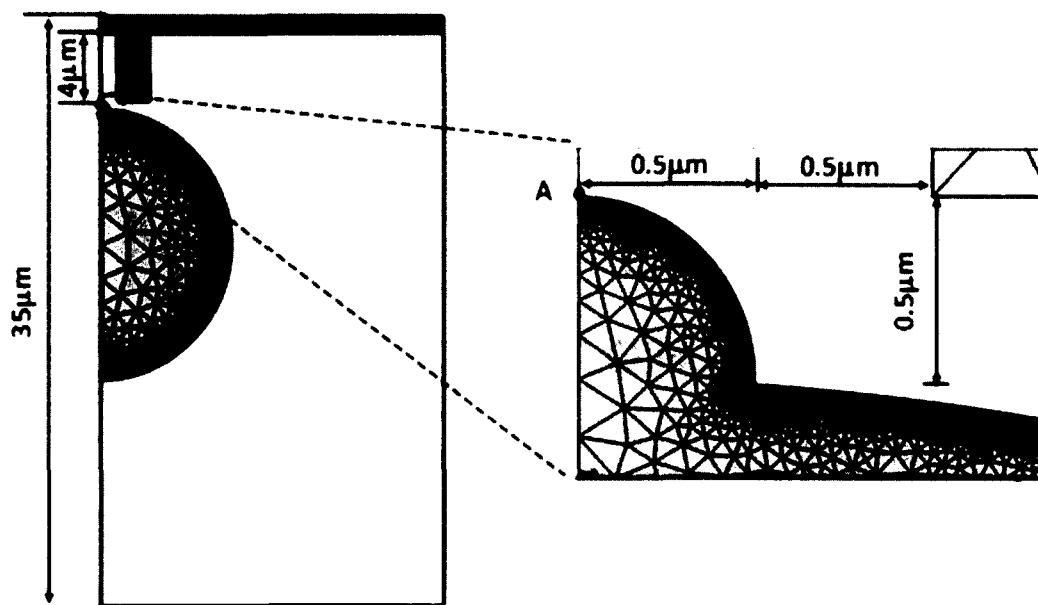


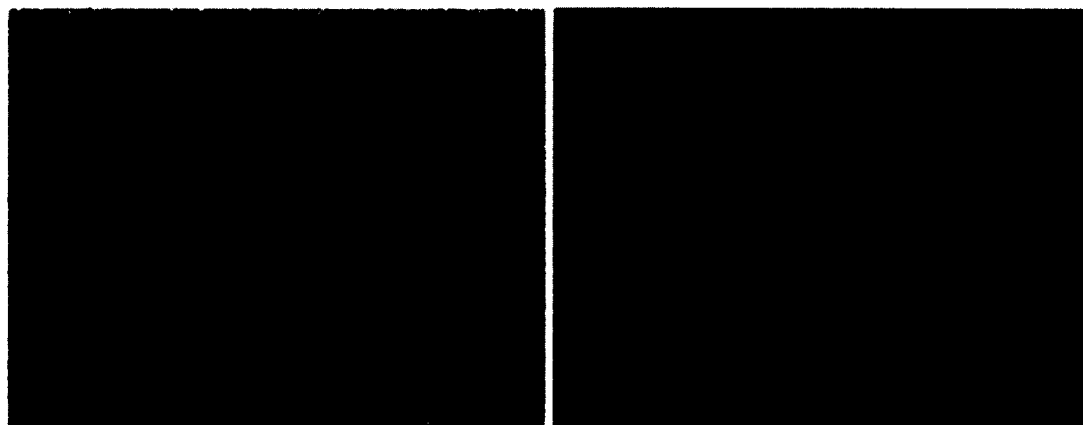
Figure 3-3: The model geometry and mesh setup for the electric field simulation of a single micropillar protruding towards a single cell. Location “A” is the chosen point in later transmembrane potential calculation.

3.4 Results and Discussion

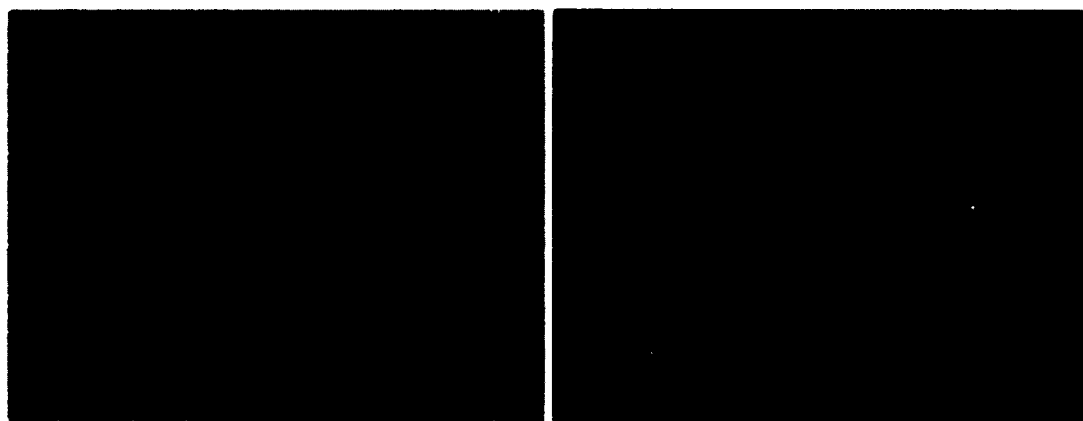
3.4.1 Enhancement of MAE on reporter gene transfection

We first did MAE electroporation on 3T3 cells and K562 cells for DNA plasmid delivery. For comparison purposes, electroporation using both a commercial system (designated as “BTX”) and another configuration with two closely placed plain electrodes but no micropillar pattern (designated as “Au Plain Plate”) was also done in conjunction. Successful transfection was observed in all three cases with many cells expressing green fluorescence protein (GFP) (Figure 3-4 and Figure 3-5a). Their quantitative difference on GFP-positive cells was further measured. As shown in Figure 3-5b, the transfection efficiency with two closely placed plain plate electrodes ($43.6 \pm 1.6\%$ for K562 cells and $44.1 \pm 1.8\%$ for 3T3 cells) is generally much better than that from BTX (K562: $25.7 \pm 1.8\%$, 3T3: $25.4 \pm 3.6\%$). When micro-pillar array is introduced on the electrode surface,

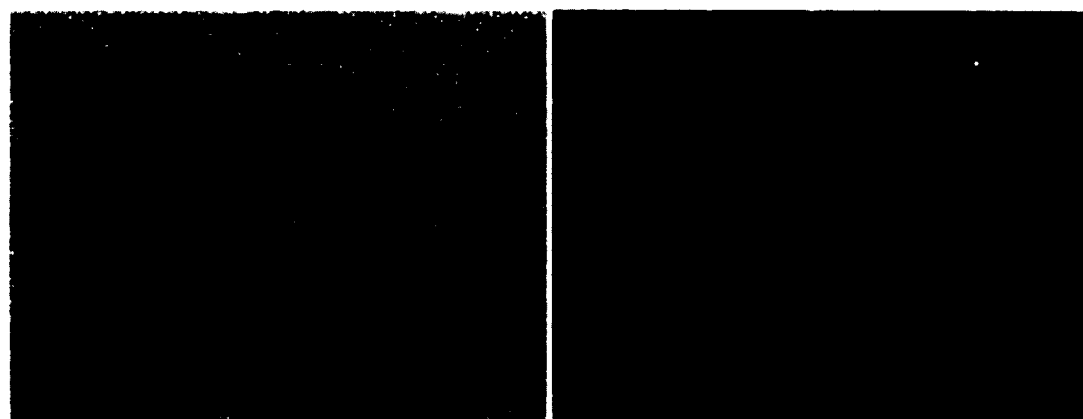
the transfection percentage is further improved (K562: $70.3 \pm 2.5\%$, 3T3: $65.1 \pm 3.7\%$). These results confirm the enhancement of MAE on plasmid transfection for mammalian cells and the improvement is indeed attributed to both the micro-pillar features and the closely placed electrode configuration. Some loss on the cell viability ($\sim 10\text{-}15\%$) is observed, but not statistically significant (Figure 3-5c). This is not surprising considering the actual voltage used in current MAE setup (10 V) is still beyond the threshold for electrochemical hydrolysis of water (~ 1.3 V). Its negative impact on cell survival is minimized, but not completely avoided.



Commercial electroporation (BTX)



Close-patterned plain plate electroporation



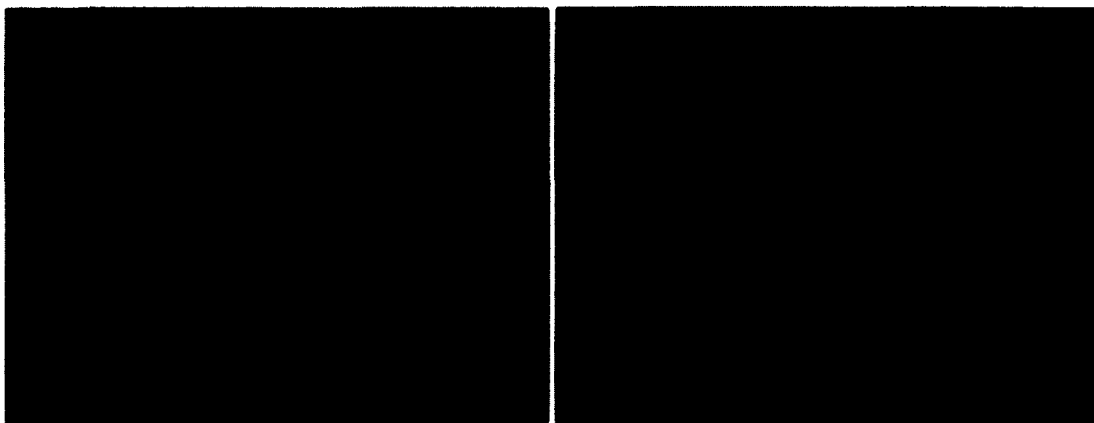
MAE electroporation

Figure 3-4: Fluorescence and phase contrast microscopic images of pGFP plasmid transfection by a commercial system (“BTX”) and MAE on K562 cells.

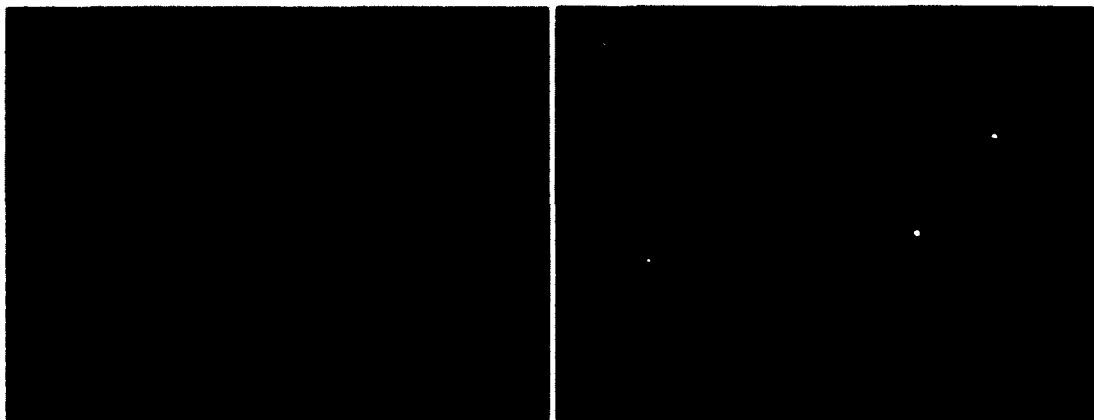


(a)

Commercial electroporation (BTX)



Close-patterned plain plate electroporation



MAE electroporation

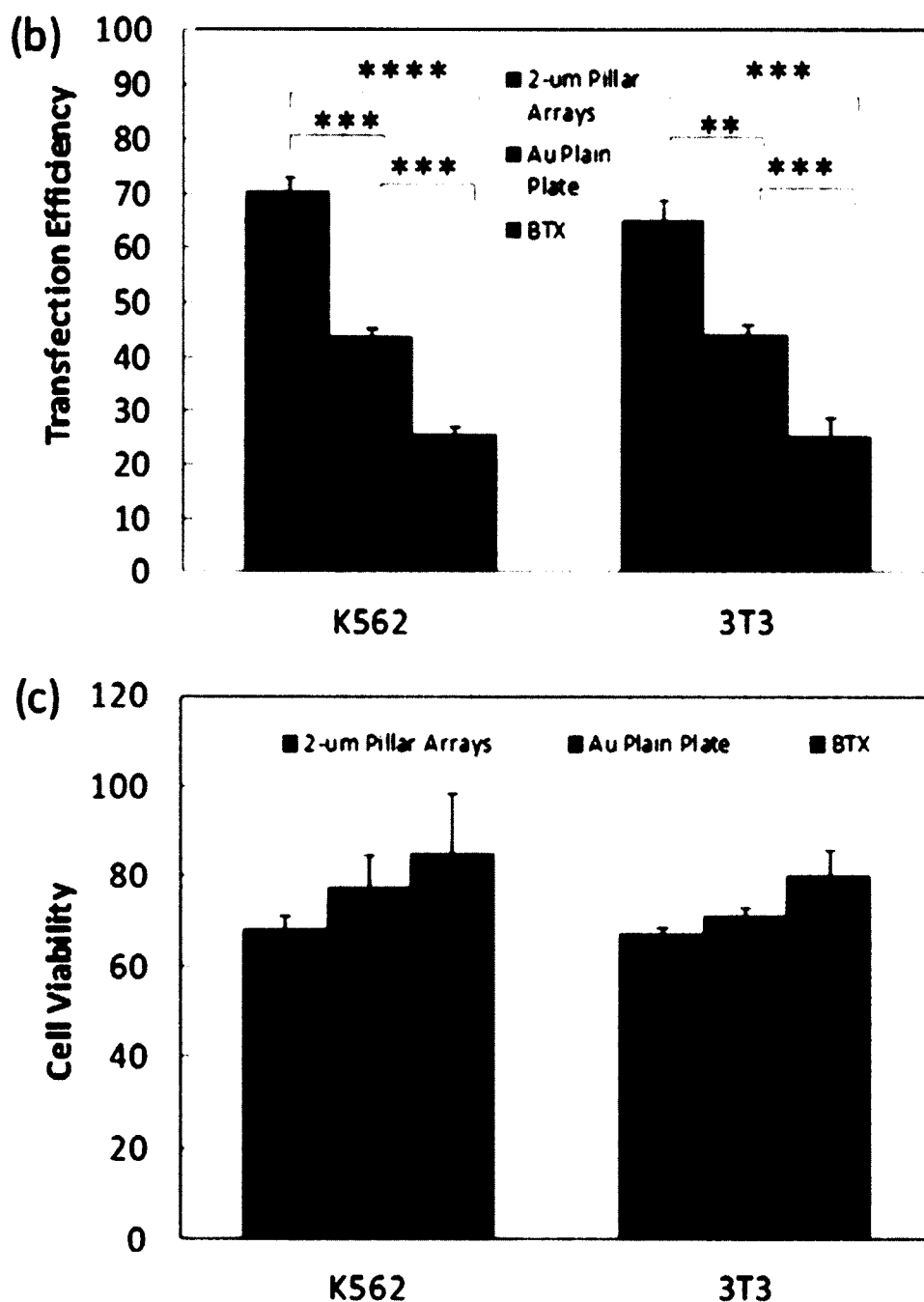


Figure 3-5: Transfection enhancement of pGFP plasmids in 2- μ m micropillar MAE. (a) Phase contrast and fluorescence microscopic images of NIH 3T3 cells after transfection by a commercial system (“BTX”), “Au plain plate”, and MAE; quantitative results of transfection efficiency (b) and cell viability (c) for 3T3 cells and K562 cells, respectively. (**) represents $p < 0.01$, (***) represents $p < 0.005$, (****) represents $p < 0.0001$.

Such transfection enhancement is attributed to the synergistic effects of the electric field focusing, localized electroporation, and size-dependent treatment in MAE. The first two effects benefitted cell membrane permeabilization at benign pulse conditions and its better recovery afterwards, while the size-dependent treatment allocates the number and area of the transient openings on individual cell membrane to ensure homogeneous treatment on cells of various sizes. Their specific contributions are discussed in the following sections.

3.4.2 Focusing of the Electric Pulses

Like what occurs in many micro/nanofluidic electroporation proof-of-concepts, micropillars in MAE help focus the electric field with their microscale at the far end that protrudes towards the cell membrane (Figures 3-6a-3-6b). According to the continuity of the electric field, the focusing level depends on the surface area (or size) of the micropillars. As the focused electric pulses affect mainly a tiny portion of the cell membrane that each micropillar faces, this gives additional localized electroporation benefit on the subjected cell. However unlike micro/nanofluidic electroporation, MAE does not require fluidic components to trap cells to accomplish these benefits. Its operation is therefore more compatible and similar to the commercial electroporation systems. As demonstrated by the COMSOL simulation (Figure 3-6c), the transmembrane potential near the micropillar is much higher than that without micropillar when the overall field strength is held constantly at 625 V/cm for all three cases. As a consequence of high transmembrane potential, these locations are more inclined to form temporary openings than elsewhere on the cell membrane during electroporation.

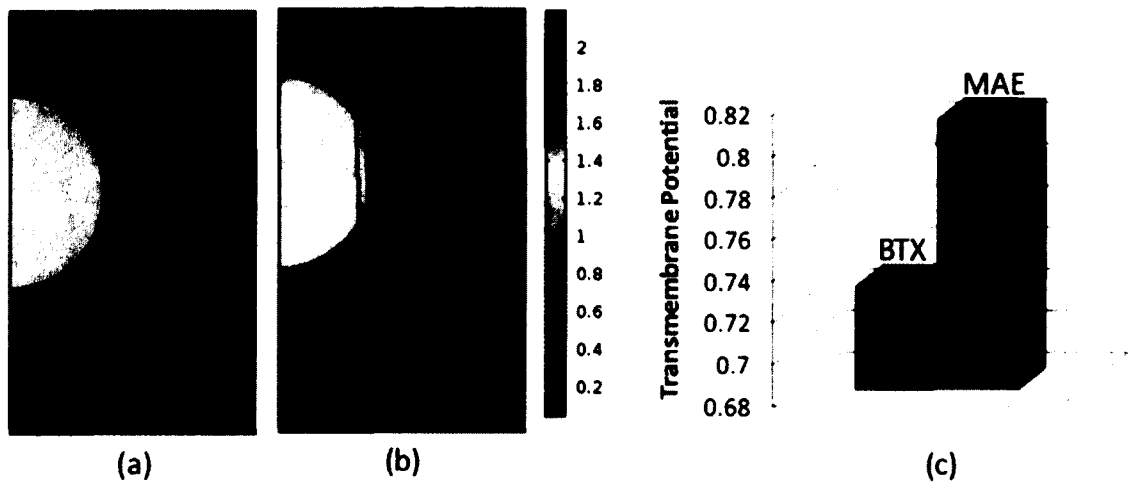
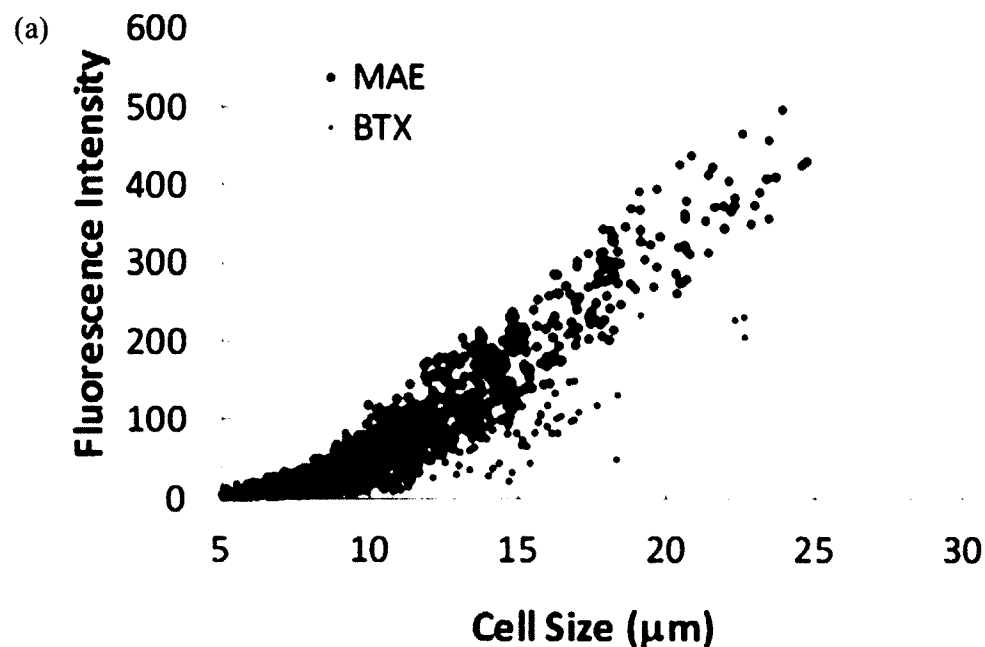


Figure 3-6: COMSOL simulation of the calculated electric potential and field lines around a cell facing an “Au plain plate” electrode (a) and a 2-μm micropillar (b). (c) The calculated transmembrane potential at location “A” (marked in Figure 3-3) of the cell.

3.4.3 Cell Size-Dependence Transfection

The number of induced pores and the transient permeable area on the cell membrane varies with the size of individual cells when the design of the micropillar array is fixed. With well-patterned array configuration, such size-dependent treatment of MAE is not affected by the randomly located sites of the cells. In other words, a big cell faces more micropillars and should have more porated locations and larger permeable areas to facilitate cellular uptake. To verify our hypothesis, the transgene expression of pGFP inside individual cells was measured, together with the cell size using NIH Image J. According to our size specific electroporation rationale, the size of the cells has a constant correlation to the number of micropillars they face, regardless their random dispersion. Therefore, the cellular uptake of DNA plasmids for cells of different sizes also represents similar relation to the number of micropillars they have faced early.

As shown in Figure 3-7a, despite the large scattering of data, the GFP intensity clearly shows a proportional increase with the cell size, particularly for large cells ($> 10 \mu\text{m}$). Different from the BTX system whose GFP signal is accumulated mainly in a specific size range ($< 12 \mu\text{m}$), the signal from MAE is stronger and extends to a broader size range. Similar trends are also observed in the dot-plots of the flow cytometry results (Figures 3-7b and 3-7c). This suggests that MAE works effectively for cells of many different sizes, unlike the commercial system which works best for cells of certain size populations. This is reasonable as the recommended electroporation protocols for most commercial systems are generally identified by a trial-and-error process and the optimal performance must be tied with effective transfection to cells of the dominated size population.



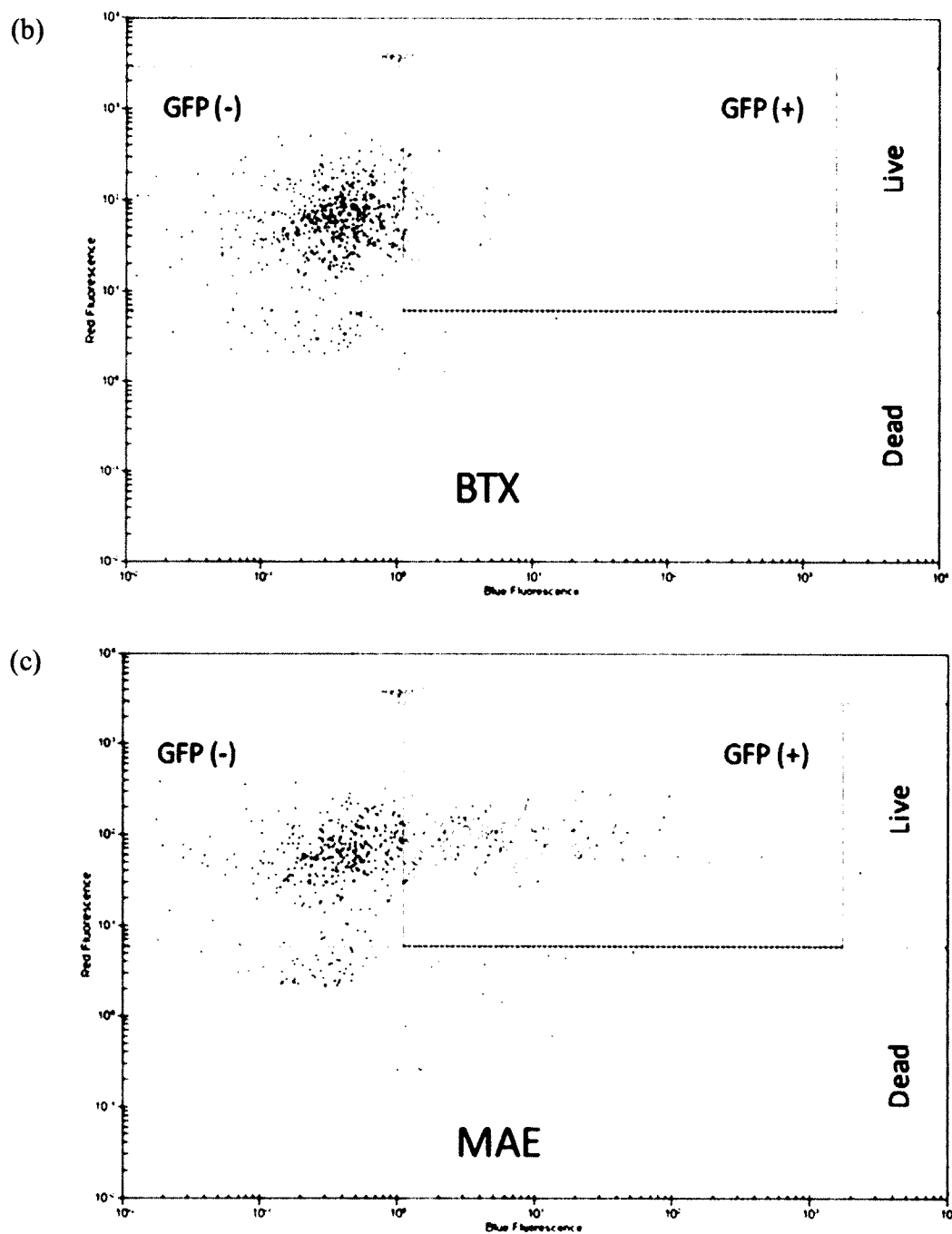


Figure 3-7: The plot of fluorescence intensity of GFP in transfected K562 cells to the cell size in a commercial bulk electroporation system (“BTX”, panel a and b) and a 2- μ m micropillar MAE system (a, c).

3.4.4 Effect of Size and Density of Micro-pillars on Electroporation Enhancement

Besides the cell size, the dimensions of individual micropillar and their pitch size in the array also decide the number of micropillars each cell faces and the consequent cell transfection. To simplify the case, we fabricated micropillars of two different diameters (6 μm and 2 μm) with a fixed pitch size (2 μm). As shown in Figure 3-8a, K562 cells face ~2-4 6- μm micropillars on average (full coverage) with a maximum of 6-9 micropillars (partial coverage) for some giant cells. Many covering events are incomplete and heterogeneous, largely depending on the actual size of the cells and their settling locations on micropillars. As a comparison, on 2- μm micropillar electrode, more micropillars cover each cell (with as many as 16 for some large cells) and incomplete coverage is hardly observed despite the random location of cells. Therefore, the cell coverage on 2- μm micropillars varies more constantly with the actual size of the individual cells. As a consequence, the number of locally porated openings and the total permeable area on the cell membrane should become more size specific and the DNA delivery dosage to cells of various size populations are improved. As demonstrated in Figure 3-8b, the transfection efficiency of 2- μm micropillar MAE is ~65% and ~70% for 3T3 cells and K562 cells, respectively, while only ~55% and ~59% for those using 6- μm micropillars, though both were much higher than the one using 2-mm cuvettes (~25%). This additional gain on the transfection efficiency is believed to be the result of more accurate allocation of the pulse on the cells based on their size in 2- μm micropillar MAE. Its electroporation works more effectively to cells of different sizes than the 6- μm ones and accomplishes better transfection performance.

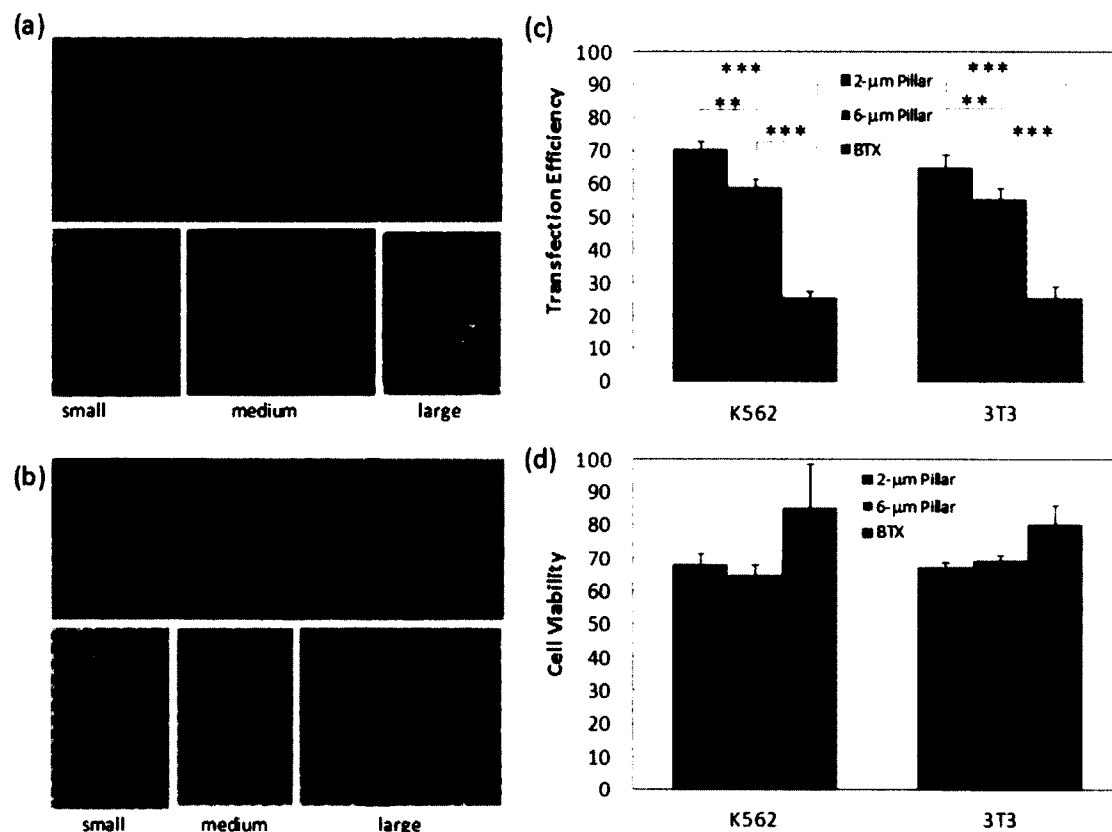


Figure 3-8: The effect of micropillar size and density on MAE electroporation enhancement. (a-b) Phase contrast images of cell coverage on 6-μm micropillar array (a) and 2-μm micropillar array (b); the comparison on the enhancement performance for MAE based on micropillars of various sizes: transfection efficiency (c) and cell viability (d). (**) represents $p < 0.01$, (***) represents $p < 0.005$.

3.5 Conclusions

We developed a micropillar array electroporation (MAE) platform and evaluated its contributions to the delivery efficiency of DNA probes with both anchor cells and suspension cells. The well-defined micropillar array ensures size specific treatment to a large number of cells regardless of their various sizes and random dispersion states. The close-configured microelectrodes allow low-voltage pulse conditions for electroporation through focused pulse strength and localized poration to the cell membrane. The delivery efficiency was evaluated with both model anchor cells (i.e., NIH 3T3) and suspension

cells (i.e., K562), together with their impact on cell viability. The advantages of this MAE system varied with the number, size, and density of the micropillars while its electroporation performance was similar for both gold-coated and carbon-based micropillar electrodes.

Although more DNA probes were introduced and the expression level of certain proteins were largely regulated, no significant increase of toxicity was found when compared to a commercial electroporation system. Besides the benefits of this MAE system demonstrated here, our design might help bridge two important, but long separated electroporation fields: single cell electroporation and cell electroporation of a large population (bulk electroporation). This system, as evidenced for its great improvement on DNA delivery efficiency, could also facilitate the discovery on cellular uptake dynamics and electroporation mechanism. Its success may help simplify the tedious, cell-specific protocol searching process and benefit the whole life science and biomedical community where a safe and effective non-viral gene delivery approach is needed on a daily basis.

CHAPTER 4

CARBON ELECTRODE MICRO-PILLAR ARRAY ELECTROPORATION

4.1 Introduction

Electroporation, known as a physical gene delivery method, is widely used for breaking the primary barrier, cell membrane, to achieve the transport of molecules and ions between the interior and the exterior of a cell. Since the early 1980s, conventional electroporation is typically applied in short electric pulses in a certain intensity and duration to a cuvette embedded with electrodes inside. In the parallel manner, the electrode materials are usually aluminum, stainless-steel, platinum, gold and/or graphite.

The last chapter describes the benefits brought from the introduction of the micro structure electroporation system. The micron structure of the electrode was processed by thermal evaporator to evaporate a layer of inert metal on the micron pillar array. This treatment is a very good solution to solve the problem of non-conductive organic polymer. However, there are some problems that emerged gradually in the actual operation.

One is the persistent problem of the device. Although thermal evaporation can coat metal uniformly on the substrate surface, the binding between inert metal and organic polymer in repeated use will be challenged. In the laboratory environment, after multiple uses (5-10 times), we can clearly observe the phenomenon of falling metal.

Although subsequent equipment preparation introduced an annealing process to reduce the internal stress of the metal works, the improvement was not obvious. On the other hand, since the surface of the conductive layer after multiple uses shed the problem, equipment reliability considerations reintroducing conductive layer is a necessary means. However this naturally raises consideration of production costs. Based on the above, to find a reliable way to introduce the conductive layer, the preparation cost can be reduced.

In this chapter, we combined our MAE system with conductive carbon material. With the same device structure used in Chapter 3, we attempted different fabrication method on electrode material. We loaded cells in a micro-scaled channel. We evaluated its transfection enhancement of reporter genes (pMaxGFP and gWizLuc). Both anchor cells (e.g., NIH 3T3 and A549 cells) and suspension cells (e.g., K562 cells) were tested to demonstrate its broad effectiveness. A significant improvement of gene transfection and excellent bio-competitive were expected. Additionally, small interfering RNA was tested to demonstrate its broad effectiveness.

4.2 Materials and Methods

4.2.1 Materials and Reagents

Small interfering RNA (siRNA) used for silencing GFP (expressed by pMaxGFP) and Luciferase genes were synthesized by Thermo Scientific (Pittsburgh, PA) and the sequences were as follows: siRNA for GFP silence, sense strand, 5'-CGCAUGACCAACAAGAUGAUU-3'; antisense strand, 5'-UCAUCUUGUUGGUCAUGCGGC-3'; Luciferase GL3 Duplex (Luc-siRNA), sense strand, 5'-CUUACGCUGAGUACUUCGA-3'; antisense strand, 5'-UCGAAGUACUCAGCGUAAG-3'. All other chemicals were purchased from

Sigma-Aldrich and the cell culture reagents were purchased from Life Technologies (Carlsbad, CA) unless specified.

4.2.2 Cell Culture

NIH/3T3 cells (ATCC, CRL-1658) were routinely grown and maintained in high glucose DMEM supplemented with 10% newborn calf serum (NCS), 1% penicillin and streptomycin, 1% L-glutamine, and 1% sodium pyruvate. K562 cells (ATCC, CCL-243) and A549 (ATCC, CCL-185) were cultured in RPMI 1640 supplemented with 10% NCS, 100 µg/mL penicillin, 100 µg/mL streptomycin, and 100 µg/mL L-glutamine. All cultures were maintained at 37° C with 5% CO₂ and 100% relative humidity.

4.2.3 Small Interfering RNA

In this chapter, with carbon electrode fabricated, another genetic particle called small interfering RNA was tested. Small interfering RNA (SiRNA) was first discovered by David Baulcombe's group and reported about 15 years ago (Hamilton & Baulcombe, 1999). It has a well-defined structure, double-stranded RNA molecules with 20-25 base pairs. In the past 15 years of research, SiRNA can play many roles in today's laboratory. However, the most frequency used is the RNA interference (RNAi) pathway. SiRNA functions are also known as a silencing RNA. It can lead to mRNA transcription breaking down. It interferes with the expression of specific genes and results in no translation. Here, we evaluated its transfection enhancement of reporter genes (pMaxGFP and gWizLuc) and their corresponding siRNAs. Both anchor cells (e.g., NIH 3T3 and A549 cells) and suspension cells (e.g., K562 cells) were tested to demonstrate its broad effectiveness.

4.2.4 Micro-Pillar Array Fabrication

Micro-pillar arrays were fabricated by MEMS technologies. SU-8 photoresist was applied on a Si (100) wafer and the pattern was transferred from a Cr photomask via the photolithography process. Micro-pillars with a pillar size of 2 or 6 μm and a pitch size of 2 μm (Figure 3-1b) were defined in many 6-mm radius disc regions (Figure 3-1c). The photo-lithography was processed as follow:

1. Wafer was cut into small 1 by 1 inch squares by a dicing saw (Microautomation).
2. Cleaning. Typically, the wafers were prepared by soaking in acetone, isopropyl alcohol, and rinsed by deionized water (DI H_2O). Since the dicing step introduced contamination, a standard RCA clean procedure was applied. The silicon wafer was immersed in the following solutions according to priority and are thoroughly rinsed with deionized water and dried by air between each step.

- SC-1: to remove organic contamination and particles

DI H_2O : ammonium hydroxide (NH_4OH) : hydrogen peroxide H_2O_2 = 5:1:1 At 80°C, for 10 minutes.

- Buffered oxide etchant (BOE): while the SC-1 step removed organic contamination and particles, a thin layer would form of silicon dioxide on the wafer's surface. The BOE is for removing the oxide layer.

Hydrofluoric acid (HF) : ammonium fluoride (NH_4F) = 1:7 At 25°C, for 1 minute.

- SC-2: to remove ionic and metallic contamination

DI H_2O : hydrochloric acid (HCl) : H_2O_2 = 5:1:1 At 80°C, for 10 minutes.

3. Pre-bake. After cleaning, the wafer was baked on the hot plate at 180 °C for about 15 minutes to remove the residual water on and inside of the wafer.

4. Photoresist (PR) application. Both Shipley Microposit S1800 series positive photoresist and MicroChem SU 8 - 2000 series permanent epoxy negative photoresist were used for patterning the pillar structure. The wafer was placed on resist spinner (CEE, model 100 programmable). According to the thickness requirement adjusted, the spin rate was from 800 to 5000 rpm for 30 - 120 seconds. The PR would form a uniform thin layer and usually with uniformity within the range of 5 to 10 nanometres.

5. Soft-bake. Soft-bake process is the most important step of the photolithography technology. After PR application, in the layer of the resist, it contains a remaining solvent concentration depending on the resist, the solvent, the resist film thickness, and the resist coating technique. The soft-bake can reduce the remaining solvent content. It is important because of the following reason:

- avoid mask contamination and/or sticking to the mask,
- prevent popping or foaming of the resist by N_2 created during exposure,
- improve resist adhesion to the substrate,
- minimize dark erosion during the developing process,
- prevent prior coated layer dissolving from the following photoresist coating,
- extrude bubble for the following process.

The soft-bake temperature and time varies up to the PR. Typically for S1813, it is in the range of 90 to 100°C and 30 to 60 seconds on a hotplate. For the SU-8, it depends

on the thickness of the coating. A longer and slower heating is required for a thicker layer of resist.

6. Exposure. After soft-bake, the photoresist is exposed under an intense light resource. EV 420 Mask Aligner (ELECTRONIC VISIONS) was used for aligning the mask and wafer together. Exposure time is calculated by the equation:

$$\text{Dose} \left(\frac{mJ}{cm^2} \right) = \text{Intensity} (mW/cm^2) \times \text{Exposure time} (s)$$

7. Post-exposure bake (PEB). A post-exposure bake (PEB) is performed after exposure. For SU-8 photoresist, PEB is necessary. It can reduce the interference patterns caused by the incident light. Wafer was baked on the hot plate at 95°C for about 3 minutes.

8. Developing. By immersing the wafer into photoresist developer, the desired pattern or structure would emerge. Different photoresists should work in their specific developer. Presented in this dissertation, positive photoresist, 1813s, developed with MF 319 and negative photoresist, SU-8, developed in SU-8 developer. Due to the designed pattern size, photoresist applied thickness and exposure time, development time varies.

9. Hard bake. A hard bake can be performed after development in order to increase the thermal, chemical, and physical stability of developed resist structures for subsequent processes such as electroplating, wet- and dry-chemical etching. Hereby, the following mechanisms have to be considered.

4.2.5 Carbonization

Carbonization is a complex process to produce conductive glass-like carbon. Polymer or organic compounds experience three major steps during pyrolysis process:

pre-carbonization, carbonization and annealing. Each step plays a different role as shown in **Table 1**

Table 1: Different steps of pyrolysis

Pre-carbonization (typically $T < 300^{\circ}\text{C}$)	Defecating molecules solvent and unreacted monomer from the polymeric precursor
Carbonization	<p>300 to 500°C</p> <p>Eliminating heteroatoms, such as oxygen and halogens, caused a rapid mass loss. The beginning of hydrogen atoms are eliminated. Rudiment carbon systems formed.</p>
	<p>500 to 1200°C</p> <p>completely eliminate heteroatoms (hydrogen, oxygen and nitrogen atoms) the aromatic network (carbon-carbon bond) is forced to connect.</p> <p>decreases: permeability,</p> <p>increase: Young's modulus, density, hardness and electrical conductivity.</p>
Annealing	Stabilize carbon structural system and remove thermal stress.

The final chemical constitution (carbonization and the residual heteroatoms) are determined by polymeric precursor and pyrolysis. Generally, 90% of the carbon content is expected in the residue at final pyrolysis temperature 900°C and more than 99% at 1300° C (Rodrigo, 2014).

4.2.5.1 Micro-Pillar Array Electrode Carbonization Protocol. As described previously, micro-pillar array electrode was carbonized through a pyrolysis process. With our work, carbonization of negative SU-8 photoresist takes place in a tube furnace (structure shown in Figure 4-1) under a nitrogen preventing atmosphere (N₂ flow at 2000 mL/min). A quartz tubes with an internal diameter of 1 inch has been used.

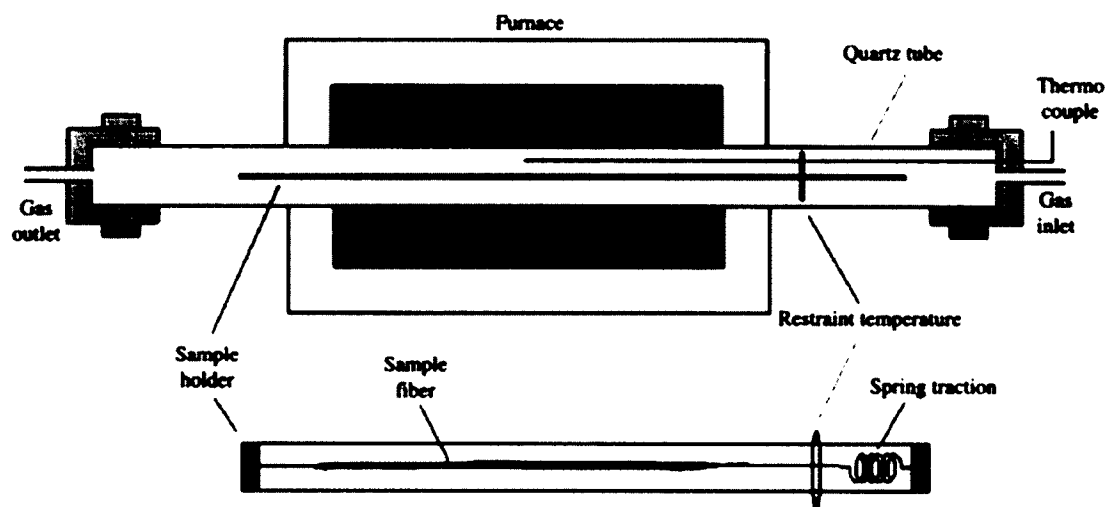
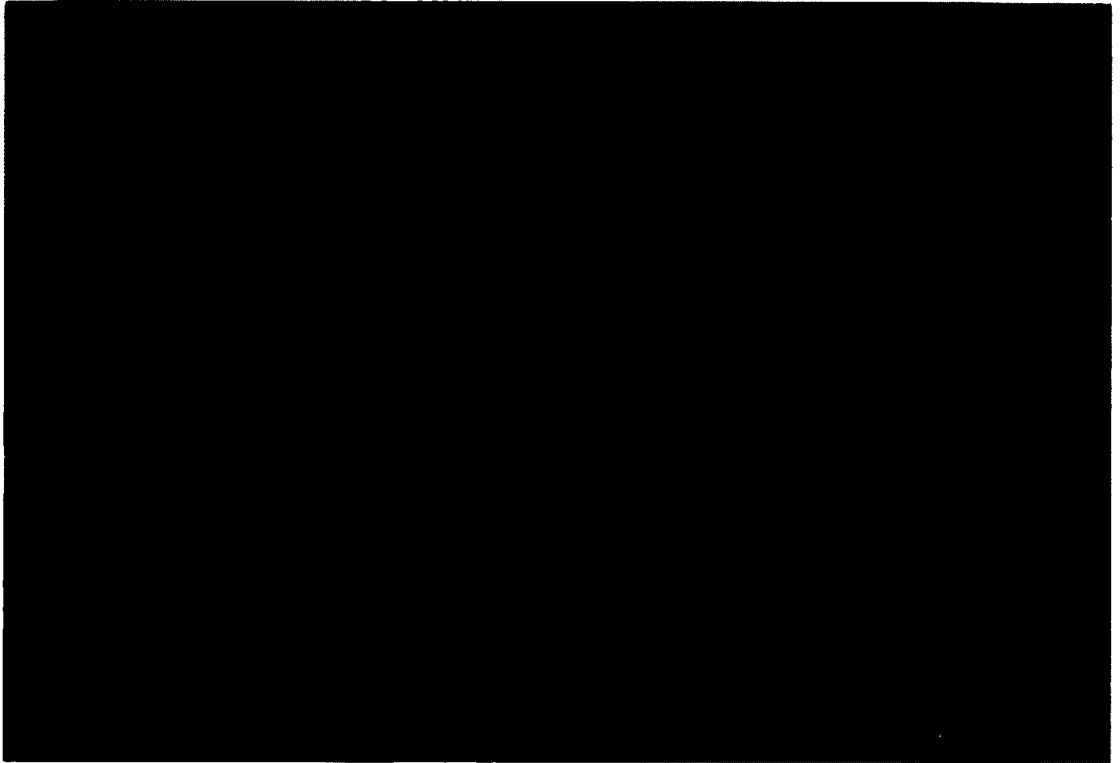


Figure 4-1: Carbonization set up used for produce conductive carbon material (http://www.scielo.br/img/revistas/mr/2012nahead/aop_1346fig01.jpg).

Samples were loaded on the sample holder at the midpoint of the quartz tube. Different protocols were tested to figure out the appropriate procedure generating the best mechanical and electrical properties. **Table 2** lists primary tested protocols with a brief result. All protocols started at room temperature (RT). Temperature is the form of Celsius. Figure 4-2 shows images from protocols I (a); II (b) and III (c).

Table 2: Protocols tested for carbonization.

	pyrolysis process			Results
	Pre-carbonization	carbonization	annealing	
I	RT→280 in 60 min. Dwell 90 min.	280→600 in 100 min. Dwell 60 min. 600→900 in 100 min. Dwell 60 min.	900→600 in 100 min. Dwell 60 min. 600→RT in 100 min.	craze crack; shedding
II	RT→200 in 18 min. Dwell 30 min.	200→900 in 70 min. Dwell 60 min.	900→RT in 60 min.	Slightly crack
III	RT→200 in 40 min. Dwell 60 min.	200→900 in 0 min. Dwell 60 min.	900→RT in 60 min.	Even uniform; Serious shrink
IV	RT→200 in 40 min. Dwell 90 min.	200→900 in 46 min. Dwell 60 min.	900→RT in 60 min.	Even uniform; slightly shrink



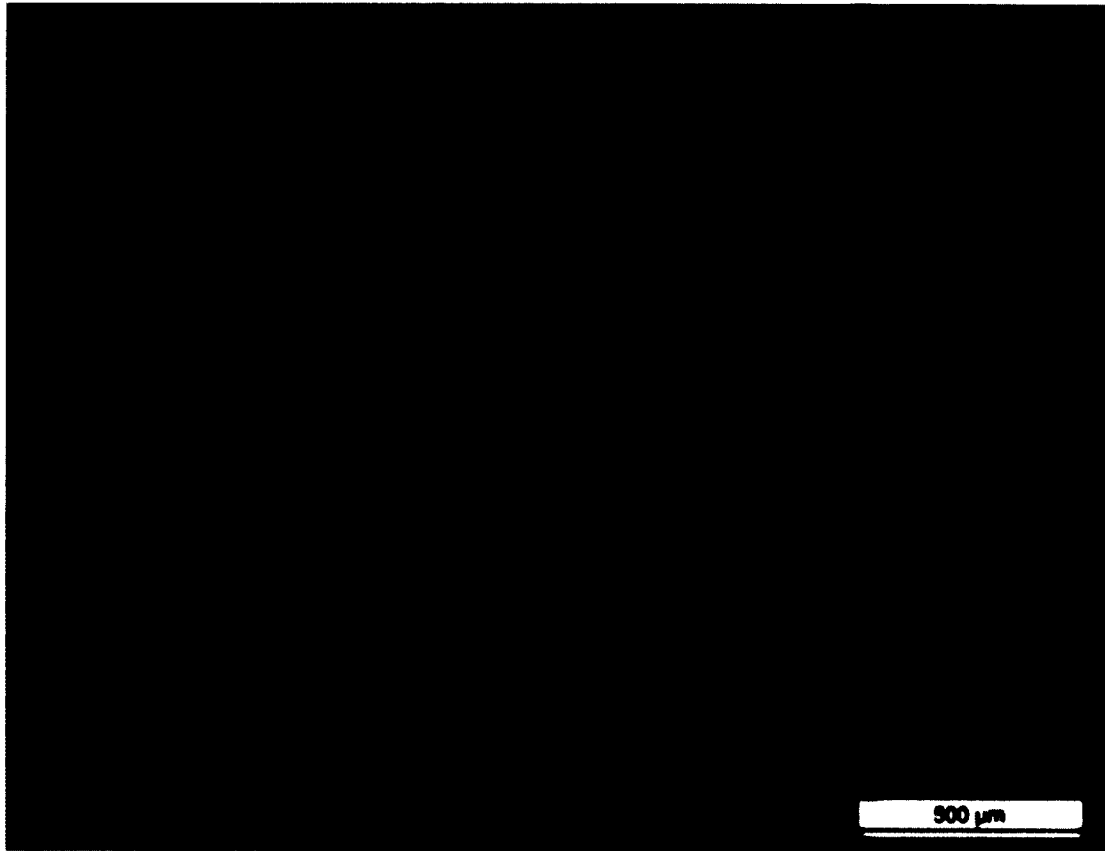


Figure 4-2: Images for pyrolysis protocols I (a); II (b) and III (c).

As shown in Table 2, the protocol IV was finally considered as standard pyrolysis process procedure for photoresist material SU-8. It is featured as three stages: (1) temperature from room temperature to 200°C at the heating rate of 5°C/min, followed by a 30-min dwell at 200°C; (2) temperature from 200°C to 900°C with the rate of 15°C/min with a one-hour dwell at 900°C to complete carbonization; and (3) a natural cool down to room temperature. This process was summarized and plotted in Figure 4-3.

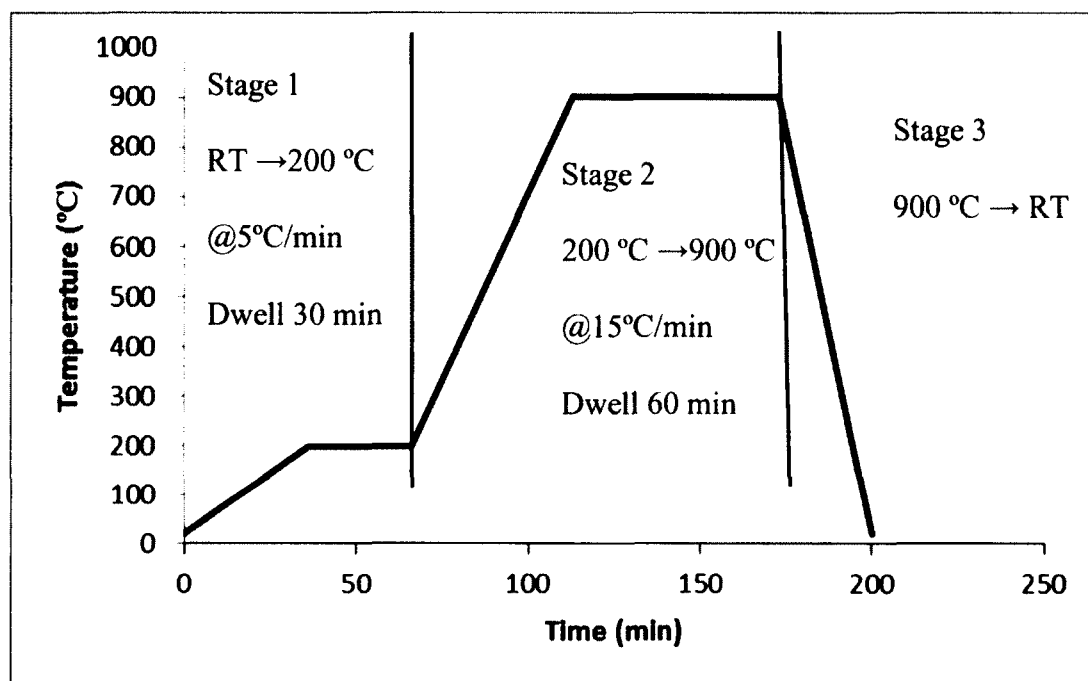


Figure 4-3: Three stages of SU-8 carbonization protocol.

4.2.6 Transfection Efficiency and Cell Viability

The expression of pGFP plasmids was evaluated both qualitatively by visualizing cells with green fluorescence within some representative areas under an inverted fluorescence microscope (Olympus, Japan) and quantitatively by counting cells using an Agilent 2100 Bioanalyzer (Agilent Technologies, Santa Clara, CA). The fluorescence intensity of GFP was measured using the Cell Assay Module with live cells stained with carboxy-naphthofluorescein (CBNF). The results were analyzed with Agilent 2100 Expert Software and 500-1,500 events were counted for each sample. The transfection efficiency of pGFP is defined as the number of cells emitting fluorescence signal to the total number of cells in a sample (gated fluorescence signal of GFP). The Luciferase expression was quantified by One-Glo™ Luciferase assay system (Promega, Madison, WI). One-Glo™ reagent of 100 μ L was added to the cell growth medium of 100 μ L in a

96-well plate. Luminescence was measured with a plate reader (FLUOstar OPTIMA, BMG LABTECH, Germany) after 10 min incubation at room temperature for complete cell lysis. The transfection efficiency of pLuc is presented as the luminescence of the total live cells in a sample.

The cell viability was evaluated by an MTS cell proliferation assay (Promega, Madison, WI). Briefly, the cells in 100 μ L/well of medium were transferred to a 96-well plate and incubated. CellTiter 96 AQueous One solution (Promega, Madison, WI) of 20 μ L was added to each well and all samples were incubated at 37°C for another 4 hr. Absorbance was measured at 492 nm on an automated plate reader (Elx 800, Biotek, VT). Data points were represented as the mean \pm standard deviation (SD) of triplicates, unless otherwise indicated. The cell viability is calculated as the ratio of light absorbance of an electroporated cell sample to that of the negative control cell sample in MTS assay 24 hours post electroporation.

4.3 Results and Discussions

4.3.1 Structure Characterization by Scanning Electron Microscopy (SEM)

SEM (AMRAY, 1830) was used to observe the structure of carbon micro-pillar. The PAN nano-fiber samples were coated with 15 nm of metal by a sputter coater (CRESSINGTON, 208 HR). SEM images are shown in Figure 4-4.

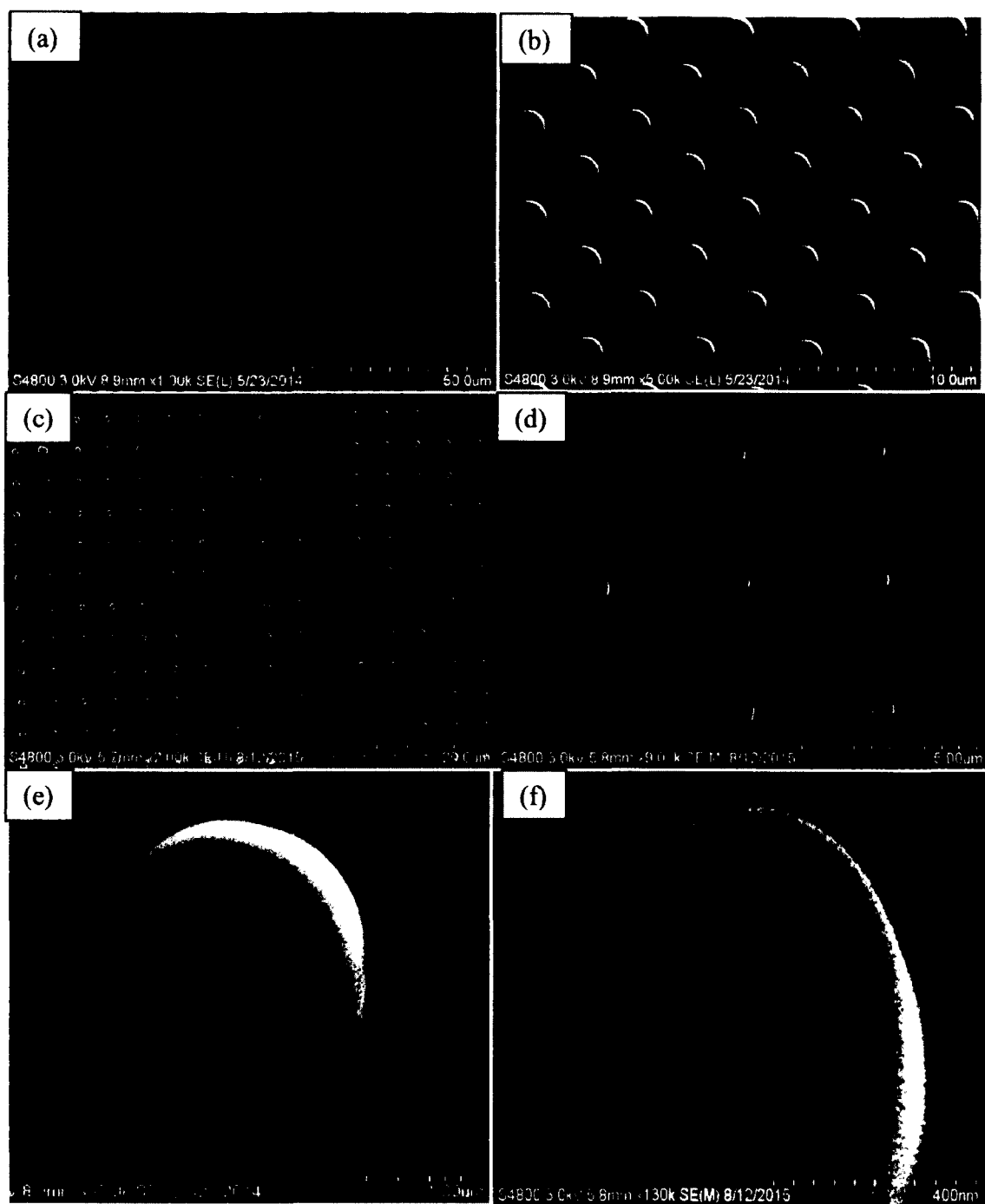


Figure 4-4: SEM images (a) and (b) SU-8 micro-pillar array, (c) and (d) carbon micro-pillar array, (e) single SU-8 micro-pillar (f) single carbon micro-pillar.

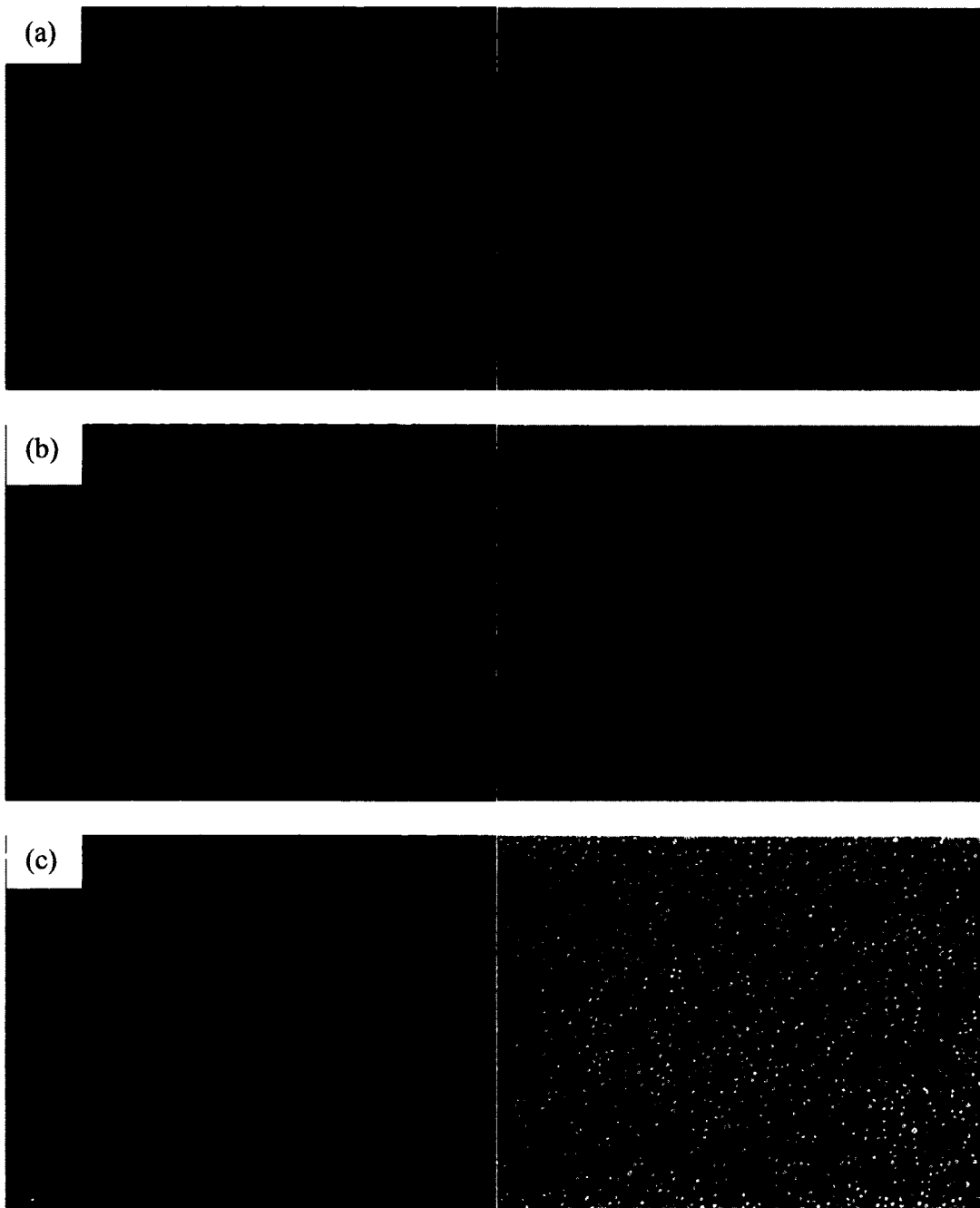
4.3.2 Carbon Micro-Pillar Array Electroporation

The same cells, 3T3 cells and K562, were used for both BTX, MAE and plain plate systems, adopting a pulse protocol (625 V/cm, single 10 ms pulse) early optimized with WizGFP plasmids. For the BTX system with 2-mm gap cuvettes, this is designated to a 125 V pulse and for MAE and plain plate, they are 10 V. The two close-placed plain electrodes with gold coating surface (no micro-pillar pattern) were also done simultaneously for electroporation as a comparison with the carbon plain plate system. Successful transfection was observed in all those cases: BTX, gold/carbon-coated plain plate electrodes, and gold-coated/carbon micro-pillar electrodes. Figure 4-5 shows transfection enhancement of pGFP plasmids in fluorescence microscopic and phase contrast images of gold coated plain plate, carbon coated plain plate, gold coated MAE and carbon coated MAE.

Many cells in each case expressed green fluorescence protein (GFP) 24 hours after electroporation (Figure 4-5). More quantitative comparison was done by counting the percentage of GFP-positive cells (Figure 4-6a). Efficiency of pGFP transfection for carbon coated and gold coated with closed-placed parallel plain electrodes stayed at the same level (~40% for both K562 cells and 3T3 cells), which as expected was generally much better than that from BTX (K562: $25.7 \pm 1.8\%$, 3T3: $25.4 \pm 3.6\%$), similar to some early micro-scale electroporation observations^{40, 42}. When we focus on the micro-pillar array system, the introduction of carbonization did not show up too much affection on the transfection percentage (K562: ~70%, 3T3: ~65%).

Such results confirm the enhancement of MAE system to the plasmid transfection of mammalian cells. As shown in Figure 4-6, similar transfection performance was found

for MAE processes using both carbon-based and gold-coated micro-pillar electrodes in terms of the transfection efficiency and cell viability. Their enhancement level to the commercial system is also about the same. This result offers us some flexibility on the choice of MAE electrode material. Considering the availability of large-scale manufacturing lines (such as hot embossing and microinjection molding facilities), the fabrication of micropillar array using SU-8 or other polymer materials (which can be converted into conductive carbon later) could be done quickly without expensive fabrication facilities and cleanroom environment. Therefore, the findings here could make MAE production largely eliminate the dependence on cleanroom facility and become truly competitive in cost with available commercial electroporation setup. In our tests below, carbon-based MAE setup was adopted.



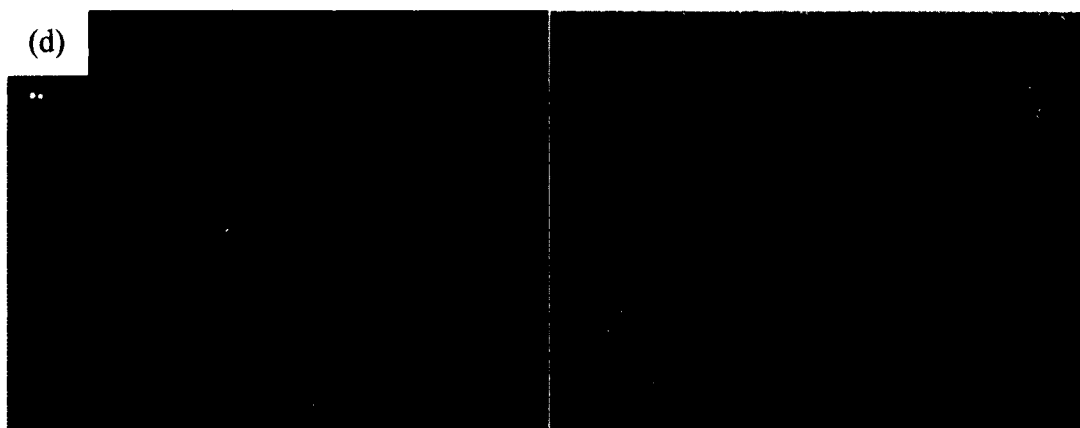
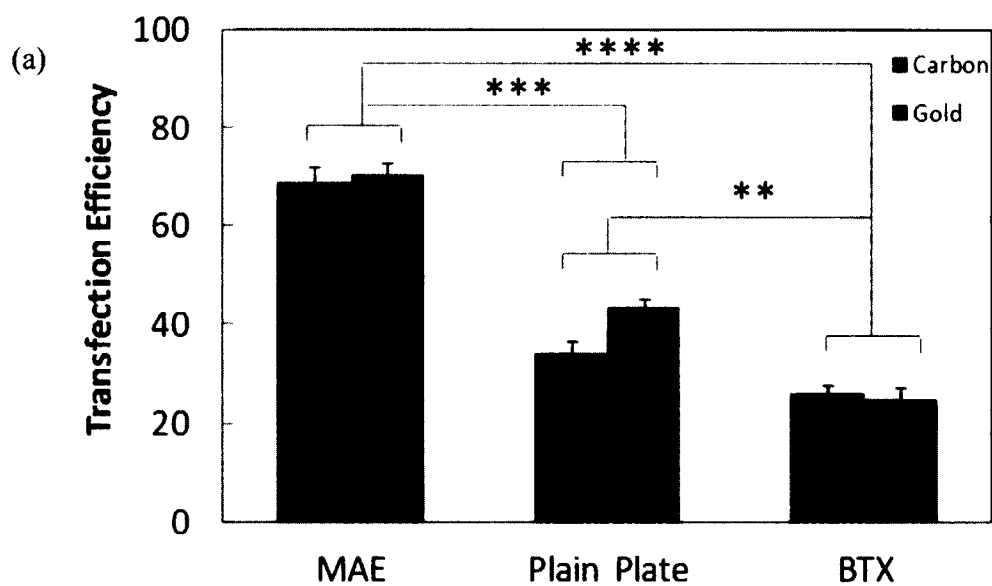


Figure 4-5: Transfection enhancement of pGFP plasmids in fluorescence microscopic and phase contrast images (a) gold coated plain plate; (b) carbon coated plain plate; (c) gold coated MAE; (d) carbon coated MAE.



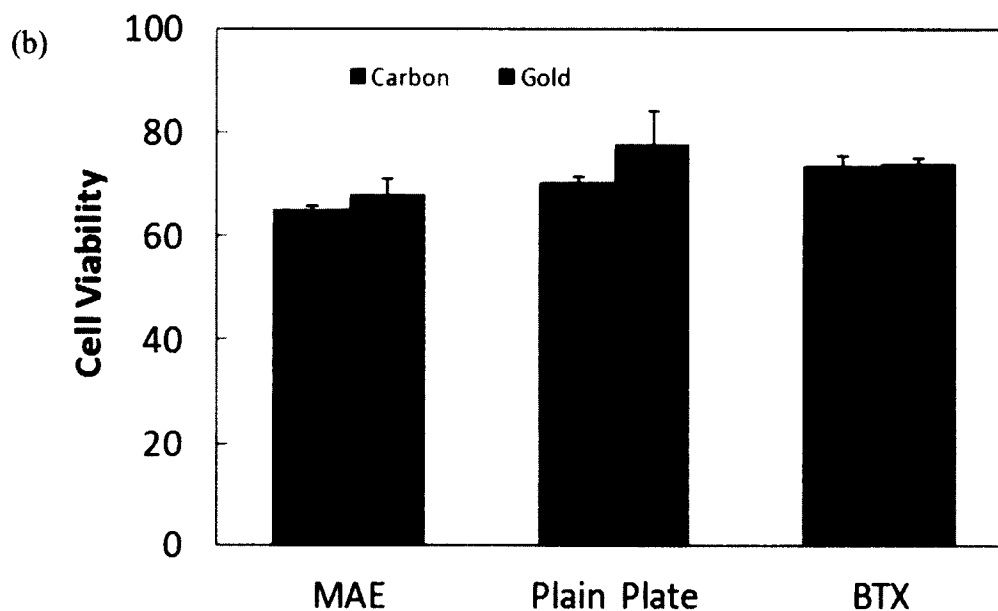
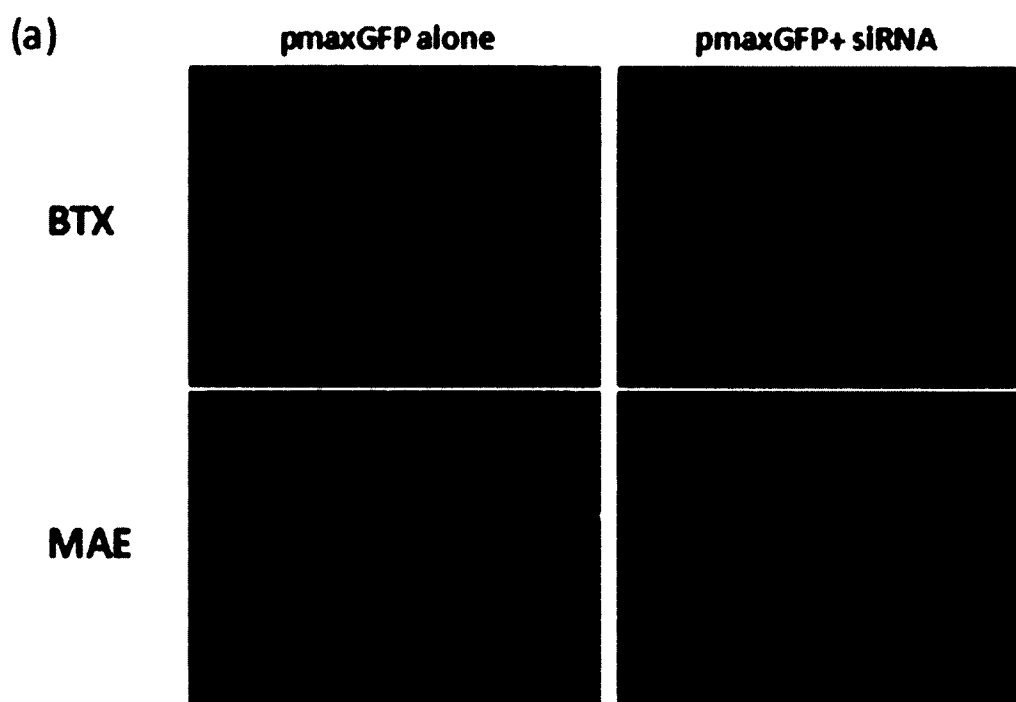


Figure 4-6: The effect of micropillar materials on electroporation performance. The transfection efficiency (a) and the cell viability (b) comparison of gold-coated electrodes and carbon-based electrodes: for micropillar array electrode (“MAE”), plain plate electrode without micropillar pattern (“Plain Plate”), and a commercial system (“BTX”). (**) represents $p < 0.01$, (***) represents $p < 0.005$, (****) represents $p < 0.0001$.

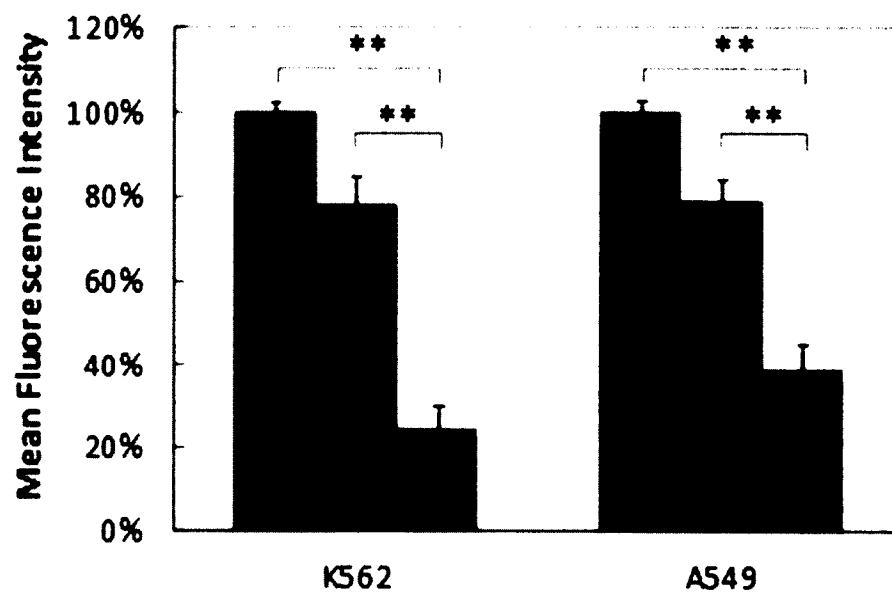
4.3.3 Enhancement of Micro-pillar Array Electroporation on Sirna Delivery

To further demonstrate the effectiveness of MAE to RNA interference applications, we chose small interfering RNA (siRNA) with sequences that could specifically silence the expression of GFP and Luciferase. Their knockdown efficiency was evaluated by co-transfecting with pGFP or pLuc plasmids. As shown in Figure 4-7a, clear suppression of GFP expression is observed when co-delivering pMaxGFP and their corresponding siRNA of 5 pmol to K562 cells in both commercial electroporation system (“BTX”) and MAE. More GFP expression is turned off by MAE, with a ~53% further drop of GFP than that in BTX and an overall knockdown level below 30% (Figure 4-7b). Similar knockdown enhancement was also observed in A549 cells (Figure 4-7b), confirming its broad effectiveness.

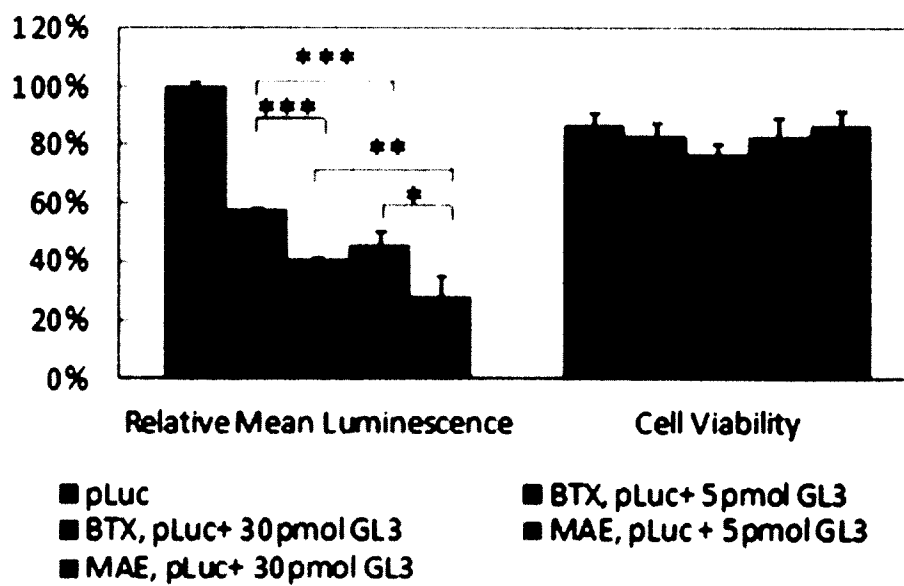
It is worth pointing out that as the co-transfection of plasmids and siRNA was used here, the delivery enhancement on the targeted reporter gene and its corresponding siRNA occurred simultaneously in MAE. It must shut off more proteins than the BTX system to reach the similar protein expression level. Down regulation of Luciferase plasmid ("pLuc") was also evaluated by co-transfecting with its corresponding siRNA ("GL3"). Compared to the knockdown result from BTX, an additional ~11% drop of Luciferase signal was found in MAE when 5 pmol siRNA was used (Figure 4-7c). However unlike the knockdown of pMaxGFP with MAE, a larger dosage (i.e., 30 pmol) of siRNA GL3 is needed to shutoff the Luciferase expression level below 30%. Although more siRNA probes were introduced into the treated cells by MAE and additional protein expression was suppressed, no significant loss of cell viability was found (Figures 4-7c and 4.7d).



(b) ■ pMax ■ BTX, pMax+ siRNA ■ MAE, pMax+ siRNA



(c)



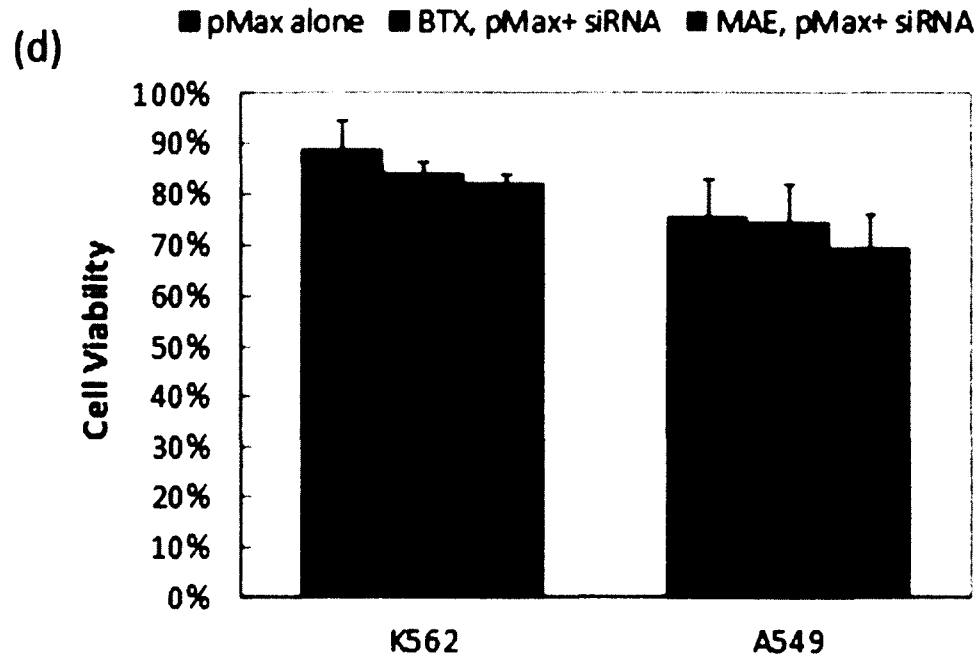


Figure 4-7: Enhancement on siRNA delivery in 2- μ m micropillar MAE. (a) Fluorescence images of K562 cells and (b) fluorescence intensity measurement on GFP expression level in K562 and A549 cells when co-transfecting pMaxGFP and its corresponding siRNA; (c) the luminescence measurement on Luciferase expression level in K562 cells and cell viability when co-transfecting pLuc and knockdown siRNA probe (“GL3”); (d) cell viability of K562 and A549 cells in panel (b). (*) represents $p < 0.05$, (**) represents $p < 0.01$, (***) represents $p < 0.005$.

4.4 Conclusions

A new synthesis procedure of conductive material, glass-like carbon, was developed and evaluated for its contributions to the delivery efficiency of DNA with both anchor cells and suspension cells. The advantages of this MAE system varied with the number, size, and density of the micropillars while its electroporation performance was similar for both gold-coated and carbon-based micropillar electrodes. The series of test results showed identical performance on both glass-like carbon and conventional conductive materials. Proleptically, the MAE still showed 2.5~3 folds improvement on the transfection efficiency of the plasmid DNA while the cell viability stayed at the same

level compared with the popular commercial electroporation system. While there was a 2.5~3 folds improvement on the transfection efficiency of plasmid DNA, the enhancement on the siRNA delivery heavily relied on the probe dosage when co-transfection strategy was adopted. Thus, well-defined micro-pillar array ensures size specific treatment to a large number of cells regardless of their various sizes, and random dispersion states were proven again.

CHAPTER 5

FLOW GUIDED MICRO-PILLAR ARRAY ELECTROPORATION

5.1 Introduction

In recent years, micro-fluidic technology developed rapidly. Different kinds of new device designs start to appear. Scientists favor micro-fluidic-based electroporation design because of its unique miniaturization and integration. Its advantage is unique. First, through standard microfabrication techniques, such as photolithography, the manufacturing of the micro-fluidic electroporation system becomes easy to achieve. Secondly, the various micro-electrodes are incorporated into the device which can produce the desired electric field. Reduced distance between the electrodes to tens of microns or even created subcellular size. Due to the proximity of electrodes required, voltage can be remarkably reduced to a few volts. Third, since operating space is reduced, a single cell can be manipulated on the chip to detect cell heterogeneity.

Miniaturized system also makes them well suited for reducing rare cells involved and expensive reagent consumption. Fourth, another advantage of system miniaturization is the material of choice diversification. It brings immediate benefits, such as transparent materials (such as polydimethylsiloxane (PDMS) and the conductive glass) microchip in real-time observation during the electroporation process, which is propitious to exploring electric mechanism. Finally, the system also has the advantage that small microfluidic devices can generate small current. It is conducive to chemical environment stability and

rapid cooling. In addition, the micro-fluidic electroporation combined with other analysis methods such as dielectrophoresis (DEP), electro-osmosis and hybridization to implement a total analysis of the analytical system. This is important for applications related to the content of intracellular analysis use.

In this chapter, we present novel micro-fluidic electroporation system owing much less invasive and more efficient on gene delivery called Flow guided Micro-pillar array Electroporation (FME). We loaded cells in a micro-scaled channel. Cells flowed continuously between micro-pillar electrode and plain surface electrode. A batch of certain frequency low voltage electric pulses was applied to achieve gene delivery. We observed a significant improvement of gene transfection with minimal cell damage.

5.2 Materials and Methods

5.2.1 Cell Culture

NIH/3T3 cells (ATCC, CRL-1658) were routinely grown and maintained in high glucose DMEM supplemented with 10% newborn calf serum (NCS), 1% penicillin and streptomycin, 1% L-glutamine and 1% sodium pyruvate. K562 cells (ATCC, CCL-243) and A549 (ATCC, CCL-185) were cultured in RPMI 1640 supplemented with 10% NCS, 100 U/mL penicillin, 100 µg/mL streptomycin, and 100 µg/mL L-glutamine. All cultures were maintained at 37°C with 5% CO₂ and 100% relative humidity.

5.2.2 Fabrication and Assembly of Microfluidic Device

The flow guided micro-pillar array electroporation (FME) device consists of a PDMS gasket with a straight channel in the middle and sandwiched with a piece of micro-pillar structure electrode and a gold or carbon coated plate electrode. The fixed composition was embedded in a pair of polymethylmethacrylate (PMMA) film (Fisher

Scientific Inc., USA) holder with tubing used for load and collect cells. As shown in Figure 5-1, after loaded, cells would experience a 150 μm height, 1 mm width and a 2.54 mm length channel.

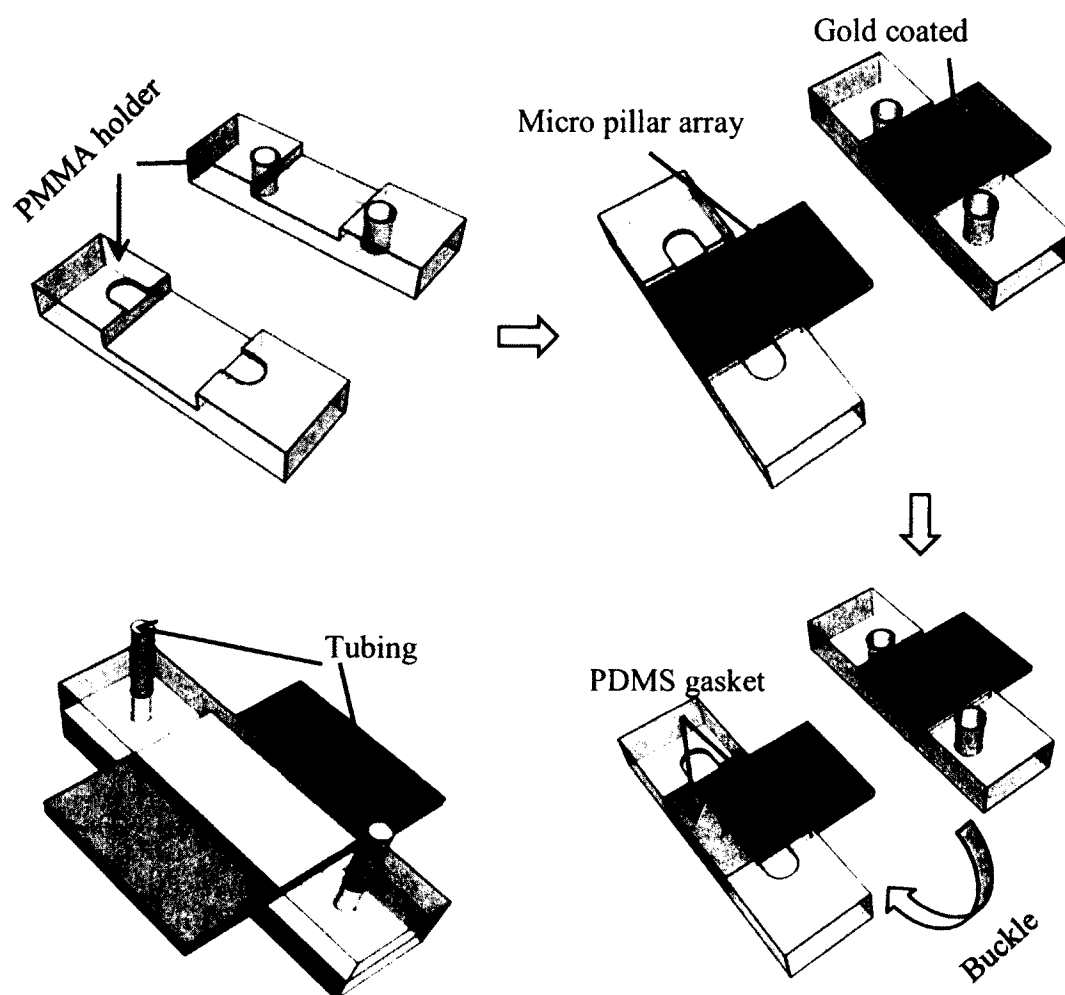


Figure 5-1: Micro-fluidic device assembling.

In order to remove all contaminants on the surface, the micro-fluidic device was exposed under UV light overnight and then cleaned with 70% alcohol successively rinsed with phosphate-buffered saline (PBS).

5.2.3 Electroporation Procedure

Bulk electroporation was processed according to the procedure described in Section 3.2. The micro-pillar structure enhanced micro-fluidic electroporation system includes a multi-functional pulse generator (BTX 830), a syringe with a pump and the unit device. The multi-functional pulse generator is able to generate square wave pulse. The technical specifications of the multi-functional pulse generator are given in **Table 3**.

Table 3: Technical specifications of the multi-functional pulse generator.

Methods	BE	MME
Voltage (V)	220	10
Pulse duration (ms)	10	10
No. of pulses	1	27
Pulse Frequency (Hz)	N/A	1

In this system, target cells was suspended in 100 μ l fresh OPTI-MEM I (a serum free medium) at a density of 0.5×10^6 cells/ml. Plasmid DNA (pGFP or pLuc) of 10 μ g was then added to make the electroporation sample solution. Afterwards, the sample solution would be loaded in a syringe and fixed on a syringe pump. By connecting with the tubing, the cells would go through the micro-fluidic device and collected in the tubing which was fixed at the other end. The syringe pump was set up at 13.5 ml/h. While the cells fulfilled the micro-channel, the multi-functional pulse generator started to provide twenty-seven electric pulses at a frequency of 1. This system settlement ensured each single cell suffered and only suffered one pulse during the whole flowing process.

After collecting all the solution, the cells were transferred to a 12-well plate with 1 ml culture media in each well. As introduced in Chapter 3, the transfection efficiency and cell viability were measured at 24 hours after electroporation.

5.2.4 Polymer Based Nano-Fiber Fabrication

Nano-fiber electrode material was fabricated through electrospinning process. Polyacrylonitrile (PAN, average MW 150,000), N, N-dimethylformamide (DMF, 99.8%) were purchased from Sigma-Aldrich (St Louis, MO). Typically, a 10 wt% PAN/DMF solution was first prepared by dissolving PAN powders in DMF stirring overnight at 80°C. The suspension was then loaded in a 10 ml plastic syringe fix on a syringe pump at a flow rate of 0.75 ml h⁻¹. The suspension was extruded through a 30 G stainless steel needle (from Nordson EFD Corporation). A grounded aluminum pan was placed at a 15 cm distance from the end of needle. A directional current electric bias (24 kV) was added between the needle end and the aluminum pan collector through Gamma ES- 40P power supply (Gamma High Voltage Research, Inc.). Figure 5-2 shows the electrospinning process.



Figure 5-2: Schematic diagram of fiber formation by electrospinning process where a droplet of a polymer solution is elongated by a high electrical field. (http://nano.mtu.edu/Electrospinning_start.html).

5.2.5 Nano-Fiber Electrode Carbonization Protocol

Similar with the SU-8 photoresist process, three stages were needed during PAN fiber carbonization. Particular parameters were justified as (1) a temperature ramp from room temperature to 280°C at 2°C/min, followed by a 360 min dwell at 280°C in an open air environment ; (2) a temperature ramp from 280 to 700°C at 10°C/min with a one-hour dwell at 700°C to complete carbonization under flowing N₂ at 2000 mL/min; and (3) cool down to room temperature at 5°C/min in N₂ flow. This protocol is shown in Figure 5-3.

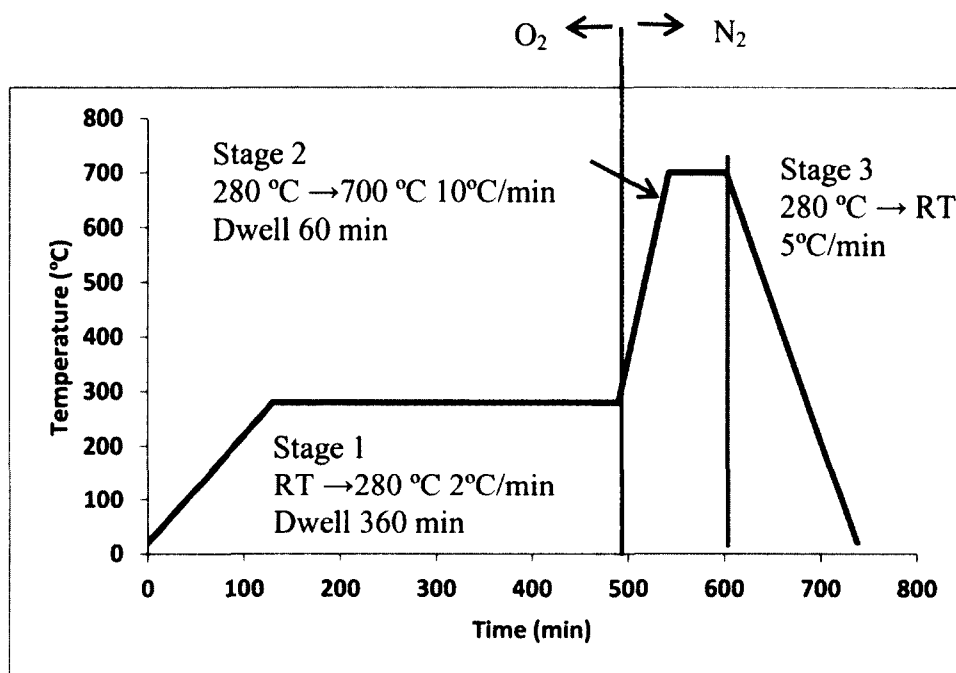


Figure 5-3: Three stages of PAN nano-fiber carbonization protocol.

5.3 Results and Discussions

5.3.1 Comparison of FME with Bulk Electroporation

For comparison purpose, plasmid GFP was used as reporter gene. K562 cells (ATCC, CCL-243) and A549 cells (ATCC, CCL-185) were used as model cells. Conventional bulk electroporation (designated as BTX) and MFE were tested. A significant improvement was expected of green fluorescence protein (GFP) expression by using the FME method over the conventional bulk electroporation method. Simultaneously in the FME system, due to a much lower electric voltage applied, cell viability achieved the same level of the conventional bulk electroporation method.

As expected, it is easily visualized from Figures 5-4 and 5-5 that successful transfection was observed in all three cases with many cells expressing green

fluorescence protein (GFP). However, for (a) and (b) which present the micro-pillar structure enhanced micro-fluidic electroporation gained more pGFP plasmids expressed. It is further proven again by the quantitative difference on GFP-positive.

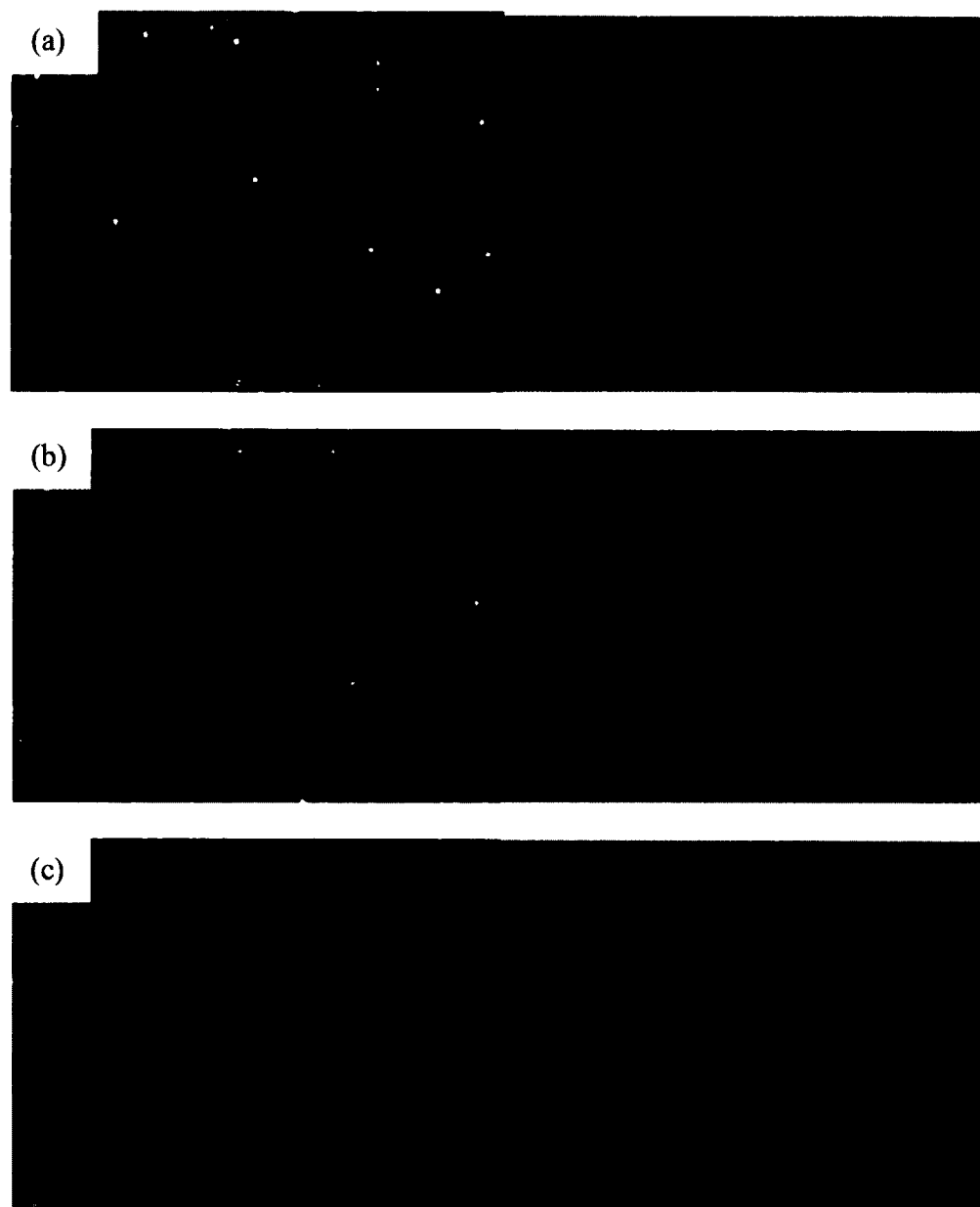


Figure 5-4: Transfection enhancements of pGFP plasmids in FME. Fluorescence microscopic and phase contrast images of K562 cells after transfection by 2 μm (a) and 6 μm (b) pillar structure enhanced microfluidic electroporation and conventional bulk electroporation (“BTX”) (c).

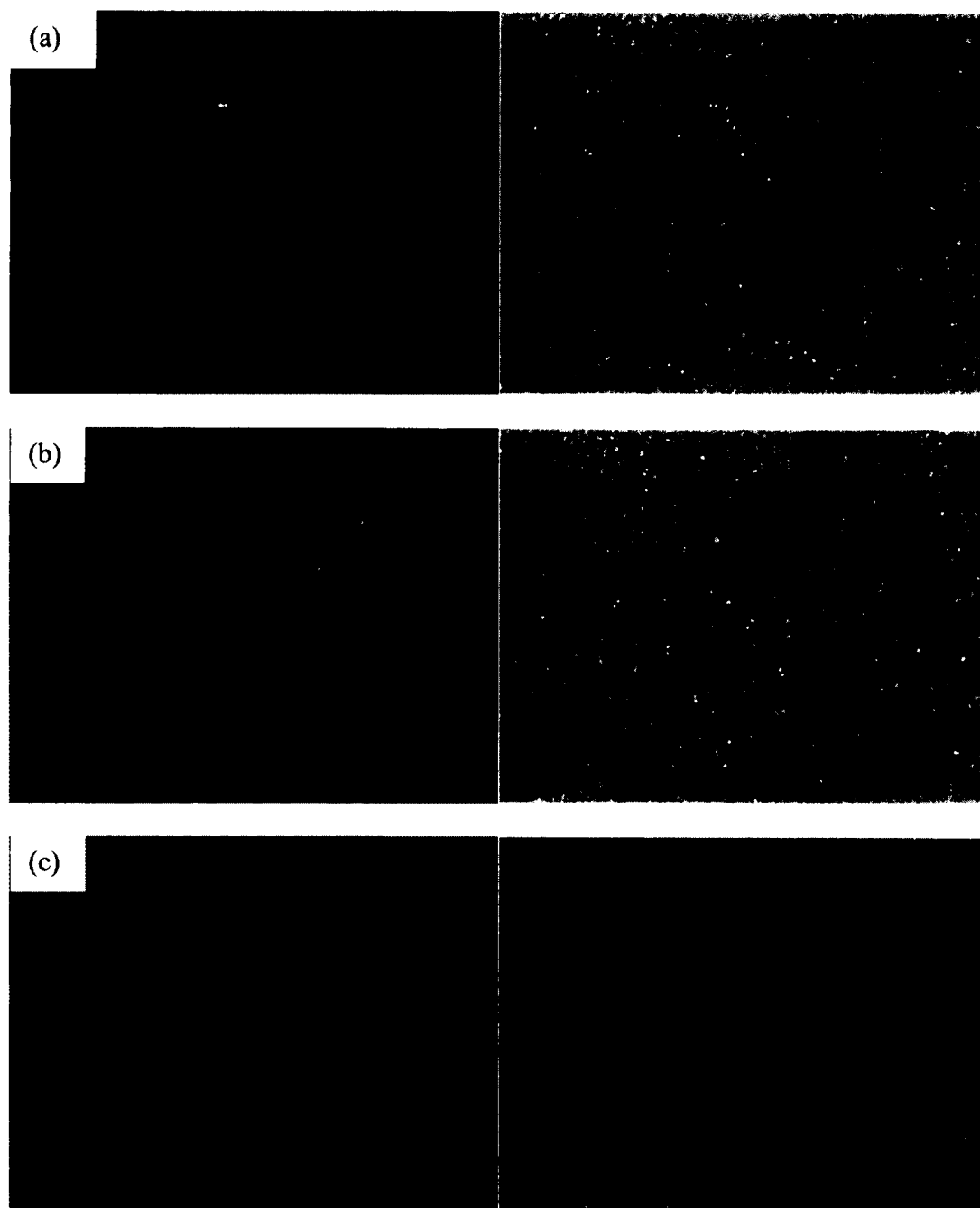
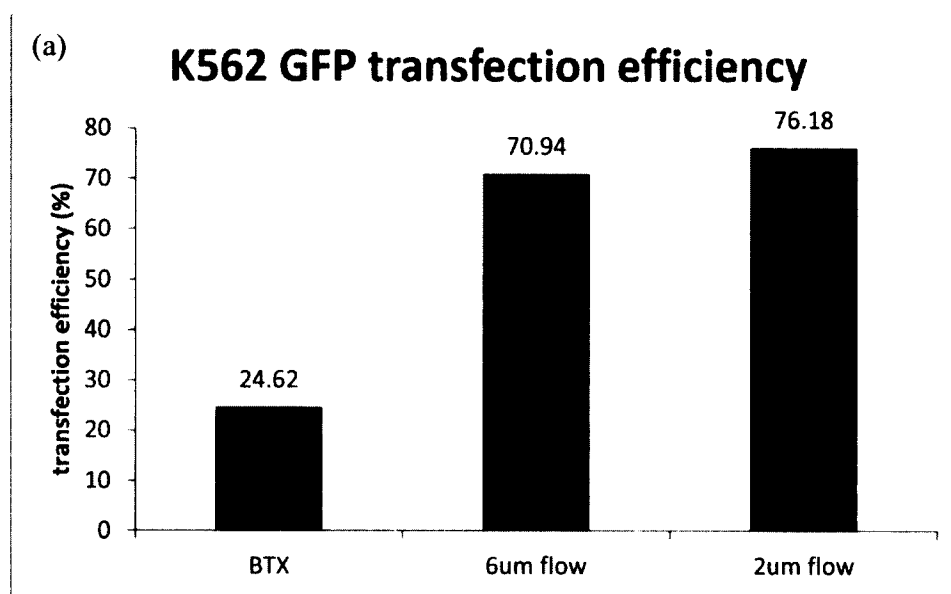


Figure 5-5: Transfection enhancements of pGFP plasmids in MFE. Fluorescence microscopic and phase contrast images of A549 cells after transfection by 2 μm (a) and 6 μm (b) pillar structure enhanced microfluidic electroporation and conventional bulk electroporation (“BTX”) (c).

As shown in Figures 5-6 and 5-7, the transfection efficiency with micro-pillar structure enhanced micro-fluidic electroporation ($73.68 \pm 0.94\%$, $71.27 \pm 1.6\%$ for 2 μm ,

6 μm A549 cells, and $76.18 \pm 2.1\%$, 70.94 ± 1.1 for 2 μm , 6 μm K562 cells) is generally much better than that from BTX (A549: $22.05 \pm 0.87\%$, K562: $24.62 \pm 0.67\%$).

Meanwhile, the quantitative differences on cell viability shown in Figures 4-4 and 4-5 indicate that there is no more loss on the MFE system ($80.68 \pm 0.30\%$, $81.54 \pm 0.30\%$ for 2 μm , 6 μm A549 cells, and $82.57 \pm 0.76\%$, 83.56 ± 0.15 for 2 μm , 6 μm K562 cells) compare with BTX (A549: $78.64 \pm 0.20\%$, K562: $80.35 \pm 0.50\%$). These results confirm the enhancement of FME on plasmid transfection for mammalian cells. This is not surprising considering the actual voltage used in the current FME setup (10 V) is still beyond the threshold for electrochemical hydrolysis of water (~ 1.3 V). Its negative impact on cell survival is minimized, not completely avoided.



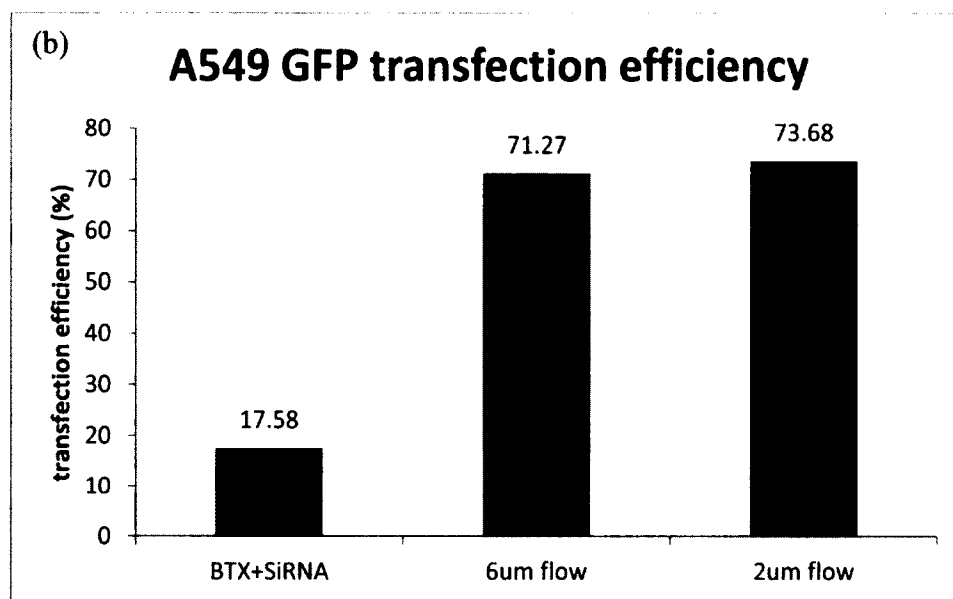
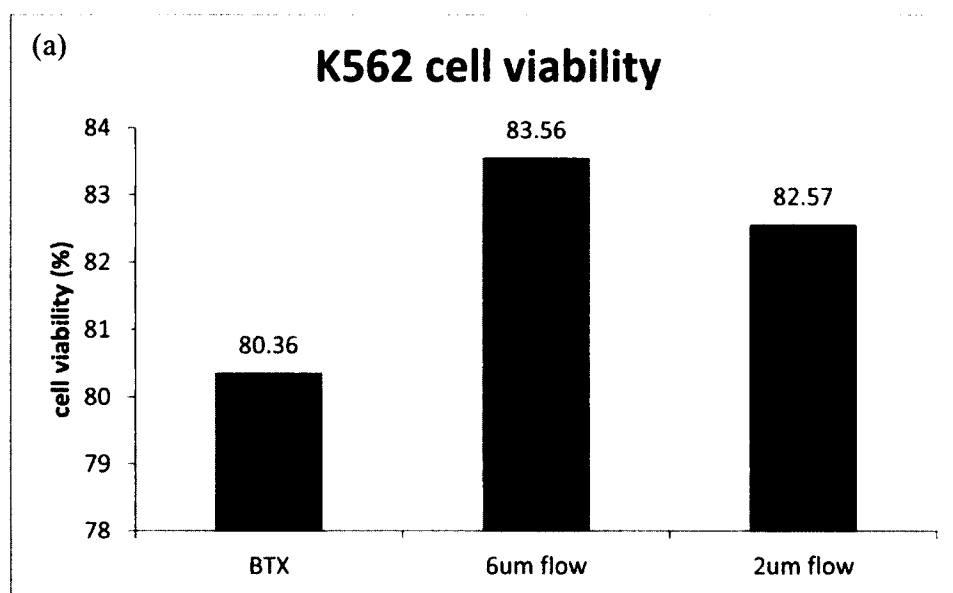


Figure 5-6: Quantitative results of pGFP plasmids transfection efficiency for K562 (a) and A549 (b) cells by 2 μm and 6 μm pillar structure enhanced micro-fluidic electroporation and conventional bulk electroporation (“BTX”).



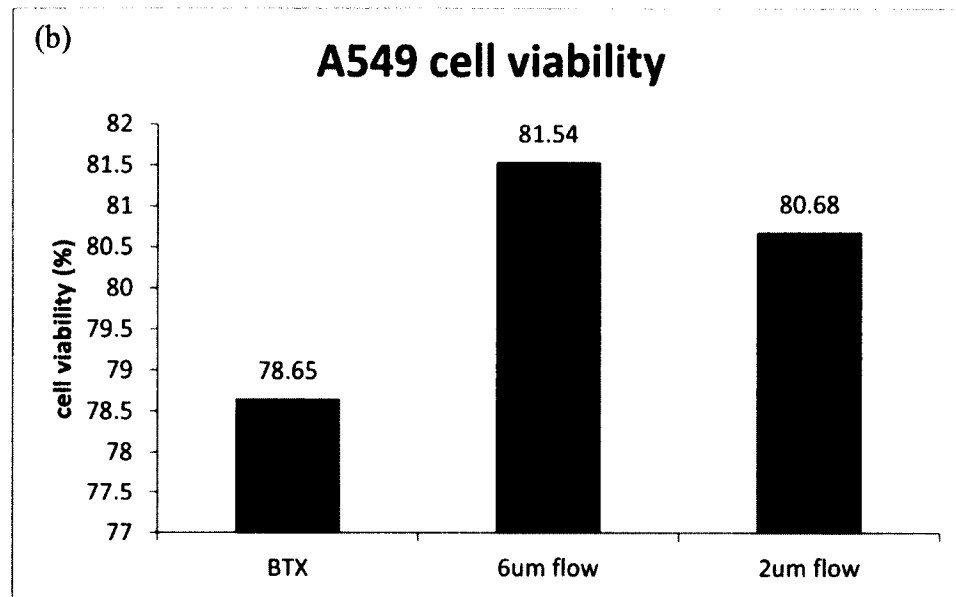


Figure 5-7: Quantitative results of electroporation cell viability for K562 (a) and A549 (b) cells by 2 μm and 6 μm pillar structure enhanced micro-fluidic electroporation and conventional bulk electroporation (“BTX”).

5.3.2 Comparison of MFE with Different Pulse Frequency

Considering the results from Section 5.3.1, since the FME cell viability performs even better than BTX, it provides us much confidence in improving our electroporation protocol on the MFE system further. A logical idea is to create more opportunities on forming transient pores on cell membrane. A straight shoot is to increase the electroporation pulse number. Thus, K562 cells were chosen as the model cells. Most parameters are kept as in Section 5.3.1. Pulse frequency varied as 1 Hz, 10 Hz, and infinite (which means a DC current was applied); 24 hours fluorescence microscopic and phase contrast images are shown in Figure 5-8.

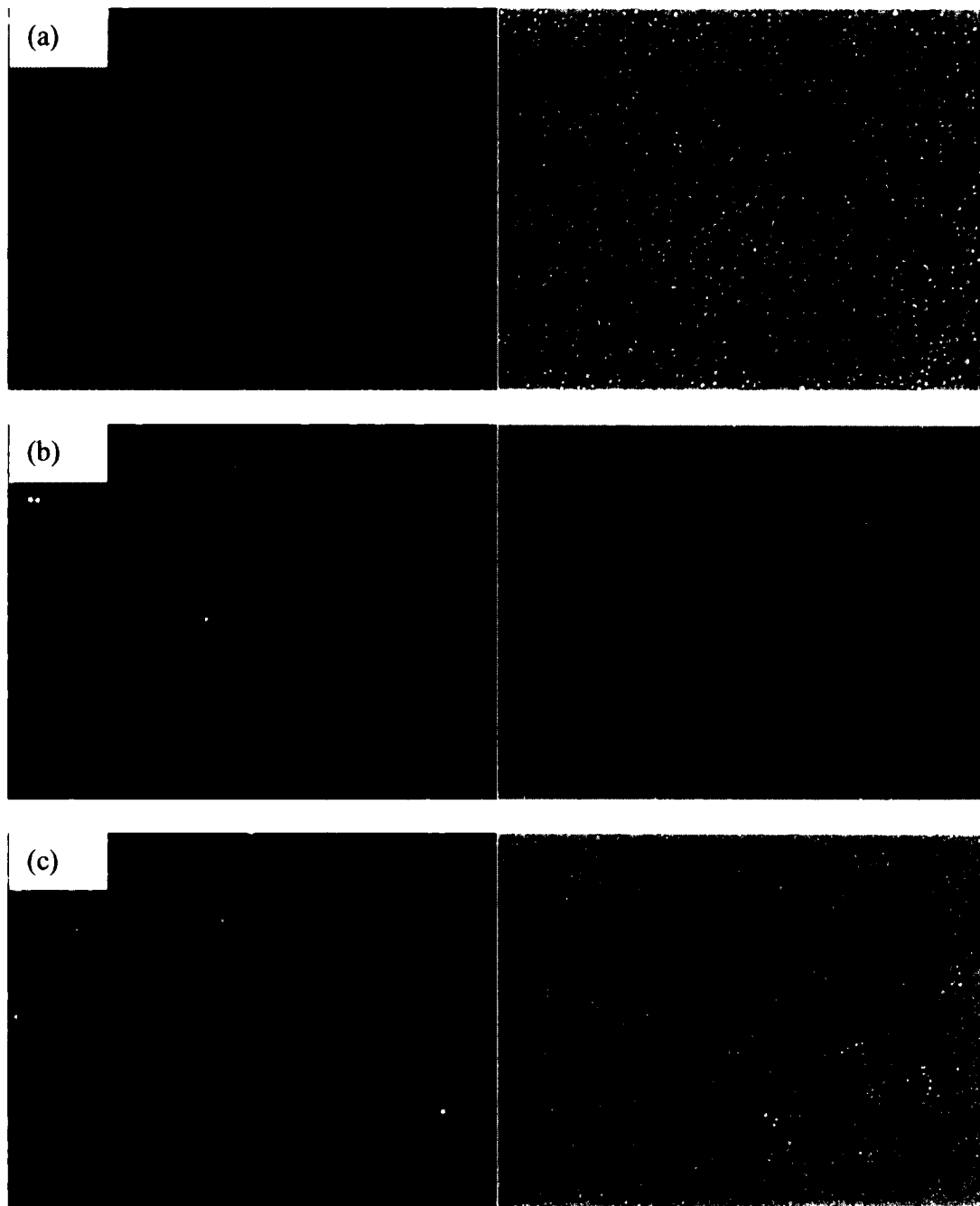
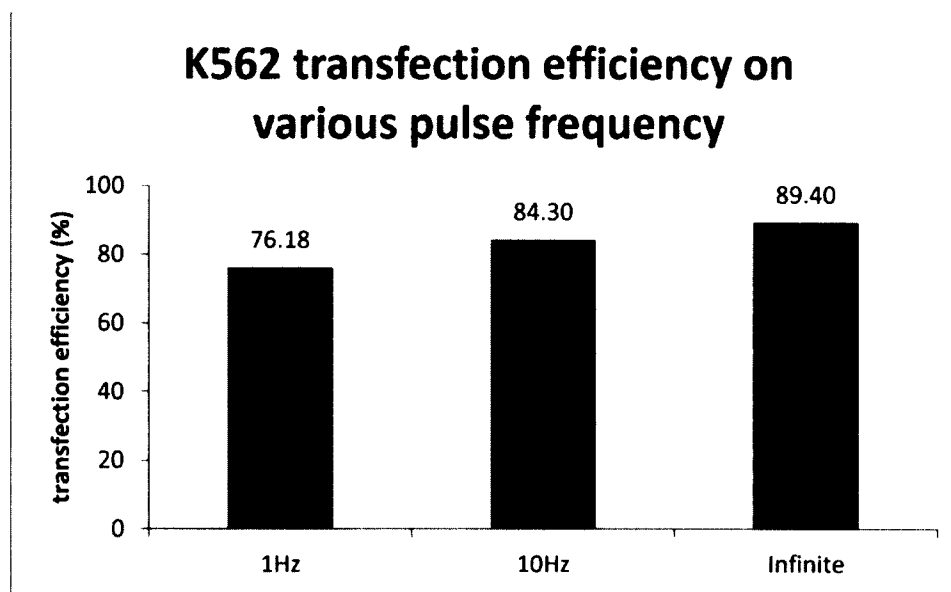


Figure 5-8: Transfection enhancements of pGFP plasmids in FME. Fluorescence microscopic and phase contrast images of K562 cells 24 hours after electroporation by 2 μm pillar structure enhanced micro-fluidic electroporation for pulse frequency 1 Hz, 10 Hz, and infinite (a, b and c).

Successful transfection was observed in all three cases with many cells expressing green fluorescence protein (GFP). All these cases present a high level on transfection efficiency.

Figure 5-9 provides the particular data. The transfection efficiency ($76.18 \pm 2.1\%$ for 1 Hz, $84.30 \pm 3.07\%$ for 10 Hz, and $89.40 \pm 2.57\%$ for infinite) was generally kept in the same range of 75% to 90%. However, when we look at cell viability, it is a different story. For 1 Hz and 10 Hz the viabilities are, respectively, $82.57 \pm 0.95\%$ and $78.18 \pm 5.05\%$, which can be considered indiscriminate. There is approximately a 30% drop on infinite pulse frequency ($51.99 \pm 3.67\%$). The significant difference brings us to ascribe the harm came from a continual current.



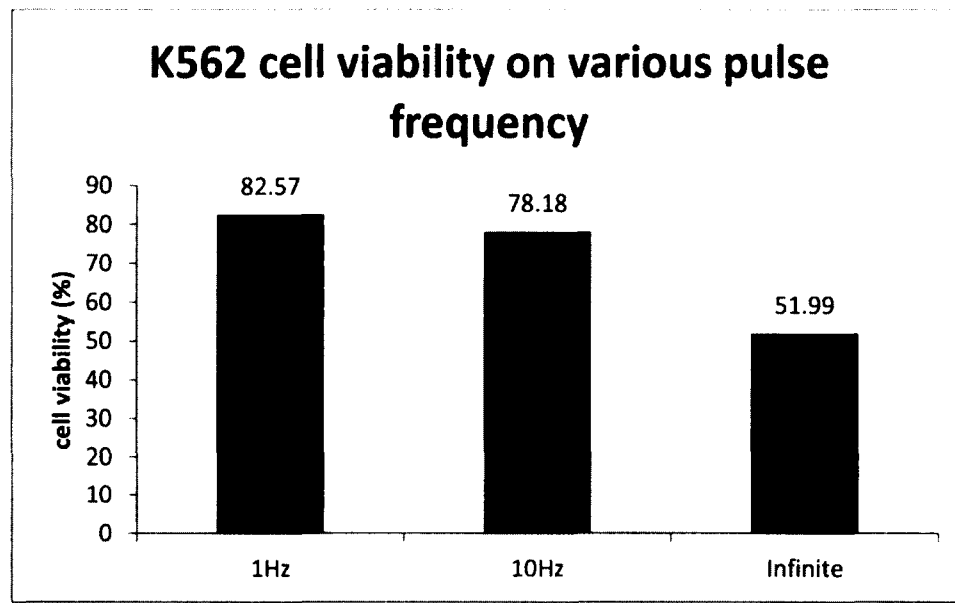


Figure 5-9: K562 cell transfection efficiency and cell viability on various pulse frequencies.

5.3.1 Comparison of MFE with Different Pulse Frequency

Using the same material and set up with carbon micro-pillar based electroporation, a comparison made between plain plate, carbon micro-pillar and carbon nano-fiber based electroporation. Figure 5-10 shows transfection enhancement of pGFP plasmids in fluorescence microscopic and phase contrast images of carbon nano-fiber based electroporation.

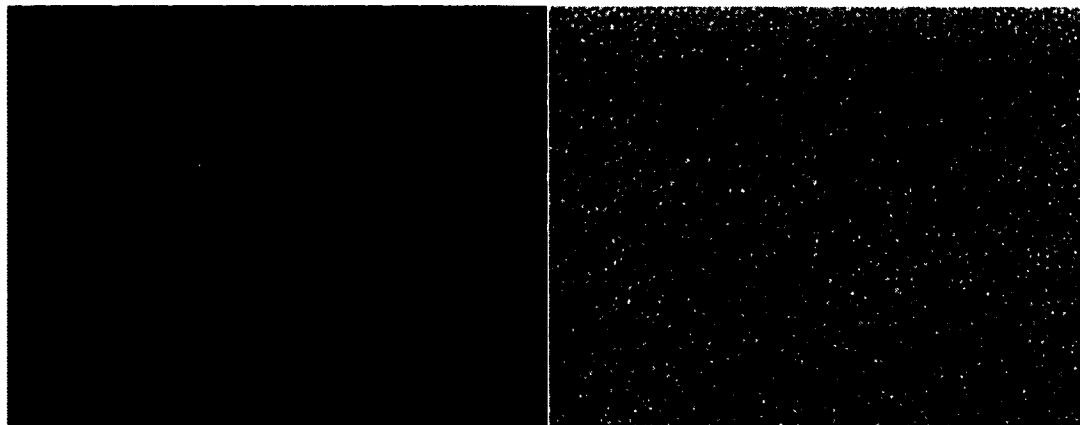


Figure 5-10: Transfection enhancement of pGFP plasmids in fluorescence microscopic and phase contrast images of carbon nano-fiber based electroporation.

In all cases, green fluorescence protein (GFP) were expressed 24 hours after electroporation (Figure 5-10). More quantitative comparisons were done by counting the percentage of GFP-positive cells (Figure 5-11a). Efficiency of pGFP transfection for plain plate carbon fiber and carbon pillar increased the gradatim (~40% for plain plate, ~55% for carbon fiber and ~70 for carbon pillar), which was genenally expected to be much better than that from BTX (K562: $25.7 \pm 1.8\%$, 3T3: $25.4 \pm 3.6\%$). For the cell viability, all of them showed great bio-stability.

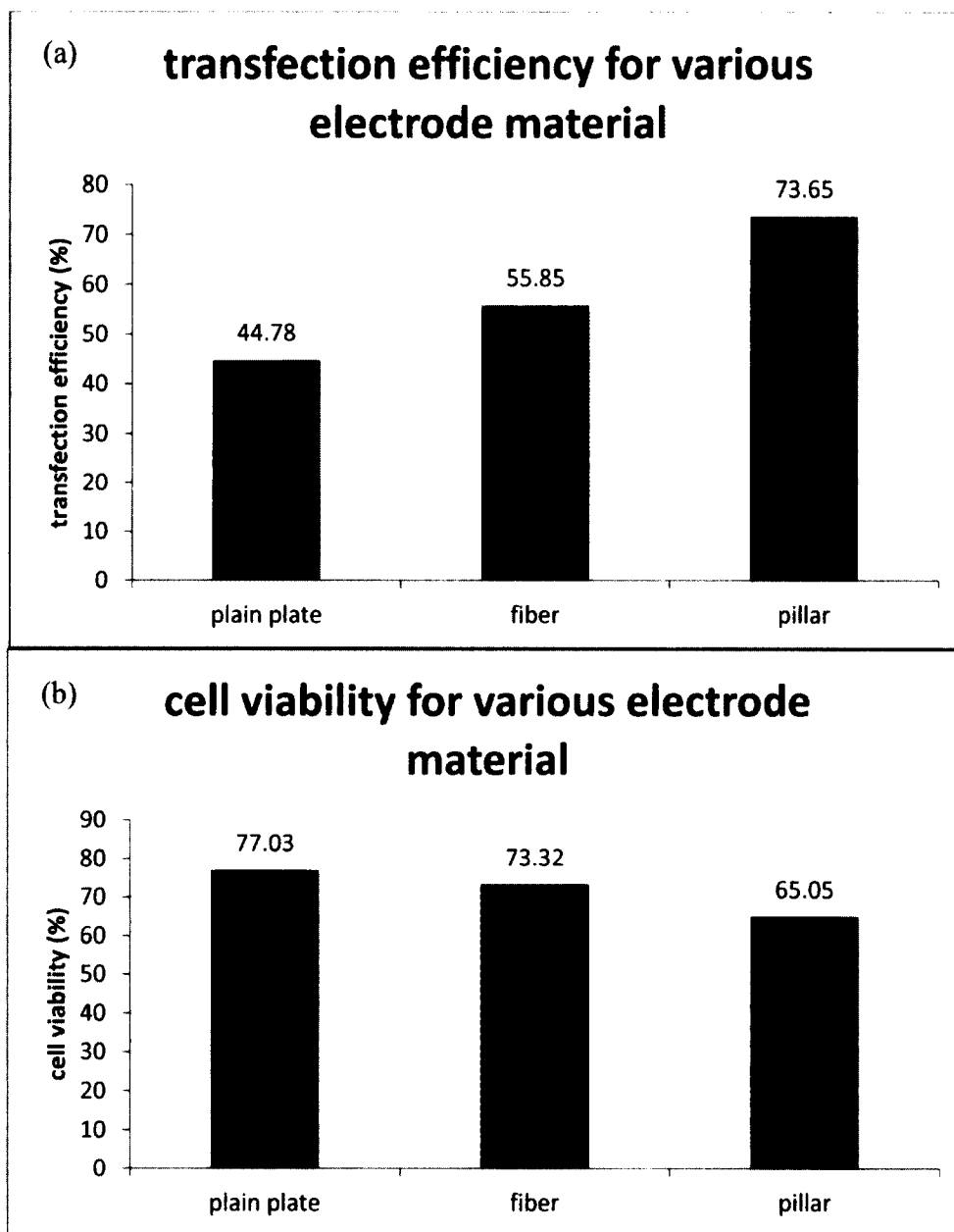


Figure 5-11: Presents the pGFP transfection efficiency (a) and cell viability (b) difference between plain plate, fiber-based and pillar-based electroporation.

5.4 Conclusions

A new micro-pillar structure enhanced by the micro-fluidic electroporation (FME) system approach was demonstrated using plasmids GFP as model materials. K562 cells (ATCC, CCL-243) and A549 cells (ATCC, CCL-185) were tested, and a significant

improvement in transgene expression was observed compared to current electroporation techniques. In the MFE method, the focused electric field enhances cell permeabilization at a low electric voltage, leading to high cell viability; more important, the micro-pillar configuration is able to provide better electric field distribution near the cell surface, facilitating gene delivery into the cells.

Successful examples of in vitro electroporation trials have been done on animal and human patients. Since typically cells or tissues from the patients are very limited and therapeutic materials such as plasmids and oligonucleotides are very expensive, our FME method with the ability to deal with a small number of cells with high transfection efficiency and cell viability offers a great impossibility for ex vivo gene therapy. The applicability of the MSE method to primary cells and hard-to-transfect cells (such as mouse embryonic stem cells and leukemia cells) is currently under investigation in our laboratory.

CHAPTER 6

CONCLUSIONS

A new micro-pillar array electroporation (MAE) approach was developed and demonstrated using plasmids GFP and gWiz Luciferase as reporter genes. Several cell lines, such as NIH 3T3 fibroblasts, K562 cells (ATCC, CCL-243) and A549 (ATCC, CCL-185) cells, were tested and a significant improvement in transgene expression and cell viability was observed compared to current electroporation techniques. In the MAE method, the focused electric field enhances cell permeabilization at a lower electric voltage, leading to high cell viability. Furthermore, the micro scaled pulse applied space is able to provide better gene confinement near the cell's surface, facilitating gene delivery into the cells.

We also demonstrated the use of polymer pyrolysis technic to fabricate low cost, multiple reutilized conductive carbon electrodes. By applying carbon material on our MAE system, we observed the same high gene transfection and excellent cell viability as the gold coated electrodes compared to that achieved with the bulk electroporation methods. The good performance on carbon electrodes provides new choices on the electrodes material for biological environment.

For large volume production, a flow guided MAE electroporation system was successfully integrated. Using plasmids GFP and gWiz Luciferase as reporter genes, K562 cells (ATCC, CCL-243) and A549 (ATCC, CCL-185) cells were tested for

electroporation. Significant improvement of gene delivery efficiency with equal or even better cell survival and recover rates were observed compared to conventional electroporation methods. Due to its ability to continuously work with assortative flowing rate and electric pulse frequency, the flow guided MAE system has the potential for large-scale industrial production.

REFERENCES

- Agarwal, A., Wang, M., Olofsson, J., Orwar, O. and Weber, S.G. (2009). "Control of the release of freely diffusing molecules in single-cell electroporation." *Anal Chem*, 81(19): 8001-8008.
- Alarcon, J.B., Waive, G.W., McManus, D.P., McManus, W. (1999). "DNA vaccines: technology and application as anti-parasite and anti-microbial agents." *Adv. Parasitol*, 42: 343-410.
- American Cancer Society "10 Must-Know Cancer Statistics for 2014," (2014)
<http://www.cancer.org/research/acsresearchupdates/more/10-must-know-cancer-statistics-for-2014>
- American Cancer Society "Cancer Statistics 2014," (2014)
<http://www.cancer.org/research/cancerfactsstatistics/cancerfactsfigures2014/>
- American Cancer Society "Cancer Immunotherapy," (2014)
<http://www.cancer.org/acs/groups/cid/documents/webcontent/003013-pdf.pdf>
- Ansorge, W. and Pepperkok, R. (1988). "Performance of an automated system for capillary microinjection into living cells." *J Biochem Biophys Methods*, 16(4): 283-292.
- Bernhardt, J. and Pauly, H. (1973). "On the generation of potential differences across the membranes of ellipsoidal cells in an alternating electrical field." *Radiation and Environmental Biophysics*, 10(1), 89-98.
- Bhatt, D.L., Gaylor, D.C. and Lee, R.C. (1990). "Rhabdomyolysis due to pulsed electric fields." *Plast Reconstr Surg*, 86, 1-11.
- Bloquel, C., Bessis, N., Boissier, M.C., Scherman, D., and Bigey, P. (2004). "Gene therapy of collagen-induced arthritis by electrotransfer of human tumor necrosis factor-alpha soluble receptor I variants." *Hum Gene Ther*, 15(2):189-201.
- Boussif, O., Lezoualc'h, F., Zanta, M.A., Mergny, M.D., Sherman, D., Demeneix, B. and Behr, J.P. (1995). "A versatile vector for gene and oligonucleotide transfer into cells in culture and in vivo: Polyethylenimine." *Proc Natl Acad Sci*, 92(16): 7297- 7301.

- Campbell, R.S. and Robinson, W.F. (1998). "The comparative pathology of the lentiviruses." *J Comp Pathol*, 119(4):333-395.
- Cemazar, M., Parkins, C.S., Holder, A.L., Chaplin, D.J., Tozer, G.M. and Sersa, G. (2001). "Electroporation of human microvascular endothelial cells: evidence for an anti-vascular mechanism of electrochemotherapy." *Br J Cancer*, 84, 565-570.
- Centers for Disease Control and Prevention (2011). "Vaccines are our most effective and cost-saving tools for disease prevention, preventing untold suffering and saving tens of thousands of lives and billions of dollars in healthcare costs each year." A CDC framework for preventing infectious diseases.
- Coffin, J.M., Hughes, S.H. and Varmus, H.E., (1997). "Principles of retroviral vector design. eds. *Retroviruses*." Cold Spring Harbor, N.Y: Cold Spring Harbor Laboratory Press.
- Comerota, A.J., Thom, R.C., Miller, K.A., *et al.* (2002). "Naked plasmid DNA encoding fibroblast growth factor type 1 for the treatment of end-stage unreconstructible lower extremity ischemia: preliminary results of a phase I trial." *J Vasc Surg*. 35(5):930-936.
- Cooray, S., Howe, S.J. and Thrasher, A.J. (2012). "Retrovirus and lentivirus vector design and methods of cell conditioning." *Methods Enzymol*, 507:29-57.
- Cui, Z. and Mumper, R. J. (2003). "The effect of co-administration of adjuvants with a nanoparticle-based genetic vaccine delivery system on the resulting immune responses." *Eur J Pharm Biopharm*, 55(1): 11-18.
- Daugimont, L., Vandermeulen, G. and Defresne, F. (2011). "Antitumoral and antimetastatic effect of antiangiogenic plasmids in B16 melanoma: higher efficiency of the recombinant disintegrin domain of ADAM 15." *Eur J Pharm Biopharm*, 78(3):314-319.
- Davis, M. E. (2002). "Non-viral gene delivery systems." *Curr Opin Biotechnol*, 13(2): 128-131.
- Davis, V.A., Ericson, L.M., Parra-Vasquez, ANG, Fan, H., Wang, Y., Prieto, V., Longoria, A.J., Ramesh, S., Saini, K. R., Kittrell, C., Billups, W. E., Adams, W.W., Hauge, R., Smalley, R. and Pasquali, M. (2004). "Phase Behavior and Rheology of SWNTs in Superacids." *Macromolecules*, 37:154–60.
- Douek, D.C., Roederer, M. and Koup, R.A. (2009). "Emerging Concepts in the Immunopathogenesis of AIDS." *Annu. Rev. Med*, 60: 471–84.

- Escoffre, J. M., Portet, T., Wasungu, L., Teissié, J., Dean, D. and Rols, M. P. (2009). "What is (still not) known of the mechanism by which electroporation mediates gene transfer and expression in cells and tissues." *Molecular Biotechnology*, 41(3), 286-295.
- Fei, Z., Hu, X., Choi, H.-W., Wang, S., Farson, D. and Lee, L. J. (2010). "Micronozzle array enhanced sandwich electroporation of embryonic stem cells." *Anal. Chem*, 82, 353-358
- Felgner, P. L., Gadek, T. R., Holm, M., Roman, R., Chan, H. W., Wenz, M., Northrop, J. P., Ringold, G.M. and Danielson, M. (1987). "Lipofection: A highly efficient, lipid-mediated DNA-transfection procedure." *Proc Natl Acad Sci USA*, 84(21): 7413-7417.
- Fiore, A.E., Bridges, C.B. and Cox N.J. (2009). "Seasonal influenza vaccines." *Curr. Top. Microbiol. Immunol*, 333: 43–82.
- Fisher, Bruce, Harvey, Richard P. and Champe, Pamela C. (2007). "Lippincott's Illustrated Reviews." *Microbiology (Lippincott's Illustrated Reviews Series)*.
- Fitzer, E., Kochling, K.H., Boehm, H.P. and Marsh, H. (1995). "Recommended terminology for the description of carbon as a solid." *Pure Appl. Chem*, 67, 473–506.
- Gabriel, B. and Teissie, J. (1997). "Direct observation in the millisecond time range of fluorescent molecule asymmetrical interaction with the electroporabilized cell membrane." *Biophysical Journal*, 73(5), 2630-2637.
- Gehl, J. and Geertsen, P. (2000). "Efficient palliation of hemorrhaging malignant melanoma skin metastases by electrochemotherapy." *Melanoma Res*, 10, 585–589.
- Gehl, J., Skovsgaard, T. and Mir, L.M. (1998). "Enhancement of cytotoxicity by electroporabilization: an improved method for screening drugs." *Anticancer Drugs*, 9, 319–325.
- Gehl, J., Skovsgaard, T. and Mir, L.M. (2002). "Vascular reactions to in vivo electroporation: characterization and consequences for drug and gene delivery." *Biochim Biophys Acta*, 1569, 51–58.
- Ginn, S.L., Alexander, I.E., Edelstein, M.L., Abedi, M.R. and Wixon, J. (2013) "Gene therapy clinical trials worldwide to 2012 – an update." *J Gene Med*, 15(2):65-77.
- Gudmundsdottir, L., Sjödin, A., Boström, A.C., Hejdeman, B., Theve-Palm, R., Alaeus, A., Lidman, K. and Wahren, B. (2006). "Therapeutic immunization for HIV." *Springer Semin Immunopathol*, 28(3):221-230.

- Hamilton, A.J. and Baulcombe, D.C. (1999). "A species of small antisense RNA in posttranscriptional gene silencing in plants." *Science*, 286 (5441), 950-952.
- Hibino, M., Shigemori, M., Itoh, H., Nagayama, K. and Kinoshita, K. (1991). "Membrane conductance of an electroporated cell analyzed by submicrosecond imaging of transmembrane potential." *Biophysical Journal*, 59(1), 209-220.
- How, S. E., Yingyongnarongkul, B., Fara, M.A., Diaz-Mochon, J. J., Mittoo, S. and Bradley, M. (2004). "Polyplexes and lipoplexes for mammalian gene delivery: From traditional to microarray screening." *Comb Chem High Throughput Screen*, 7(5): 423-430.
- Huang, S., Deshmukh, H., Rajagopalan, K. and Wang, S. (2014). "Gold nanoparticles electroporation enhanced polyplex delivery to mammalian cells." *Electrophoresis*, 35, 1837-1845.
- Jenkins, G. and Kawamura, K. (1971). "Structure of glassy carbon." *Nature*, 231, 175-176.
- Jenkins, G., Kawamura, K. and Ban, L. (1972). "Formation and structure of polymeric carbons." *Proc. R. Soc. Lond. A Math. Phys. Sci*, 327, 501-517.
- John Wiley and Sons Ltd. (2013) "Gene Therapy Clinical Trials Worldwide," <http://www.abedia.com/wiley/>.
- Jordan, M. and F. Wurm (2004). "Transfection of adherent and suspended cells by calcium phosphate." *Methods*, 33(2): 136-143.
- Joshi, R. and Schoenbach, K. (2000). "Electroporation dynamics in biological cells subjected to ultrafast electrical pulses: A numerical simulation study." *Physical Review E*, 62 (1 Pt B): 1025-33.
- Kakinoki, J. (1965). "A model for the structure of 'glassy carbon'." *Acta Crystallogr*, 18, 578.
- Kamimura, K., Suda, T., Zhang, G. and Liu, D. (2011). "Advances in Gene Delivery Systems." *Pharm Med*, 25 (5): 293-306.
- Kim, J. A., Cho, K., Shin, Y. S., Jung, N., Chung, C. and Chang, J. K. (2007). "A multi-channel electroporation microchip for gene transfection in mammalian cells." *Biosens. Bioelectron*, 22, 3273-3277.
- Kim, J. A., Cho, K., Shin, M. S., Lee, W.G., Jung, N., Chung, C. and Chang, J. K. (2008). "A novel electroporation method using a capillary and wire-type electrode." *Biosens Bioelectron*, 23(9): 1353-1360.
- Kinoshita, K. and Tsong, T.Y. (1977b). "Formation and resealing of pores of controlled sizes in human erythrocyte membrane." *Nature*, 268, 438-441.

- Kulangara, K., Yang, Y., Yang, J. and Leong, K.W. (2012). "Nanotopography as modulator of human esenchymal stem cell function." *Biomaterials*, 33, 4998-5003.
- Li, S. and Huang, L. (2000). "Nonviral gene therapy: promises and challenges." *Gene Ther*, 7(1):31-34.
- Ma, B., Zhang, S., Jiang, H., Zhao, B. and Lv, H. (2007). "Lipoplex morphologies and their influences on transfection efficiency in gene delivery." *J Control Release*, 123(3): 184-194.
- McFeely, S.P., Kowalczyk, S.P., Ley, L., Cavell, R.G., Pollak, R.A. and Shirley, D.A. (1974). "X-ray photoemission studies of diamond, graphite, and glassy carbon valence bands." *Phys. Rev. B*, 9, 5268–5278.
- Mehrle, W., Hampp, R. and Zimmermann, U. (1989). "Electric pulse induced membrane permeabilisation. spatial orientation and kinetics of solute efflux in freely suspended and dielectrophoretically aligned plant mesophyll protoplasts." *Biochimica Et Biophysica Acta (BBA)-Biomembranes*, 978(2), 267-275.
- Mi, Y, Hu, W, Dan, Y and Liu, Y. (2008). "Synthesis of carbon micro-spheres by a glucose hydrothermal method." *Mater Lett*, 62:1194–6.
- Mintzer, M. A. and Simanek, E. E. (2009). "Nonviral vectors for gene delivery." *Chem Rev*, 109(2): 259-302.
- Nadjm, B. and Behrens, R.H. (2012). "Malaria: An update for physicians." *Infectious Disease Clinics of North America*, 26 (2): 243–59.
- National Cancer Institute. (2014). "Cancer Treatment." <http://www.cancer.gov/about-cancer/treatment>
- National Vital Statistics Report (NVSR). (2014). "Deaths: Final Data for 2014." The complete version of this report, 64, 2.
- Nayak, S. and Herzog, R.W. (2009). "Progress and prospects: immune responses to viral vectors." *Gene Ther*, 17(3):295-304.
- Neumann, E., Schaefer-Ridder, M., Wang, Y. and Hofschneider, P.H. (1982). "Gene transfer into mouse lyoma cells by electroporation in high electric fields." *The EMBO Journal*, 1 (7): 841–5.
- Neumann, E. (1992). "Membrane electroporation and direct gene transfer." *Bioelectrochemistry and Bioenergetics*, 28(1), 247-267.
- Neumann, E., Kakorin, S., Tsoneva, I., Nikolova, B. and Tomov, T. (1996). "Calcium-mediated DNA adsorption to yeast cells and kinetics of cell transformation by electroporation." *Biophys J*, 71, 868–877.

- Nikol, S., Baumgartner, I., Van Belle, E., Diehm, C., Visoná, A., Capogrossi, M., Ferreira-Maldent, N., Gallino, A., Wyatt, M., Wijesinghe, L. D., Fusari, M., Stephan, D., Emmerich, J., Pompilio, G., Vermassen, F., Pham, E., Grek, V., Coleman, M. and Meyer, F. (2008). "Therapeutic angiogenesis with intramuscular NV1FGF improves amputation- free survival in patients with critical limb ischemia." *Mol Ther*, 16(5):972-978.
- Nisole, S. and Saib, A. (2004) "Early steps of retrovirus replicative cycle." *Retrovirology*, 1:9.
- O'Brien, J. A. and Lummis, S. C. (2011). "Nano-biolistics: a method of biolistic transfection of cells and tissues using a gene gun with novel nanometer- sized projectiles." *BMC Biotechnol*, 11: 66.
- Olofsson, J., Levin, M., Stromberg, A., Weber, S. G., Ryattsen, F. and Orwar, O. (2007). "Scanning electroporation of selected areas of adherent cell cultures." *Anal Chem*, 79(12): 4410-4418.
- Pagano, J. S. and Vaheri, A. (1965). "Enhancement of infectivity of poliovirus RNA with diethylaminoethyl-dextran (DEAE-D)." *Arch Gesamte Virusforsch*, 17(3):456-464.
- Peng, K.W. (1999). "Strategies for targeting therapeutic gene delivery." *Mol Med Today*, 5(10):448-453.
- Pesin, L.A. (2002). "Structure and properties of glass-like carbon." *J. Mater. Sci*, 37, 1–28.
- Pesin, L.A. and Baitinger, E.M. (2002). "A new structural model of glass-like carbon." *Carbon*, 40, 295–306.
- Pinto, U.M., Pappas, K.M. and Winans, S. (2012). "The ABCs of plasmid replication and segregation." *Nat Rev Microbiol*, 10(11):755-765.
- Powell, R.J., Simons, M., Mendelsohn, F.O., Daniel, G., Henry, T.D., Koga, M., Morishita, R. and Annex, B.H. (2008). "Results of a double-blind, placebo-controlled study to assess the safety of intramuscular injection of hepatocyte growth factor plasmid to improve limb perfusion in patients with critical limb ischemia." *Circulation*, 118(1):58-65.
- Ranganathan, S., McCreery, R., Majji, S.M. and Madou, M. (2000). "Photoresist-derived carbon for microelectromechanical systems and electrochemical applications." *J. Electrochem. Soc*, 147, 277-282.
- Robinson, H.L., Pertmer, T.M. and Pertmer (2000). "DNA vaccines for viral infections: basic studies and applications." *Adv. Virus Res*, 55: 1-74.

- Rodrigo Martinez-Duarte. (2014). "SU-8 Photolithography as a Toolbox for Carbon MEMS." *Micromachines*. 5, 766-782.
- Rols, M.P., Delteil, C., Serin, G. and Teissie, J. (1994). "Temperature effects on electrotransfection of mammalian cells." *Nucleic Acids Res*, 22, 540.
- Rothwell, W. (1968). "Small-angle X-ray scattering from glassy carbon." *J. Appl. Phys*, 39, 1840-1845.
- Sakuma, T., Barry, M.A. and Ikeda, Y. (2012). "Lentiviral vectors: back to translational." *Biochem J*, 443(3):603-618.
- Sandstrom, E., Nilsson, C., Hejdeman, B., Bråve, A., Bratt, G., Robb, M., Cox, J., Van Cott, T., Marovich, M., Stout, R., Aboud, S., Bakari, M., Pallangyo, K., Ljungberg, K., Moss, B., Earl, P., Michael, N., Birx, D., Mhalu, F., Wahren, B., Biberfeld, G. and HIV Immunogenicity Study 01/02 Team. (2008). "Broad immunogenicity of a multigene, multiclade HIV-1 DNA vaccine boosted with heterologous HIV-1 recombinant modified vaccinia virus Ankara." *J Infect Dis*, 198(10):1482-1490.
- Seaman, M.S., Xu, L., Beaudry, K., Martin, K.L., Beddall, M.H., Miura, A., Sambor, A., Chakrabarti, B.K., Huang, Y., Bailer, R., Koup, R.A., Mascola, J.R., Nabel, G.J. and Letvin, N.L. (2005). "Multiclade human immunodeficiency virus type 1 envelope immunogens elicit broad cellular and humoral immunity in rhesus monkeys." *J Virol*, 79(5):2956-2963.
- Sersa, G., Cemazar, M., Miklavcic, D. and Chaplin, D.J. (1999). "Tumor blood flow modifying effect of electrochemotherapy with bleomycin." *Anticancer Res*, 19, 4017-4022.
- Del Solar, G., Giraldo, R., Ruiz-Echevarría, M.J., Espinosa, M. and Díaz-Orejas, R. (1998). "Replication and control of circular bacterial plasmids." *Microbiol Mol Biol Rev*, 62(2):434-464.
- Spain, I. (1981). "Electronic Transport properties of graphite, carbons, and related materials. In *Chemistry and Physics of Carbon*." Walker, P.L., Ed.; Marcel Dekker, Inc.: New York, NY, USA. pp 119-304.
- Spira, M. S. and Hai, A. (2013). "Multi-electrode array technologies for neuroscience and cardiology." *Nat Nanotechnol*, 8, 83-94.
- Stewart, D. A., Gowrishankar, T. R., Smith, K. C. and Weaver, J. C. (2005). "Cylindrical cell membranes in uniform applied electric field: validation of a transport lattice method." *IEEE Trans. Biomed. Eng*, 52, 1643–1653.
- Sugar, I.P. and Neumann, E. (1984). "Stochastic model for electric field-induced membrane pores electroporation." *Biophysical Chemistry*, 19 (3): 211-25.

- Teissie, J., Golzio M. and Rols M. P. (2005). "Mechanisms of cell membrane electroporation: A minireview of our present knowledge." *Biochim Biophys Acta*, 1724(3): 270-280.
- Teissie, J. and Rols, M. P. (1993). "An experimental evaluation of the critical potential difference inducing cell membrane electroporation." *Biophysical Journal*, 65(1), 409-413.
- Thrasher, A.J., Gaspar, H.B., Baum, C., Modlich, U., Schambach, A., Candotti, F., Otsu, M., Sorrentino, B., Scobie, L., Cameron, E., Blyth, K., Neil, J., Abina, S.H., Cavazzana-Calvo, M. and Fischer, A. (2006). "Gene therapy: X-SCID transgene leukaemogenicity." *Nature*, 443(7109):E5-6; discussion E6-7.
- Uchida, M., Li, X.W., Mertens, P. and Alpar, H.O. (2009). "Transfection by particle bombardment: delivery of plasmid DNA into mammalian cells using gene gun." *Biochim Biophys Acta*, 1790(8): 754-764.
- Ulasov, A.V., Khramtsov Y.V., Trusov G.A., Rosencranz A.A., Sverdlov E.D. and Sobolev A.S. (2011). "Properties of PEI-based polyplex nanoparticles that correlate with their transfection efficacy." *Mol Ther*, 19(1): 103-112.
- Urnov, F.D., Miller, J.C., Lee, Y-L, Beausejour, C.M., Rock, J.M., Augustus, S., Jamieson, A.C., Porteus, M.H., Gregory, P.D. and Holmes, M.C. (2005). "Highly efficient endogenous human gene correction using designed zinc-finger nucleases." *Nature*, 435:646-651.
- Van der Linde, W.E. and Dieker, J.W. (1980). "Glassy carbon as electrode material in electro-analytical chemistry." *Anal. Chim. Acta*, 119, 1-24.
- Van Krevelen, D.W. (1950). "Graphical-statistical method for the study of structure and reaction processes of coal." *Fuel*, 29:269-84.
- Vancha, A. R., Govindaraju S., Parsa K. V., Jasti M., Gonzalez-Garcia M., Ballesteros R. P.. (2004). "Use of polyethyleneimine polymer in cell culture as attachment factor and lipofection enhancer." *BMC Biotechnol*, 4: 23.
- Vivian, A, Murillo, J, and Jackson, R.W. (2001). "The roles of plasmids in phytopathogenic bacteria: mobile arsenals." *Microbiol*, 147(pt 4):763-780.
- Walther, W. and Stein, U. (2000). "Viral vectors for gene transfer: a review of their use in the treatment of human diseases." *Drugs*, 60(2):249-271.
- Wang, S., Hu, X. and Lee, L. J. (2008). "Electrokinetically induced asymmetric transport in polymeric nanonozzles." *Lab Chip*, 8, 573-581.
- Wang, S. and Lee, L. J. (2013) "Micro/nanofluidics based cell electroporation." *Biomicrofluidics*, 7, 011301/1-14.

- Weaver, J. C., Chizmadzhev and Yu, A. (1996). "Theory of electroporation: A review." *Bioelectrochemistry and Bioenergetics*, 41 (2): 135-60.
- Weaver, J. C. (2000). "Electroporation of cells and tissues." *Plasma Science, IEEE Transactions*, 28(1), 24-33.
- Weaver, J. C. (2003). "Electroporation of biological membranes from multicellular to nano scales." *Dielectrics and Electrical Insulation, IEEE Transactions*, 10(5), 754-768.
- Wolff, J.A., Malone, R.W., Williams, P., Chong, W., Acsadi, G., Jani, A. and Felgner, P.L. (1990). "Direct gene transfer into mouse muscle in vivo." *Science*, 247(4949 Pt 1):1465-1468.
- Xie, C., Lin, Z., Hanson, L., Cui, Y. and Cui, B. (2012). "Intracellular recording of action potentials by nanopillar electroporation." *Nat Nanotechnol*, 7, 185-190.
- Yamada, S. and Sato, H. (1962). "Some physical properties of glassy carbon." *Nature*, 193, 261-262.
- Yang, S. and May, S. (2008). "Release of cationic polymer-DNA complexes from the endosome: A theoretical investigation of the proton sponge hypothesis." *J ChemPhys*, 129(18): 185105.
- Yoshida, A., Kaburagi, Y. and Hishiyama, Y. (1991). "Microtexture and magnetoresistance of glass-like carbons." *Carbon*, 29, 1107-1111.
- Yu, S-H, Cui, X., Li, L., Li, K., Yu, B., Antonietti, M. and Cölfen, H. (2004). "From starch to metal/carbon hybrid nanostructures: hydrothermal metal - catalyzed carbonization." *Adv Mater*, 16:1636-40.
- Zerbib, D., Amalric, F. and Teissie, J. (1985). "Electric field mediated transformation: isolation and characterization of a TK+ subclone." *Biochem Biophys Res Commun*, 129, 611-618.
- Zhou, H.S., Liu, D.P., and Liang, C.C. (2004). "Challenges and strategies: the immune responses in gene therapy." *Med Res Rev*, 24(6):748-761.
- Zimmermann, U., Pilwat, G. and Riemann, F. (1974). "Dielectric breakdown of cell membranes." *Biophysical Journal*, 14(11), 881-899.
- Zittel, H.E. and Miller, F.J.A. (1965). "Glassy-carbon electrode for voltammetry." *Anal. Chem*, 37, 200-203.
- Zuhorn, I. S., Kalicharan, R. and Hoekstra, D. (2002). "Lipoplex-mediated transfection of mammalian cells occurs through the cholesterol-dependent clathrin- mediated pathway of endocytosis." *J Biol Chem*, 277(20): 18021-18028.